



Zoltan Ferenc Magosi, Msc

# **Advanced Phenomenological Radar Sensor Model for Full Vehicle Virtual Validation in Automated Driving**

## **Doctoral Thesis**

to achieve the university degree of  
Doktor der technischen Wissenschaften  
Doctoral degree programme: Mechanical Engineering

submitted to

**Graz University of Technology**

Supervisor and 1st evaluator  
Assoc.-Prof. Dipl.-Ing. Dr. techn. Arno Eichberger  
Institute of Automotive Engineering

2nd evaluator  
Assoc.-Prof. Dr. Zsolt Szalay  
Budapest University of Technology and Economics  
Automated Drive Laboratory

Graz, November 2022



# Affidavit

I declare that I have authored this thesis independently, that I have not used other than the declared sources/resources, and that I have explicitly indicated all material which has been quoted either literally or by content from the sources used. The text document uploaded to TUGRAZonline is identical to the present master's thesis.

---

Date

---

Signature



# Contents

<b>Affidavit</b>	<b>iii</b>
<b>Acknowledgement</b>	<b>ix</b>
<b>Abstract</b>	<b>xi</b>
<b>Kurzfassung</b>	<b>xiii</b>
<b>List of Publications and Supervised Theses</b>	<b>xv</b>
<b>Abbreviations</b>	<b>xxi</b>
<b>List of symbols</b>	<b>xxv</b>
<b>1. Introduction</b>	<b>1</b>
1.1. Motivation . . . . .	1
1.2. Research objectives . . . . .	2
1.3. Structure of the thesis . . . . .	3
<b>2. State of the Art</b>	<b>5</b>
2.1. The Challenge in Automotive Testing . . . . .	5
2.2. Vehicle Development Phase . . . . .	5
2.3. Type Approval Phase . . . . .	6
2.4. Consumer Protection Phase . . . . .	6
2.5. Vehicle Development Process . . . . .	7
2.6. State-of-the-Art Radar Sensor Modelling Approaches . . . . .	9
2.7. Classification from the System Integrator's Perspective . . . . .	12
2.7.1. Operational Model . . . . .	14
2.7.2. Functional Models . . . . .	14
2.7.3. Technical Models . . . . .	15
2.7.4. Individual Model . . . . .	16
2.8. Research Contributions . . . . .	17
<b>3. Development process flow and procedure of the radar sensor model approach</b>	<b>21</b>
3.1. Process flow of sensor modelling . . . . .	21
3.2. Model development procedure . . . . .	22
3.2.1. Development of a suitable measurement setup . . . . .	22
3.2.2. Driving Scenario Definition . . . . .	23
3.2.3. Identifying Radar Detection Phenomena . . . . .	23
3.2.4. Implementation in Matlab . . . . .	25

3.2.5. Calibration . . . . .	26
3.2.6. Assessment Method and Benchmark . . . . .	26
<b>4. Methodology</b>	<b>28</b>
4.1. Experimental methodology . . . . .	28
4.1.1. Vehicle Set-Up and Measurement System . . . . .	28
4.2. Sensor modelling . . . . .	32
4.2.1. Operating Principle of Frequency Modulated Continuous Wave Radar Detectors . . . . .	32
4.2.2. Modular Structure . . . . .	33
4.2.3. Functional model / design philosophy . . . . .	33
4.3. Evaluation methodology . . . . .	47
4.3.1. Dynamic Ground Truth Sensor Model Validation approach . . . . .	47
4.3.2. On-Road Measurements . . . . .	47
4.3.3. Re-Simulation of Experiments . . . . .	49
4.3.4. Commercial Radar Sensor Model . . . . .	50
4.3.5. Parameter Setting of the Sensor Model . . . . .	50
4.3.6. Labelling of Radar Measurement Data . . . . .	51
4.3.7. Evaluation Procedure . . . . .	51
4.3.8. Validation Metrics for Comparing Probability Distributions . . . . .	52
<b>5. Results and discussion</b>	<b>55</b>
5.1. Survey on Modelling of Automotive Radar Sensors and Modelling Approaches . . . . .	55
5.2. Process chain for implementing the sensor model development method . . . . .	55
5.3. Driving manoeuvre definition . . . . .	56
5.4. Evaluation of modelling approach of the presented radar sensor model . . . . .	58
5.4.1. Performance assessment of the presented radar sensor model . . . . .	59
5.4.2. RCS performance assessment of the presented radar sensor model . . . . .	60
5.5. Evaluation of modelling approach IPG-RSI . . . . .	61
5.5.1. Performance assessment - IPG-RSI . . . . .	63
5.6. Discussion . . . . .	64
<b>6. Summary</b>	<b>69</b>
<b>Bibliography</b>	<b>74</b>
<b>A. Summary of Papers</b>	<b>86</b>
A.1. Paper 1 . . . . .	86
A.2. Paper 2 . . . . .	86
A.3. Paper 3 . . . . .	87
A.4. Paper 4 . . . . .	88
A.5. Paper 5 . . . . .	89
A.6. Paper 6 . . . . .	89
A.7. Paper 7 . . . . .	90
A.8. Paper 8 . . . . .	90

## Contents

---

A.9. Paper 9 . . . . .	91
A.10. Paper 10 . . . . .	91
<b>B. Additional results</b>	<b>93</b>





# Acknowledgment

The present thesis with the research objective **Advanced Phenomenological Radar Sensor Model for Full Vehicle Virtual Validation in Automated Driving** was developed during my work as a scientific project researcher at the Institute of Automotive Engineering at the Graz University of Technology in cooperation with MAGNA STEYR Engineering AG & Co KG.

I would like to take this opportunity to thank everyone who supported me during my doctoral thesis, but also all those who supported and accompanied me on my way. I would like to thank my main supervisor, Assoc. Prof. Dipl.-Ing. Dr. techn. Univ.-Doz. Arno Eichberger from the Institute of Automotive Engineering at the Graz University of Technology for making it possible for me to work on this research topic, for giving me the necessary freedom and for providing me with excellent and continuous support during my research work. Furthermore, I would like to thank Dr. Rudolf Seller and Prof. Dr. József Pávó from the Department of Electrical Engineering at the Institute for Broadband Info-communications and Electromagnetic Theory at the Budapest University of Technology and Economics for their expert advice and the many interesting discussions we had together, and especially for the exclusive tutorials that helped me to better understand the physics of high-frequency EM waves and radar terminology, and enabled me to improve my understanding of radar technology applied in automotive radar engineering.

I would also like to express my gratitude to my second supervisor Assoc.-Prof. Dr. Zsolt Szalay for his review and contribution to the success of this doctoral thesis.

To make this work possible, the greatest thanks go to my wife Viktoria, who has supported my work from the beginning to the present day with her unstinting patience and encouragement, and to our daughters Adél-Viktoria, Dóra and Anna, who have had to do without their father so many times while working on this thesis.



# Abstract

Automated driving is being intensively developed for reasons of road safety, driver comfort, efficiency of energy consumption and traffic flow, and the introduction of new mobility concepts. The enormous amount of test kilometres required for safety validation of Advanced Driver Assistance Systems, SAE Level 0-2, and higher-level Automated Driving Functions SAE Level 3-5, demonstrates the need to integrate virtual development. However, virtual test methods for verification and validation of Automated Driving Functions are being developed to reduce testing time and costs, the modelling of machine perception and the proof of its validity are not yet fully solved. Due to the complexity of modelling high-frequency wave propagation, signal processing and perception algorithms, sensor models aiming for a high degree of accuracy are difficult to simulate. Therefore, a variety of different modelling approaches have been presented previously, mainly developed for a specific use case.

The present work focuses on a novel modelling approach for automotive radar sensors to simulate realistic radar point cloud data. The modelling approach aims to provide a real-time, modular, flexible and platform-independent radar sensor model. The presented method uses a semi-physical modelling approach based on experiments. The selected commercial automotive radar was used in road tests where ground truth was recorded with a precise measurement system installed in the ego and target vehicle. Observations of high-frequency phenomena were made and reproduced in the model using physical modeling where possible such as antenna characteristics and the radar equation, otherwise mathematical approximation by deriving suitable error models from the measurements.

The model was evaluated against performance metrics also developed in this thesis and compared to a commercial radar sensor model. The results show that the model achieves remarkable accuracy while maintaining the real-time performance required for X-in-the-loop applications, evaluated against the probability density functions of the radar point clouds and using Jensen-Shannon divergence. The model provides radar cross-section values for the radar point clouds that correlate well with measurements comparable to the Euro-NCAP Global Vehicle Target Validation process.



# Kurzfassung

Die Entwicklung des automatisierten Fahrens wird aus Gründen der Verkehrssicherheit, des Fahrerkomforts, der Effizienz des Energieverbrauchs und des Verkehrsflusses sowie der Einführung neuer Mobilitätskonzepte intensiv vorangetrieben. Die enorme Menge an Testkilometern, die für die Sicherheitsvalidierung von Fahrerassistenzsystemen, SAE Level 0-2, und höherwertigen automatisierten Fahrfunktionen, SAE Level 3-5, erforderlich ist, zeigt die Notwendigkeit, in die virtuelle Entwicklung weiter zu entwickeln. Aktuell werden virtuelle Testmethoden zur Verifizierung und Validierung von automatisierten Fahrfunktionen werden entwickelt um die Testzeit und -kosten zu reduzieren, die Modellierung der maschinellen Wahrnehmung und der Nachweis ihrer Gültigkeit ist jedoch noch nicht vollständig gelöst. Aufgrund der Komplexität der Modellierung der hochfrequenten Wellenausbreitung, der Signalverarbeitung und der Wahrnehmungsalgorithmen sind Sensormodelle, die einen hohen Genauigkeitsgrad anstreben, schwierig zu realisieren. Daher wurde bisher eine Vielzahl unterschiedlicher Modellierungsansätze vorgestellt, die hauptsächlich für einen bestimmten Anwendungsfall entwickelt wurden.

Die vorliegende Arbeit konzentriert sich auf einen neuartigen Modellierungsansatz für automotive-Radarsensoren zur Simulation realistischer Radarpunktwolkendaten. Der Modellierungsansatz zielt darauf ab, ein echtzeitfähiges, modulares, flexibles und plattformunabhängiges Radarsensormodell bereitzustellen. Die vorgestellte Methode verwendet einen semi-physikalischen Modellierungsansatz, der auf Experimenten basiert. Der ausgewählte kommerzielle Radar wurde in Straßentests eingesetzt, bei denen die Ground Truth mit einem präzisen Messsystem aufgezeichnet wurde, das im Ego- und Zielfahrzeug installiert war. Beobachtungen von Hochfrequenzphänomenen wurden durchgeführt und im Modell nachgebildet, wobei nach Möglichkeit physikalische Modelle wie Antenneneigenschaften und die Radargleichung verwendet wurden, andernfalls mathematische Näherungen durch Ableitung geeigneter Fehlermodelle aus den Messungen.

Das Modell wurde anhand von Leistungskennzahlen, die ebenfalls in dieser Arbeit entwickelt wurden, bewertet und mit einem kommerziellen Radarsensormodell verglichen. Die Ergebnisse zeigen, dass das Modell eine bemerkenswerte Genauigkeit und gleichzeitig die für X-in-the-Loop-Anwendungen erforderliche Echtzeitfähigkeit erreicht. Die Prognosefähigkeit des Modells wird anhand der Wahrscheinlichkeitsdichtefunktionen der Radarpunktwolken bewertet und unter Verwendung der Jensen-Shannon-Divergenz. Das Modell liefert Radar Cross Section Werte für die Radarpunktwolken, die gut mit Messungen korrelieren, die mit dem Euro-NCAP Global Vehicle Target Validation Prozess vergleichbar sind.



# List of Publications and Supervised Theses

1. Holder, M., Rosenberger, P., Winner, H., D'hondt, T., Makkapati, V. P., Maier, F. M., Schreiber, H., **Magosi, Z. F.**, Slavik, Z., Bringmann, O., Rosenstiel, W. (2018). Measurements revealing Challenges in Radar Sensor Modeling for Virtual Validation of Autonomous Driving. in 2018 21st International Conference on Intelligent Transportation Systems (ITSC) (S. 2616 - 2622) <https://doi.org/10.1109/ITSC.2018.8569423>
2. Tihanyi, V., Tettamanti, T., Csonthó, M., Eichberger, A., Ficzero, D., Gangel, K., Hörmann, L. B., Klaffenböck, M., Knauder, C., Luley, P., **Magosi, Z. F.**, Magyar, G., Németh, H., Soós, G., Szántay, D., Reckenzaun, J., Remeli, V., Rövid, A., Ruether, M., ... Szalay, Z. (2021). Motorway measurement campaign to support RnD activities in the field of automated driving technologies. *Sensors*, 21(6), 1-35. [2169]. <https://doi.org/10.3390/s21062169>
3. **Magosi, Z. F.**, Li, H., Rosenberger, P., Wan, L., Eichberger, A. (2022). A Survey on Modelling of Automotive Radar Sensors for Virtual Test and Validation of Automated Driving. *Sensors*, 22(15), [5693]. <https://doi.org/10.3390/s22155693>
4. **Magosi, Z. F.**, Eichberger, A. (2022). A novel approach for simulation of automotive radar sensors designed for systematic support of vehicle development. Submitted to journal *Energies* on 07.11.2022
5. **Magosi, Z. F.**, Wellershaus, C., Tihanyi, V., Luley, P., Eichberger, A. (2022). Evaluation methodology for physical radar perception sensor models based on on-road measurements for testing and validation of automated driving. *Energies*, 15(7), [2545]. <https://doi.org/10.3390/en15072545>
6. Bernsteiner, S., **Magosi, Z. F.**, Lindvai-Soos, D., Eichberger, A. (2015). Radar Sensor Model for the Virtual Development Process. *ATZelektronik worldwide*, 10(2), 46–52 (2015). <https://doi.org/10.1007/s38314-015-0521-1>
7. Eichberger, A., Markovic, G., **Magosi, Z. F.**, Rogic, B., Lex, C., Samiee, S. (2017). A Car2X Sensor Model for Virtual Development of Automated Driving. *International Journal of Advanced Robotic Systems*, 14(5). <https://doi.org/10.1177/1729881417725625>
8. Höber, M., Nalic, D., Eichberger, A., Samiee, S., **Magosi, Z. F.**, Payerl, C. (2020). Phenomenological Modelling of Lane Detection Sensors for Validating Performance of Lane Keeping Assist Systems. 899-905. Beitrag in IEEE Intelligent Vehicle Symposium 2020, Virtual, Las Vegas, USA / Vereinigte Staaten. <https://doi.org/10.1109/IV47402.2020.9304832>

9. Babic, D., Babic, D., Fiolic, M., Eichberger, A., **Magosi, Z. F.** (2021). A Comparison of Lane Marking Detection Quality and View Range between Day-time and Night-Time Conditions by Machine Vision. *Energies*, 14(15), [4666]. <https://doi.org/10.3390/en14154666>
10. Li, H., Kanuric, T., Arefnezhad, S., **Magosi, Z. F.**, Wellershaus, C., Babic, D., Babic, D., Tihanyi, V., Eichberger, A., Baunach, M. C. (2021). Phenomenological Modelling of Camera Performance for Road Marking Detection. *Energies*, 15(1), [194]. <https://doi.org/10.3390/en15010194>



### Further Publications not Included in the Thesis

1. Billicsich, S., Tomasch, E., Sinz, W., Eichberger, A., Markovic, G., **Magosi, Z. F.** (2015). Potentieller Einfluss von C2X auf die Vermeidung von Motorradunfällen bzw. Reduktion der Verletzungsschwere. in 10. VDI-Tagung Fahrzeugsicherheit - Sicherheit 2.0 (Band 2265, S. 383-392).
2. Billicsich, S., Tomasch, E., Markovic, G., Eichberger, A., **Magosi, Z. F.** (2016). Evaluation of the impact of C2X systems to the accident severity in motorcycle accidents. *Transportation Research Procedia*, 14, 2129-2137.  
<https://doi.org/10.1016/j.trpro.2016.05.228>
3. Lex, C., Schabauer, M., Semmer, M., Holzinger, J., Schlömicher, T., **Magosi, Z. F.**, Eichberger, A., Koglbauer, I. V. (2017). Objektive Erfassung und subjektive Bewertung menschlicher Trajektorienwahl in einer Naturalistic Driving Study. in *Der Fahrer im 21. Jahrhundert: Der Mensch im Fokus technischer Innovationen* (Band 2311, S. 177-192). (VDI-Berichte; Nr. 2311). Springer-VDI-Verlag GmbH Co.KG. <https://www.vdi-nachrichten.com/shop/der-fahrer-im-21-jahrhundert-6/>

**Master theses co-supervised within the scope of the project:**

Master Thesis 1

**Title:** Generic Radar Model for Automotive Applications

Author: Mario Grgic

Supervisor: Dipl.-Ing.Dr.techn.Markus Neumayer

Co-supervisor: Assoc.-Prof. Dr. Arno Eichberger

Co-supervisor: Zoltan Magosi, MSc

Master Thesis 2

**Title:** Implementation of a Highway Chauffeur in a Virtual Test Environment

Author: Christian Friess

Supervisor: Assoc.-Prof. Dr. Arno Eichberger

Co-supervisor: Zoltan Magosi, MSc

Co-supervisor (MAGNA Steyr Fahrzeugtechnik AG CO&KG): Dr. Stefan  
Bernsteiner

Master Thesis 3

**Title:** Performance assessment of a physical sensor model for Automated Driving

Author: Christoph Wellershaus

Supervisor: Assoc.-Prof. Dr. Arno Eichberger

Co-supervisor: Zoltan Magosi, MSc





# Abbreviations

ACC	Adaptive Cruise Control
AD	Automated Driving
ADAS	Advanced Driver Assistance Systems
ADC	Analog-Digital-Converter
ADF	Automated Driving Functions
ADMA	Automotive Dynamic Motion Analyzer product from GeneSys GmbH
ARA	Amplitude Range Azimuth
ARS-308	Continental Automotive Radar Sensor of series 3xx
CA-CFAR	Cell Averaging Continuous False Alarm Rate
CAN	Controller Area Network
CFAR	Continuous False Alarm Rate
CPI	Coherent Process Interval
DAU	Data Acquisition Unit
DFM	Doppler Frequency Migration
DFT	Discrete Fourier Transform
DGPS	Differential-GPS
DGT-SMV	Dynamic Ground Truth - Sensor Model Validation
DiL	Driver-in-the-Loop
EC	Environment Components
EM	Electromagnetic
Euro-NCAP	European New Car Assessment Program
FFT	Fast Fourier Transform
FMCW	Frequency Modulated Continuous Wave
FOV	Field Of View
FPGA	Field Programmable Gate Array
GNSS	Global Navigation Satellite System
GSM	Global System for Mobile Communications
GT	Ground Truth
GVT	Global Vehicle Target
HF	High-frequency
HiL	Hardware-in-the-Loop
HMI	Human Machine Interface
HW/SW	Hardware/Software
I&Q	In-phase and Quadratic-phase
IMU	Inertial Measurement Unit
ISO	International Organisation for Standardisation
JSD	Jensen-Shannon Divergence
KDE	Kernel Density Estimation
KLD	Kullback-Leibler Divergence
LOS	Line Of Sight
LTI	Linear Time-Invariant
MBSE	Multi-Body Simulation Environment

MiL	Model-in-the-Loop
NCAP	New Car Assessment Program
NHTSA	National Highway Traffic Safety Administration
OEM	Original Equipment Manufacturer
OS-CFAR	Ordered Statistic Continuous False Alarm Rate
OTA	Over-The-Air
PDF	Probability Density Function
PiL	Processor-in-the-Loop
PPS	Pulse per second
RA	Range-Azimuth
RCS	Radar Cross Section
RD	Range Doppler detection
RSI	Raw Signal Interface
RTK-GPS	Real Time Kinematics/Global Positioning System
RUS	Radar-Under-Simulation
Rx/Tx	Receiver/Transceiver
SAE	Society of automotive Engineers
SB	Space Bin
SBI	SB-Indicator
SiL	Software-in-the-Loop
SNR	Signal-to-Noise Ratio
UN-ECE	United Nations Economic Commission for Europe
V&V	Validation (of intended use) and Verification (of requirements)
ViL	Vehicle-in-the-Loop







## List of symbols

$g_s(r_s, \vartheta_s, \phi_s)$	Impulse response of a point scatterer
$s$	Point scatterer
$r_s$	Distance at the point scatterer is located
$\vartheta_s$	Angular position in elevation direction
$\phi_s$	Angular position in azimuth direction
$D(r_s, \vartheta_s, \phi_s)$	Antenna directivity
$R(r_s, \vartheta_s, \phi_s)$	Path loss
$F(r_s, \vartheta_s, \phi_s)$	Propagation factor (the letter $F$ is also used for the receiver noise figure in radar literature)
$k_\lambda$	Wave number
$P_{Tx}$	Transmitted power
$P_{Rx}$	Received power
$g_{sP}(r_s, \vartheta_s, \phi_s)$	Power related impulse response
$\lambda_c$	wavelength of the carrier frequency
$G_0$	Realised antenna gain
$G_{Tx}$	Gain of transmitter antenna
$G_{Rx}$	Gain of receiver antenna
$\sigma_s$	Reflection coefficient of the point scatterer
$A$	Amplitude
$\epsilon_0$	Permittivity of the vacuum
$c$	Speed of light
$\Gamma$	Complex Fresnel reflection coefficient
$\Gamma_0$	Smooth earth reflection coefficient
$R_0$	Minimum detection range of the real radar
$\tau$	Rate constant
$\Delta R$	Difference in range between the direct path and the reflected path
$\rho_s$	Specular roughness factor
$\rho_d$	Diffuse roughness factor
$\sigma_{SBI}$	Reflection coefficient of one resolution cell
$N_{CPI_{Tx}}$	Number of required pulses for a given velocity resolution
$SBI$	Space-Bin indicator
$\mu\text{Doppler}$	Micro-Doppler
$B$	Receiver bandwidth
$P_n$	Power of the thermal noise
$k$	Boltzmann's constant
$T_0$	Ambient temperature (290 K)
$F$	Receiver noise figure (the letter $F$ is also used for the propagation factor in radar literature)
$\mathcal{P}_{ref}(x, y)$	Reference point on the target vehicle
$\zeta_r$	Vector represents the measured sensor data
$\zeta_s$	Vector represents the simulated sensor data
$\zeta_{s,\Delta}$	Deviation of the simulation data to the reference point
$\zeta_{r,\Delta}$	Deviation of the real sensor data to the reference point
$\mathcal{P}$	True discrete probability distribution
$\mathcal{Q}$	Approximation of $\mathcal{P}$



# 1. Introduction

## 1.1. Motivation

The automation of driving is being intensively pursued, as assisting the human driver in complex traffic situations can bring advantages from various points of view. Automated vehicles can significantly increase road safety and driving comfort by transferring some or all driving tasks to automated driving systems. Vehicles with a higher level of automation SAE Level 3-5 could provide access to mobility for population groups that are unable or not authorised to drive conventional vehicles. In addition to the social benefits, the expected economic improvements in terms of more efficient energy consumption and more balanced traffic flow are also driving the development of automated driving functions. As the development of motor vehicles and the market introduction of their functions are subject to strict legislation and validation measures, the validation and verification (V&V) activities of the automotive industry are closely linked to the regulatory framework. The concept of V&V is to find an appropriate way to determine whether a product, function, system or subsystem meets or complies with safety requirements, specifications and regulations. A comprehensive V&V methodology is required to ensure that the complex vehicle system functions safely in an unsafe traffic environment. The need for virtual development for safety validation of Advanced Driver Assistance Systems (ADAS), SAE Level 0-2, and higher-level Automated Driving Functions (ADF), SAE Level 3-5, has coincided with the dramatic increase in on-road test mileage. Among others, Kalra et al. quantified. [53] the total amount of test miles required for safety validation, citing values ranging from 1.6 million to 11 billion miles, depending on the question answered in a statistical survey. Testing components, functions or the entire vehicle in virtual space can bring benefits from various perspectives. From a safety perspective, for example, tests that pose a risk to the test subject or the test environment can be conducted safely and repeatedly. From a cost perspective, every test kilometre in virtual space saves manufacturers money, not to mention reducing environmental impact. The required integration of virtual models (vehicle, tyres, engine, etc.) into the vehicle development process has therefore led to the systematic use of simulation techniques that make it possible to virtually prove the correctness of the system concept already in the requirements analysis phase. As a result, perceptual sensor models have also been developed and implemented in a modern simulation tool that enables virtually based V&V of ADAS and ADFs also at the whole vehicle level. However, there is still a significant discrepancy between the results of real sensors and the results of most sensor models in terms of all possible effects that occur during signal propagation and processing, such as due to tyre splash or multipath propagation. However, it should be noted at this point that for efficient simulations, models with varying degrees of realistic representation

must be used, depending on the stage of development and the specific use case.

### 1.2. Research objectives

Despite the progress in driving automation, the market introduction of the higher level of automation has not yet been successful. One of the main reasons for this is the effort required for safety validation to prove functional safety to the customer. Virtual testing can compensate for this challenge, but the modelling of machine perception and the proof of its validity have not yet been fully solved. The present work deals with the development of a novel modelling approach for automotive radar sensors. Due to the complex high frequency physics and the corresponding signal processing and perception algorithms of automotive radar sensor, the modelling and parameterisation of virtual perception sensor models for vehicle development is challenging. Furthermore, depending on the stage of vehicle development, sensor models of varying complexity and accuracy in terms of efficiency and already implemented functions are required for testing. Consequently, a variety of different modelling approaches have been reported in the literature over the last two decades. In order to understand and categorise the heterogeneous state of the art in radar sensor modelling, an extensive literature review and survey comprehensively summarises the simulation techniques and methods. Instead of a methodology-oriented classification of the works reviewed so far, a novel classification method from the system integrator's perspective is presented on how these models can be applied in vehicle development using the V-model. Sensor models are thus divided into operational, functional, technical and individual models. The sensor modelling method presented here is based on the findings from the literature review and applies a semi-physical modelling approach based on experiments with a real radar sensor with an open data interface. The selected commercial automotive radar was used in on-road tests where ground truth was also recorded. This requires a complex measurement system that enables highly precise positioning of the test vehicles and synchronised recording of all sensor data. The development of automotive radar technology, including hardware and software components, are special fields of high-frequency technology and form market advantages for radar manufacturers. The concrete technologies, hardware and software solutions used are therefore heavily protected by copyright and are not available to the public. Therefore, no manufacturer-specific information and parameters were used for the modelling, with the exception of the parameters described in the data sheet of the sensor itself. The aim is to determine the relationship between the input and output variables as well as other influencing parameters for the system to be simulated in order to incorporate this a priori knowledge into the model development. Since the required model fidelity can vary in the different phases of vehicle development depending on the V-model, the input-output relationship also changes accordingly. In order to quantitatively measure and determine the extent of required model fidelity, this thesis also develops a practical procedure that enables a systematic assessment for perceptual sensor models on a low-level data basis. The validation framework includes firstly performing test drives on a test site where the Digital-Twin is also

available, secondly re-simulating these test drives based on the highly accurate vehicle position and dynamic state information using the provided Digital-Twin, and thirdly comparing the measured and simulated perceptual sensor outputs with statistical metrics.

### 1.3. Structure of the thesis

The present work focuses on the development of a modelling approach for the presented radar sensor model based on on-road measurements and experiments, as well as on the development of methods that allow a quantitative evaluation of perceptual sensor models. The remaining part of the thesis is structured as follows:

*Chapter 2* provides an overview of the State-of-the-Art in radar sensor models and modeling approaches. Section 2.1 summarises the challenges in motor vehicle testing procedures, which are divided into three phases according to the vehicle development life cycle, starting with vehicle development phase introduced in Section 2.2, followed by type-approval activities in Section 2.3 and ending with testing activities carried out by consumer protection organisations in Section 2.4. Section 2.5 introduces the vehicle development process and the usage of sensor models, Section 2.6 gives an overview of previous survey in radar sensor modelling, Section 2.7 introduces a new classification approach that is more useful for selection of the appropriate modelling approach. This chapter is closed with Section 2.8, which introduces a summary of the research contribution.

*Chapter 3* introduces the model development process flow in Section 3.1 and procedure in Section 3.2 by summarising the main development phases, discussed in detail in the following chapter.

*Chapter 4* describes in detail the development of the mobile measurement system in Section 4.1 implemented in test vehicles for providing ground truth (GT) information. Section 4.2 introduces the radar sensor model development method and describes in detail the mathematical and physical approach of the sensor model. In addition Section 4.3 presents the evaluation methodology including the digital twin of the driving environment, the vehicle and the assessment approach. Based on the measurement, applied on the modelling approach evaluated with the assessment tool described in this thesis.

*Chapter 5* presents the results. In Section 5.1 the outcome of the extensive literature review is presented. Section 5.2 presents the result of the development of the method used to define the modelling approach to realistically simulate a real automotive radar sensor. Section 5.3 shows the result of the method used to define driving manoeuvres by means of an example. In the following Sections 5.4 and 5.5, the combined results of the development of the radar sensor model and the evaluation methodology are presented in the form of Matlab diagrams using the driving manoeuvre as an example. The results are presented both in graphical form to illustrate the applicability of the visual evaluation and in tabular form to illustrate the informative value of the metric evaluation, discussed in Section 5.6.

*Chapter 6* summarises the key findings, the methods developed and the result presented in this thesis.

## 2. State of the Art

### 2.1. The Challenge in Automotive Testing

In recent years, more and more advanced features have been incorporated into vehicles. The robustness and reliability of these systems is highly dependent on their sensing capabilities, their processing of complex perception algorithms and their operation by electrical and/or electronic systems. The testing and validation activities for such distributed systems are already a complex task and are closely related to various national and international laws, regulations and industry standards. Szalay et al. identify in [99] three different areas of automotive testing activities according to the life cycle management process of automotive products. Figure 2.1 illustrates these different phases of vehicle development, which will be explained in the next sections. We therefore assume that the modelling approaches for radar sensors must differ in the different product development phases.

### 2.2. Vehicle Development Phase

In the first phase of the product life cycle, manufacturers are responsible for developing safe, reliable and well-functioning vehicles. The basic legal framework for the development of vehicles or safety-critical systems is laid down in product liability law. Product liability requires that the product placed on the market must provide adequate safety and must be developed according to the state of the art. These methods are laid down in national and international standards maintained by the International Organisation for Standardisation (ISO) and/or national standardisation bodies. The main objective of standardisation work is to ensure the comparability and consistency of analysis results carried out independently by different companies [18]. In the automotive industry, development processes are carried out according to the V-model proposed in ISO-26262 [48]. This approach

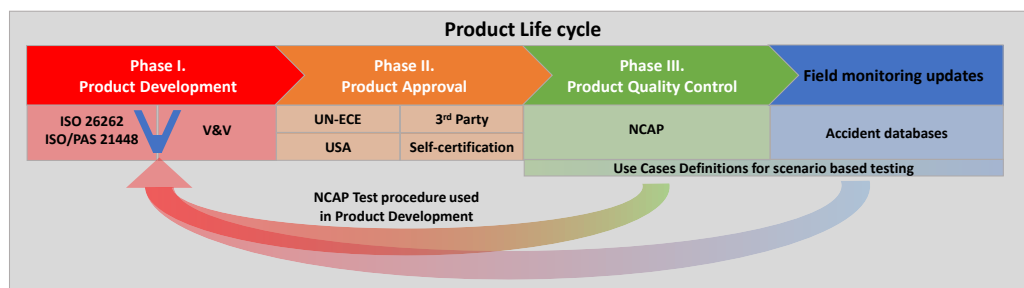


Figure 2.1.: Automotive product life cycle phases related to V&V of safety.

defines the system requirements in parallel with their verification and validation throughout the development process, including the software and hardware development phases with the corresponding test activities, in particular the various X-in-the-loop test solutions. Standardised test and validation methods are only available for driver assistant systems with lower levels of automation (SAE Level 0-2).

Requirements are usually set at the vehicle level; for longitudinal control, these are defined for adaptive cruise control (ACC) in ISO-15622 [43] and for autonomous emergency braking (AEB) in ISO-22733 [47]. For lateral guidance, there are standards for lane departure warning (LDW) systems in ISO-17361 [44], for lane change decision aids systems (LCDAS) in ISO-17387 [45], for partially automated lane change systems (PALS) in ISO-21202 [46], and for lane keeping assistance systems (LKAS) in ISO-11270 [42].

### 2.3. Type Approval Phase

In the second phase of the product life cycle, vehicles are brought to market. If an automobile manufacturer wishes to market its product in Europe, it must meet the requirements of the United Nations Economic Commission for Europe (UN-ECE) in a process known as type approval (or homologation). In type approval, vehicles are tested by an independent third party (e.g., TÜV, Dekra), and approval is granted by the authorities. In contrast, there is also the process of self-certification (e.g., in the U.S.), in which the vehicle manufacturer analyses and certifies the safety strategy through a voluntary safety self-assessment to confirm that the product meets market requirements [99]. The criticality of these testing activities is much higher than for feature development. The reason is that if type approval/homologation is successful, the vehicle is deemed safe by the authority and therefore must meet the authority's specifications and the public's expectations [18]. For longitudinal control, type approval is specified in UN-ECE R 131 for the advanced emergency braking system (AEBS) [102] and for lateral control in UN-ECE R 157 [103] for the automated lane keeping system (ALKS).

### 2.4. Consumer Protection Phase

In the third phase of the product life cycle, products are already on the market and consumer organizations demonstrate the quality of the product to protect consumers from the risk of unfair commercial interactions. In the automotive industry, the New Car Assessment Program (NCAP) is one of the best-known consumer protection organizations [99]. It was established in the late 1970s by the U.S. National Highway Traffic Safety Administration (NHTSA) and focuses on testing the major operating and safety systems of motor vehicles. Later, NCAPs were adopted by the automotive industry in other parts of the world, such as the European New Car Assessment Program (Euro-NCAP), the Japanese New Car Assessment Program (JNCAP), and the Chinese New Car Assessment Program (C-NCAP) [41]. Euro-NCAP's test protocols, developed based on real-world accident scenarios,



are not just a test and evaluation procedure for the final product. The automotive industry also uses them as a tool to directly improve safety by incorporating them into the vehicle development process. By virtually performing NCAP test evaluation protocols with various simulation methods, development engineers can elaborate and verify the vehicle's perception strategy in a time- and cost-efficient manner at an early stage of development, during the concept phase. They also provide a good basis for functional testing of software and hardware prototypes on Hardware-in-the-Loop test benches in later development phases [108].

### 2.5. Vehicle Development Process

The inherent complexity of modern systems is increasing significantly. Consequently, the system development process and verification and validation activities are becoming increasingly complex. In order to cope with this major challenge, suitable development processes have been introduced. Combining these with appropriate simulation techniques, different system designs can be evaluated and the number of physical prototypes can be reduced. The increasing complexity of modern vehicle systems requires a modular system design, both in terms of the integrated hardware components and the algorithms running on them. This means that the operation and correct behaviour of the system depend on the interactions between the modules and the content and quality of their input and output information. Therefore, it is becoming increasingly important to test and evaluate the entire system in its intended operating environment. Traditional system design methods address this complexity problem by providing appropriate process models that contain detailed specifications of all components as well as the overall system with all relevant interfaces and relationships. The product development method currently used in the automotive industry is based on the V-model as proposed in the ISO-26262 standard [48] (see Figure 2.2).

Product development starts with a hierarchical top-down analysis and design phase, followed by implementation and a reverse bottom-up integration and test phase. Test tools corresponding to the development phases, such as Model-in-the-Loop (MiL), Software-in-the-Loop (SiL), Processor-in-the-Loop (PiL) and Hardware-in-the-Loop (HiL) simulations, are also provided. The development of modern systems requires the integration of many disciplines, leading to a need for standardised interfaces and coordination between the standard methods of the disciplines involved [15]. To meet this challenge, the methodology of model-based systems engineering (MBSE) plays an increasingly important role in system design, that is, the formalised application of modelling to support the entire development process at all levels of abstraction [87]. The integration of virtual models into the vehicle development process has led to the systematic use of simulation techniques that enable virtually based V&V to prove the correctness of the system already in the requirements analysis phase. One of the key points of this methodology is the V&V concept, as different models of varying complexity can be used for the V&V activities in the different phases of the product development cycle, depending on their complexity. Once the complete system is designed, specified, and verified, it can be

## 2. State of the Art

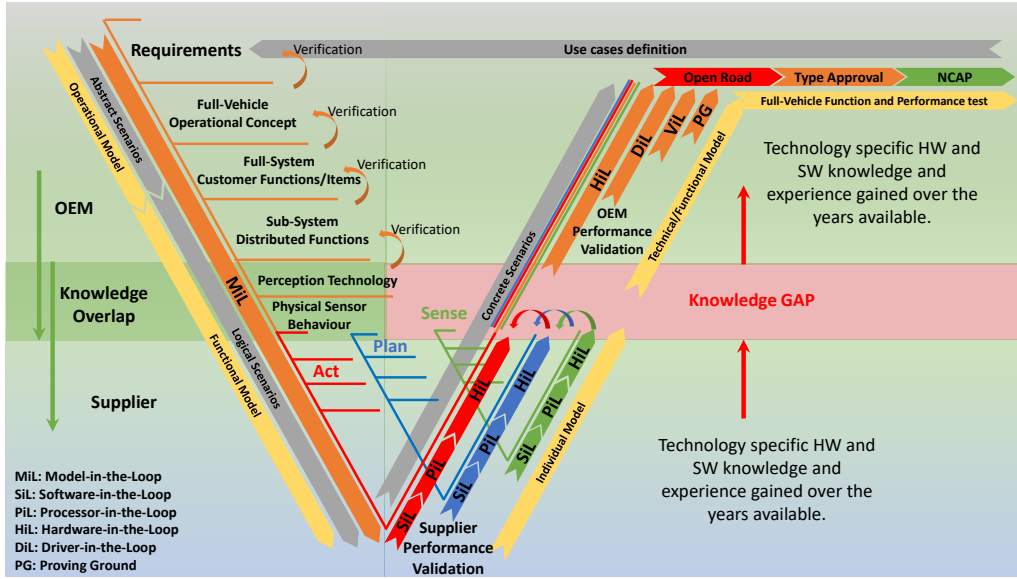


Figure 2.2.: Vehicle development process with respect to driving automation.

implemented, integrated, and validated. The validation processes are designed to ensure that all requirements arising from the 'safety by engineering' strategy along the left-hand side of the V-model in a decreasing direction are met, that known scenarios are covered, and that the system behaves as specified. In the validation processes, which represent the right side of the V-model, the verified system is tested using well-defined test methods in an ascending direction to confirm that the system meets all safety design requirements and behaves as intended and specified.

In order to validate the safety of the intended functions and systems, the vehicles are tested in all phases of development using a variety of predefined realistic test scenarios in virtual and real traffic. A number of validation tools are already defined in the standards mentioned above, such as SiL and HiL. At the level of the complete vehicle, real test drives are performed on the proving ground, but also on public roads, to ensure that the systems function properly in road traffic. Combining simulations in the above context with tests at the vehicle level is intended to establish statistical confidence in operational safety. As specified in the ISO/PAS-21448 Safety of the Intended Functionality [50] and ISO-26262 Functional Safety standards, once the vehicle with ADFs is on the market, the safety of the system will be continuously monitored through field operational test (FOT) by collecting and analysing anonymous data from the field during on-road testing.

Figure 2.2 also illustrates that there is a knowledge gap in V&V of automotive radar sensor based systems in the phase where there is a hand-over from the system supplier to the vehicle's original equipment manufacturer (OEM). It also includes a proposal of which overall modelling approaches (operational, functional, individual and technical modelling) are appropriate in the different phases. These approaches will be explained in Section 2.7.

## 2.6. State-of-the-Art Radar Sensor Modelling Approaches

In recent years, many different approaches to modelling radar sensor systems have been developed. An early example of radar sensor modelling can be found in [59], from 1990. There are a number of different approaches to generating synthetic radar data. The authors in [69] distinguish between ideal models, probabilistic models, and physics-based models. They also distinguish three fidelity levels for sensor models with increasing complexity: low-fidelity models, medium-fidelity models, and high-fidelity models [86]. Ideal sensor models simply generate ground truth data for objects in the sensor's detection range. This allows sensor-type-specific object list information to be generated for all objects in the sensor's field of view (FOV). In contrast to ideal sensor models, physics-based sensor models attempt to model the physical sensing process of the real sensor as accurately as possible. They are computationally intensive and require more computational power, often at the expense of real-time capability. In addition to the required expertise in sensor technology, a detailed description of the environmental conditions (material properties, weather conditions, etc.) is required to accurately model the physics of the sensor. The simulated output data from these models can be a raw analog signal comparable to that of the real sensor. As suggested in [70, 89], the use of probabilistic sensor models can provide a reasonable trade-off between complexity and computational efficiency. The simplified parameter set and reduced model complexity allow simulation tests to be performed faster than real time. The output of these models can be set up to provide object lists or even raw data. Even though the output data is less realistic compared to the real sensor, phenomenological models can be used at most levels of the development process to test and validate the safety of the vehicles with ADFs.

Rosenberger et al. in [81] distinguish between ground truth models that neglect any operation on the GT object list except for the transformation from world to sensor origin coordinates, idealised models that additionally cut out the FOV of the sensor from the object list, and phenomenological models that consist of stochastic and physical model parts. In radar modelling, this could mean that a ray tracing approach to physical modelling of signal propagation is accompanied by a stochastic Gaussian noise model. While pure stochastic modelling is often applied in sensor models for high-level object list output, pure physical modelling is almost completely avoided in scenario-based simulation due to the computational time required for such finite element method (FEM) simulation or the like.

In [52], the author categorises sensor models into three groups, defined as ideal, physical, and functional. Ideal sensor models directly read any measurable objects or GT information provided in the virtual environment without including any real sensor-related uncertainty. In contrast, physical models or white-box models implement the real physical sensor properties, but at the expense of real-time simulation performance. The functional model ignores the sensor hardware architecture and signal processing process. Such a black-box model focuses only on the detection result of the measured object. This type of sensor model can be implemented by combining certain geometric and selected physical properties. This improves the real-time performance of the sensor simulation without completely

ignoring the detection limits and characteristics of the real sensor.

Similarly, in [28], sensor models are classified as function-based, physics-based, or a combination of both. For simplicity and real-time capability, the function-based modelling approach includes geometric models and models dealing with scattering centres. The physics-based approach has been divided into two classes, one dealing with modelling the electronic components of the radar sensor, including the propagation channel modelled by ray-tracing techniques. The other approach considers radar and clutter echoes as well as noise. Another approach is presented that distinguishes between a radar model and a radar system model, where the radar system model includes the environment and the target vehicle model in addition to the radar model.

Holder et al., in [38], distinguish three groups of sensor models and define them as follows. The ideal sensor models generally generate a list of perfectly sensed objects from the simulation environment, that is, they do not model sensing errors. These are followed by phenomenological sensor models that already take into account additional sensor properties such as the FOV of the sensor, limited resolution, and measurement uncertainties [4, 33]. Finally, physical sensor models aim to reproduce the raw sensor data by modelling the physical phenomena specific to the sensor being modelled. The authors in [27, 106, 51] provide an assessment of radar sensor models in the literature, based on some predefined modelling criteria, with the goal of helping the modeller estimate the effort required to create such models. Based on their defined criteria, radar sensor models can be classified into three categories. In the physical sensor model, called the white-box model, all physical aspects of the radar are considered and calculated based on a detailed description of the environment [28, 57, 34]. The scattering centre sensor models exploit the property, known from radar cross-section (RCS) studies, that electromagnetic scattering from an electrically large target can be approximated by a sparse set of points at a fixed position on the target, called scattering centres (SC) [65, 5, 92]. Data-driven or black-box models do not require information about the behaviour of the radar and can only learn its operation based on recorded data from real experiments [35, 85, 106].

Schlager et al. [86] determine the accuracy of a sensor model based on its inputs, outputs, and modelling principle. Low-fidelity sensor models are based on geometric aspects such as the sensor-specific FOV and object occlusion. The input data format is object lists with ground truth information, and the output data format is also object lists but with filtered GT information [29]. Medium-fidelity sensor models take into account some physical aspects of the real sensor and material properties of the objects, as well as the sensor's field of view and detection probability. The input for medium-fidelity sensor models are object lists corresponding to ground truth. The output data formats are object lists or raw data processed, according to the modelled perceptual effects [8]. High-fidelity sensor models are the most accurate representations of real-world sensors. They incorporate rendering methods such as rasterisation or ray tracing. They combine environmental parameters and material properties as well as physical effects such as diffraction and interference. High-fidelity sensor models use the entire 3D virtual environment, a mesh grid describing objects and their surfaces, as input and

produce sensor-specific raw data as output [39].

Cao et al. [9] introduced the white-box, grey-box, and black-box classifications for sensor models. Black-box models can be used for system function verification but not for validation. White-box modelling is the simulation of electromagnetic wave propagation by solving Maxwell's equations, simulating semiconductor components and the propagation channel. Grey-box modelling is an effective combination of the above models in terms of complexity and real-time capability.

Ngo et al. [72] distinguish time-domain electromagnetic simulation techniques, ray tracing, data-driven, and idealised modelling approaches. They describe a method for evaluating a radar sensor model by comparing the results of clustering algorithms with real and synthetic radar data and provide a sensitivity analysis for the various parameters of their radar sensor model.

In a later publication, Ngo et al. [71] describe common sensor model categorisation into physics-based, probabilistic, and phenomenological. They also describe the expansion stages of their radar models, which are later used to demonstrate their multi-layer model validation study: ideal radar model (IRM), data-driven model (DDM), and ray-tracing-based model (RTM).

Holder in [40] classifies sensor models according to the information flow in the simulation, the model input (I) and output (O), and the error modelling in between. Six levels are distinguished along this path. The model input can be vectorised information such as an object list (O) or rendering (R). The output is distinguished between object list (O), detections (D), or raw data (R). With these abbreviations, a naming scheme is provided from a combination of them: for example, object in object out (OIOO) or rendering in detection out (RIDO), and so on.

To be able to test radar sensors under laboratory conditions, the virtual world can be combined with real hardware components in a special HiL test field that enables the stimulation of radar sensors [16]. Advances in analogue and digital millimetre-wave signal processing technology already offer powerful real-time radar target stimulators that complement the X-in-the-loop test portfolio and can precisely stimulate the radar signature of real targets represented by point scatterers. The general operating principle is that the receiver mixes the received radar signal into the baseband, digitises the baseband frequency signal, modifies the waveform on one or more field programmable gate arrays (FPGA), and converts it into an analog signal. Possible signal modifications include amplitude and phase changes, time delays, and frequency shifts. Finally, the mixed radar echo is transmitted back over the air at the transmitter end. In [26], an HiL approach is used that emulates a virtual radar environment corresponding to a defined test scenario. The relevant test scenarios are parameterised and then mapped to the antennas of the target stimulator.

A radar HiL test approach based on over-the-air (OTA) stimulation can be found in [96, 112]. In [112], a simulation platform is developed using multi-body simulation (MBS) software to combine traffic and scenario simulations. The radar echoes are mixed with Gaussian noise to improve the realism of the test. Based on the flexibility and scalability of available high-frequency hardware components combined with MBS, the authors presented a whole-vehicle-level testbed based on OTA radar target stimulation in [11, 17, 24]. In [2], a dynamic OTA radar

stimulator is demonstrated. The system provides the illuminated antennas with three degrees of freedom of motion to simulate more complex scenarios with different angular positions of the target vehicle. The authors in [60] calculate the radar characteristics using theoretical formulations and implement them in FPGA hardware components to produce even more realistic radar echoes. Another ViL test method based on the OTA radar target stimulation approach is presented in [64]. The ambient perception simulation is based on statistical distributions and the radar signature of the target is estimated as a function of the target vehicle dynamics. In addition to the aforementioned development and research systems, radar target stimulators are also used in series production as end-of-line (EOL) test equipment.

The commercially available integration and test platform CarMaker of IPG Automotive GmbH [49] classifies sensor models into three groups: Ideal, High-Fidelity (HiFi) and Raw Signal Interface (RSI) [32]. Ideal sensor models represent a generic interface. Object information can be accessed within the defined sensor range, and the model is technology-independent. High-fidelity models correspond to phenomenological sensor models and provide a higher level of detail than ideal models. They use ideal environmental information and overlay it with technology-dependent effects known from theory and measurements. Physical models with an RSI account for actual signal propagation. This includes the main physical effects involving the interaction of the signal with objects in the simulation and the transmission media along the propagation path.

Furthermore, most simulation tools provide different interfaces for sensor modelling with varying complexity [32]. We used the definition given in [90], which describes the complexity of the model as follows:

The ground truth model contains all information about all objects within the search radius. The geometric models take into account some basic information from the sensor's data sheet and map the detection area and field of view. The stochastic models assume some uncertainty in the detection probability and provide parallel measurements with artificially generated noise. The most complex models for perceptual sensors are physics-based models that use the physical properties of the object, wave propagation, and reflections. From the point of view of computational requirements and reduced parameter space, phenomenological models are a good alternative since mathematical methods can be used to simulate a sensor-specific phenomenon. This classification, presented in Figure 2.3, serves as the basis for a classification more focused on vehicle development applications, as described below.

### 2.7. Classification from the System Integrator's Perspective

Modeling the performance of perceptual sensors at different levels of abstraction in the development process is critical because it provides a preliminary estimate of sensing capabilities, enabling the development and verification of different sensing strategies that are essential for automated driving functions [31]. The radar sensor models available in the literature have been studied extensively by researchers and, as described earlier, have been classified into many different categories.

Modern X-in-the-loop test methods for verifying and validating the safety of

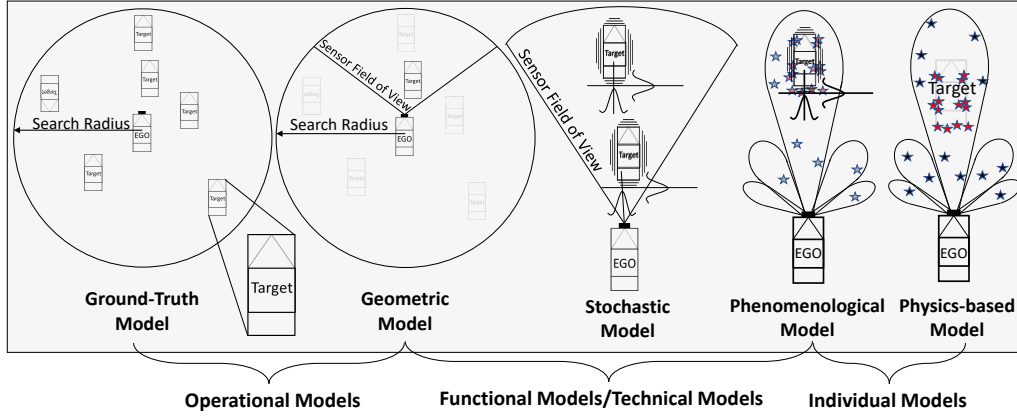


Figure 2.3.: Sensor modelling approaches

ADFs range from field tests to simulation of all subcomponents of the complete vehicle. Due to the high complexity of an ADS, test activities are shifted to the virtual test domain by replacing one or more physical components with an appropriate simulation model [70, 109]. The scenario-based method can be applied to the X-in-the-loop testing methodology throughout the development process described in Section 2.5 because the scenario description is based on different levels of abstraction or detail. Our motivation to introduce a new naming convention for the state-of-the-art radar sensor models is based on the scenario abstraction levels [67] and the X-in-the-loop test methods [6], which are jointly mapped to the phases of the development process represented in the V-model [93].

We have also defined two prerequisites: First, that the automotive manufacturer involves an DAS/ADS supplier with specialised knowledge and unique experience in the field of environmental perception sensing at the subsystem or at least component level. Second, radar sensor models with a more detailed output data level than object lists, such as target/cluster lists or raw signals, cannot be integrated into the vehicle development process by automotive manufacturers due to a lack of technological knowledge and hardware resources appropriate to high-frequency (77–79 GHz) automotive radar technology. It is assumed that these models are more likely to be used on the supplier side.

In increasing order of complexity, we introduce *operational models*, *functional models*, *technical models*, and *individual models*. The application of the different models in the vehicle development process is illustrated in Figure 2.2 and described below.

Following the V-model, the sequence of development phases is: operational → functional → individual → technical → functional. For OEMs, however, only the operational, functional, technical, and functional radar sensor models can be used. After applying the technical models in HiL testing at the component and sub-system level, functional models can be reused for Driver-in-the-Loop (DiL) and Vehicle-in-the-Loop (ViL) testing, for example, for testing the human-machine interface (HMI).

### 2.7.1. Operational Model

#### Definition

The term operational means “*in or ready for use*”; ground truth and geometric models are considered. In the concept phase, simplified sensor models can be used to specify the perception concept of the automated driving system. For example, it must be determined which areas of the vehicle environment are to be perceived and at what distance objects must be detected. For this purpose, typical sensor properties such as sensor FOV, detection range, and so on can be modelled easily and quickly even without specific knowledge of perception sensor technology.

#### Application

The automotive industry has a wide range of simulation tools to support the development process and to accelerate V&V test activities. In the concept phase, simplified sensor models can be used to specify the perception concept of the automated driving system. For example, it must be determined which areas of the vehicle environment are to be perceived and at what distance objects must be detected. In the further course of development, sensor models can support the selection of the sensor technology to be used for the automated driving system (radar, lidar, camera, etc.). For this purpose, typical sensor characteristics such as sensor FOV, detection range, and so on can be modelled. With the ability to generate the GT for each simulation step, all of these modern simulation tools have easy-to-parameterise, built-in, and technology-independent generic sensor models. These models are often referred to as idealised or geometric models and provide object lists as output data. As examples, we mention some products that are widely used in the automotive industry: in [58], TwT GmbH, TASS-PreScan, dSpace-ASM; in [31], TESIS Dyna4-Driver Assistance, MathWorks-ADAS Toolbox; in [82], CARLA, AirSim, DeepDrive, Udacity, Constellation, Helios, GLIDAR, RADSim, SIMSonic; and in [68], CarMaker from IPG Automotive GmbH, VIREs-VTD, CARLA, and AirSim can provide GT information.

In vehicle development, *operational models* are used in the descending branch of the V-model, in the early stage where the operational concept of the vehicle is tested with abstract scenarios against the requirements (see also Figure 2.2).

### 2.7.2. Functional Models

#### Definition

The term functional means “*of or having a special activity, purpose, or task*”. Stochastic, phenomenological, and data-driven models are being considered with increasing attention. Given a particular sensor technology, such as the radar sensor, a functional representation of the acquisition process can be modelled by simulating the antenna properties with a simple cone and a complex target with a cuboid. Discretised scatterers can then be generated from the object, which can additionally be overlaid with noise to provide a more realistic object list. To accommodate different design considerations, the complexity can vary over a wide range. These models may



require moderate sensor-specific knowledge to realise realistic behaviour with a reduced parameter space.

### Application

The output of a *functional model* usually does not deal with the internal processes or algorithms of the real sensor, but focuses on reproducing the effects that distinguish the sensor output from the reference data. Unlike *operational models*, *functional models* already contain more information and details about the real sensor properties. The authors in [33, 35] illustrate this point that a non-parametric modelling approach is able to model sensor range, occlusion, latency, ghost objects, and object loss without explicit programming, and can be used efficiently in real-time simulation. The same concept is developed in [4, 12], where the geometric information of the target is transformed into the sensor model, and then the signal noise and statistically based signal loss are superimposed on the original signal. The method described above has provided good estimation and modelling of relative distance, velocity, and other sensor-specific information. The data-driven approach requires a large number of experiments to obtain a statistical distribution that can be applied by the model. However, in the real world, there are often crucial parameters that affect the detection results, and a given statistical distribution may not do justice to the sensor's detection performance. Therefore, a data-driven approach based on machine learning is introduced. In the work of [68], different ML methods are investigated and used to build RCS models, demonstrating that better prediction accuracy can be achieved with ML models. In addition to data-driven methods, geometric-based approaches are also commonly used for radar feature modelling. The geometric approach focuses more on the specific details of the target and models according to the statistics of the reflection points at different locations on the surface of the target to create the sensor-specific object list.

In vehicle development, *functional models* are used in the descending branch of the V-model after the use of *operational models*, but can also be reused in the ascending branch after the use of *technical models*. For more detailed logical scenarios, *functional models* can be used at the subsystem level in the design phase to produce sensor-technology-specific outputs that are used as inputs to a sensor fusion algorithm. In addition, the models can be used to verify that real sensors meet the requirements of the system specifications. The Figure shows that *functional models* can be used not only for verification purposes in the design phase, but also in the ascending branch of the V-model in the integration phase for testing. Since *functional models* are expected to perform their task in real time or even faster than real time, they can replace the real sensors for functional testing of the vehicle's HMI in DiL testing or for testing some vehicle functions at the system level in ViL testing methods.

### 2.7.3. Technical Models

#### Definition

"Involving or concerned with applied and industrial sciences", models for over-the-air target stimulator testbeds are considered. This group of radar sensor models includes

models developed for a specific well-defined high-frequency radar target stimulator. These models have much lower performance compared to their simulation-only counterparts and are developed according to the available hardware components. These models typically provide only radial range, angular position, radial range rate, or velocity, as well as radar-cross-section information for radar signature generation in the form of a point target.

### Application

*Technical models* provide object lists with reduced content to represent a radar signature, usually in the form of a point target. The model output is the input data for a particular radar target stimulator high-frequency HiL testbed. A typical radar signature consists of: Doppler shift  $f_d$  due to relative velocity, range in the form of propagation delay  $\Delta t$ , spatial direction (azimuth  $\phi$ , elevation  $\theta$ ), and RCS  $\sigma$  describing the effective area of the identified objects. Once the concept of the perceptual sensor system is fully defined, the integration phase begins (right side of the V-model). For the integration of initial hardware prototypes with mostly limited functionality, *technical sensor models* provide input signals to validate the intended functionality on HiL, DiL, or even ViL test benches. Due to the lack of detailed technological knowledge of the subcomponents and the complex high frequency technology, the focus is on quantitative rather than qualitative or performance analysis.

Although OTA radar sensor simulation is widely used in co-simulation for HiL and ViL, the huge investment in hardware equipment is still a challenge. In addition, due to the high computational requirements of the real-time system, the effects of environmental conditions on the radar echo are often ignored or reduced to a probability distribution. Furthermore, the number of objects to be simulated is also limited.

In vehicle development, *technical models* are used in the ascending branch of the V-model, after the usage of *individual models*. The test cases are defined in concrete scenarios with well-defined requirements. *Technical models* support X-in-the-Loop on vehicle level, see also Figure 2.2.

#### 2.7.4. Individual Model

##### Definition

The term individual means "*single; separate, for a particular use*"; physically based models are considered here. Parametrisation is only possible with the expertise of the system supplier. To verify the detection performance of an individual sensor or a sensor cluster under non-optimal detection conditions, sensor-typical phenomena such as range reduction, multipath wave propagation, reflections, attenuation, or the unexpected rapid changes of the radar cross-section have to be modelled.

### Application

Under the *individual model*, physical models are considered, provided the sensor supplier has all the technology and hardware-specific parameters to perform a reliable performance evaluation. The application is in the lower part of the V-model, at the component or subsystem level, where performance verification can only be performed by the supplier. Models that provide raw data, reflection points and target lists belong to this class of models because the data processing algorithms for clustering and tracking are not known to the vehicle integrator. *Individual models* can be used effectively by system suppliers who have the technological knowledge to perform simulations of everything down to semiconductor components. Examples include ray-tracer-related models, any time-domain electromagnetic wave simulation, finite-difference time-domain (FDTD) method, finite element method (FEM), raw input-raw output (RIRO) method, raw input-object-output (RIOO) method, and so on [40].

Academic and industrial researchers are making great efforts to develop an efficient, easy-to-use sensor model that behaves like the real sensor. However, without the specific infrastructure, such as an anechoic chamber the size of a vehicle [3], or knowledge of characteristic parameters, such as the antenna radiation pattern [34], the modelling can only be based on compromises and must focus on a very specific domain or use case [100]. These compromises include simplifications and assumptions, for example:

- Replacing of the real material description model by a probabilistic material model in [91];
- Assuming the radiation pattern of the antenna is known in [34];
- Replacing complex objects by multiple scattering centres in [20];
- Treating all metallic surfaces as perfect conductors (PEC) [64], while considering all other materials as absorbing in [39].

The authors show in [113] that a virtual representation of a real perceptual sensor in the form of a physics-based model is possible if the right supplier information and resources are available. In this paper, some basic properties of radar detection are investigated by measurement and calibrated simulation, including RCS estimation using ray tracer method. The main contribution of this work is that the calibration parameters for simulation can be derived from real measurements if the key parameters of the real sensor hardware are known.

In vehicle development, *individual models* are used in the ascending branch of the V-model, after the usage of *functional models*. The test cases are defined in concrete scenarios with well-defined requirements. *Individual models* support X-in-the-loop at the component and subsystem level (see also Figure 2.2).

## 2.8. Research Contributions

Extending the state of the art described above, the new contribution of this work is the development of a comprehensive framework for modelling environmental

perception sensors. The framework enables the systematic development of perception sensor models to integrate the properties of a real radar sensor into a simulation tool in accordance with the V-model. Figure 2.4 illustrates the modules and the interface data intended to use in the different development stages. The modelling is based on the presented process steps and the novel contributions can be summarised as follows:

- A suitable measurement setup makes it possible to combine the low-processed (target) and the high-processed (object) radar data into a single post processing tool based on the spatial and temporal synchronisation of the asynchronous radar sensor output. Using this approach it was possible to identify relevant phenomena related to radar sensor detections and led to the presented modelling approach.
- The modular semi-physical modelling methodology takes into account the radar point cloud and the Radar Cross Section by modeling the antenna characteristics, the radar equation and calculation of velocities using physical effects as detected by measurements. To the best of the authors knowledge the specific modelling approach described in Section 4.2 has not been used before.
- The interface data between the modules are intentionally aligned with the V-model and available X-in-loop methods, see Figure 2.4. The model is accordingly prepared to be used over the overall development process ranging from the concept phase to future virtual vehicle homologation. It is ready for the implementation of different processing algorithms from radar sensor providers, allowing for a more realistic and adaptive simulation. Thereby the initial application of the model in early development stages (operational, functional) is also suitable for later use as individual models.
- Despite the fact that the model can be used in the overall vehicle development process it is still real-time capable which enables an implementation in different X-in-the-Loop test procedures, for example for over-the-air radar simulation test benches.
- The modelling approach requires only limited input from the sensor system providers, based on parameters given in technical data sheets and access to the radar point cloud. Hence the model can be used in development phases where the sensor supplier is not specified.

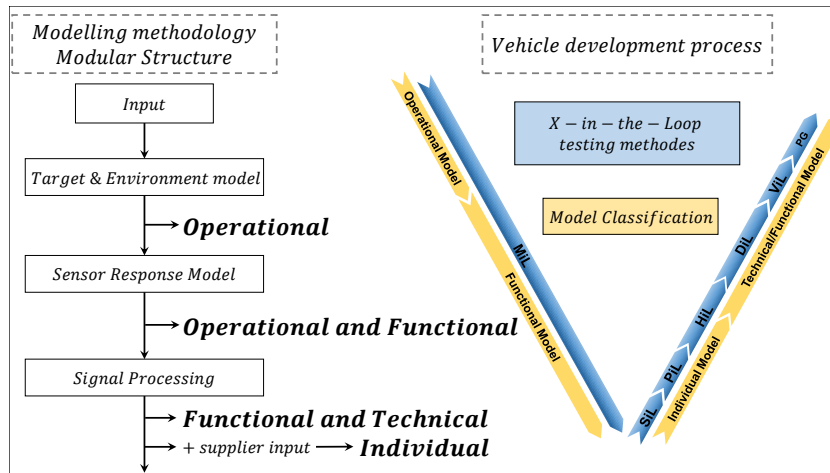


Figure 2.4.: Modular structure of the sensor model is aligned with the V-model.

In the course of the dissertation, ten peer-reviewed papers have been published in different journals. The contents of the papers as well as the authors contribution are summarized in the appendix 6. In the following scientific monograph, the contents of the following three papers are presented and the author's contributions are mentioned.

**Magosi, Z. F.**, Li, H., Rosenberger, P., Wan, L., Eichberger, A. (2022). A Survey on Modelling of Automotive Radar Sensors for Virtual Test and Validation of Automated Driving. *Sensors* , 22(15), [5693].

The contents of this paper is included in Section 2. The thesis author was responsible for evaluating the state-of-the-art methods used to radar sensor model categorisation. Developing the novel classification method and assigning the reviewed sensor modelling approaches. Defining the structure of the paper, writing and editing the publication.

**Magosi, Z. F.**, Eichberger, A. (2022). A novel approach for simulation of automotive radar sensors designed for systematic support of vehicle development. Submitted to journal *Energies* on 07.11.2022

The contents of this paper is included in Section 4.2. The thesis author was responsible for the development of the overall modelling concept. Design and implement the measurement set-up, including the preparation of the test vehicles. Definition, design and documentation of radar sensor specific driving scenarios. Preparation, coordination and execution of driving manoeuvres. Development and implementation of a suitable post-processing technique, followed by the development and implementation of the semi-physical radar sensor model both in MATLAB. Simulation and evaluation of the sensor model using the method developed in Paper 5, as well as writing and editing the publication.

**Magosi, Z. F.**, Wellershaus, C., Tihanyi, V., Luley, P., Eichberger, A. (2022). Evaluation methodology for physical radar perception sensor models based

on on-road measurements for testing and validation of automated driving. *Energies*, 15(7), [2545].

The contents of this paper is included in Section 4.3. The author of the thesis was responsible for defining the concept of the *Dynamic Ground Truth—Sensor Model Validation* method, developing the evaluation procedure, method development and implementation in MATLAB of the validation metric calculation (JSD), and writing and editing the corresponding parts including the following subsections: Driving Scenario, Vehicle Setup and Measurement System.

### **3. Development process flow and procedure of the radar sensor model approach**

#### **3.1. Process flow of sensor modelling**

Transferring the development of driving automation functions and their validation and verification activities into virtual space requires the appropriate modelling of perceptual sensors to support development through the entire process. To meet this need, commercial simulation tool vendors offer integrated sensor models of varying complexity. However, these models often use different modelling approaches that require completely different parameter sets. It is also obvious that with increasing complexity, aiming at realistic synthetic sensor data, more sensor and manufacturer specific information is needed to obtain a reasonable simulation result. This leads to the question: To what extent can the virtual sensor replicate the real one and how can the replicability be quantitatively determined? In order to reduce the simulation effort in terms of parameterisation and to be able to use the same model across the development phases through flexible scaling, the modelling was carried out under the following aspects:

- a Real measurements and the synthetic data should be transferable and interchangeable. E.g. real measurement on the test track and virtual measurement on the digital twin.
- b Modular design of the model structure. System integrators or vehicle OEMs involve radar sensor suppliers in the function development process already in the concept phase, who can also supply submodules of the entire simulation chain in the form of black-box algorithms.
- c Model parameterisation is based on data sheet information provided with the sensor and some characterizing measurements with a real sensor, but without additionally supplier information.
- d Flexibility, the model shall support different development stages according to the V-model.

A sensor model is an abstraction of the physical sensing process whose purpose is to determine the ability of the sensor being modelled to represent the environment based on the input information available to the sensor. The goal is to determine the relationship between the input and output information and other influencing factors in order to incorporate this a priori knowledge into the model development. Therefore, our model development method is based on well-designed measurements and their analysis carried out with real sensors and reference measuring devices

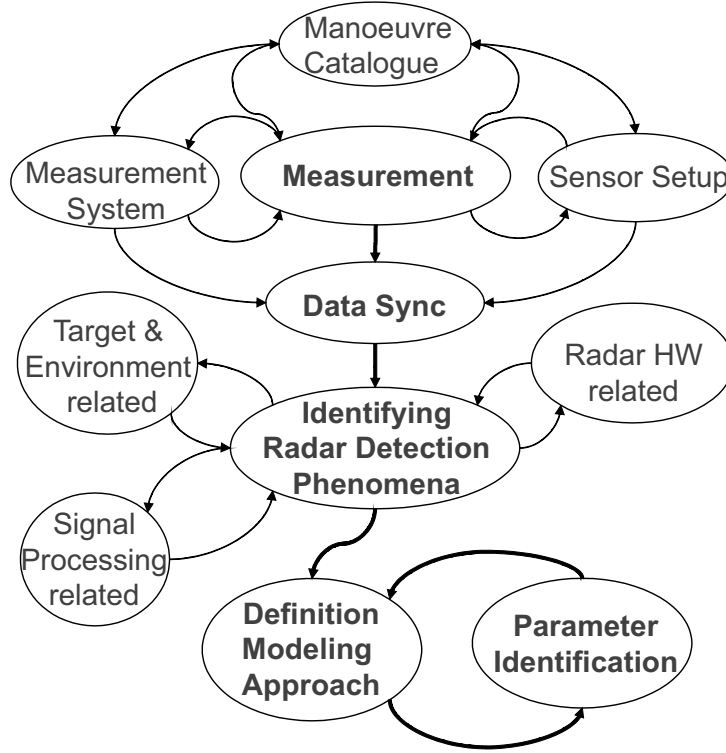


Figure 3.1.: Process flow to derive the radar sensor model

(GT). The model development process is shown in Fig. 3.1 and is explained in more detail here.

## 3.2. Model development procedure

### 3.2.1. Development of a suitable measurement setup

The measurement setup used, Fig. 3.1, allows simultaneous measurement with two radar sensors that are configured differently with respect to the processing level of the output data. In this work, the **Sensor Setup** consisted of two ARS-308 radar sensors from Continental GmbH. [13] to generate a real sensor data stream. According to the Continental terminology taken from the data sheet, the first sensor was configured to output radar *target* information that is updated in each sampling period, the second one was configured to output so-called radar *object* information that is the result of an unknown tracking algorithm. The **measurement system** used allows data **data synchronization** not only between the target and the ego-vehicle, but also between the sensors and the vehicle's CAN bus data streams. A detailed description of the measurement setup can be found in previous work [63], summarised in section 4.1. With this data acquisition method, we were able to analyse the behaviour of the sensors in different driving scenarios with a self-developed visualisation tool.



#### 3.2.2. Driving Scenario Definition

The research presented has been ongoing for several years and during this time the modelling methodology in the areas of raw data visualisation and labelling, scenario rendering and scenario definition has been continuously developed and refined based on the experience gained. However, despite the long duration, the measurement setup, the data acquisition unit (DAU) and the reference measurement system providing the GT information remained unchanged to ensure that the raw data generation remained consistent over the years. In the end, thousands of measurement kilometres and hundreds of driving manoeuvres have been accumulated in this way, which can be assigned to the various driving scenarios.

The planning of driving scenarios requires a combination of complex knowledge about the sensor capabilities, the available infrastructure of the test area and the specific requirements of the other partners involved and should be carefully defined as they serve multiple purposes. As an example, a selected driving manoeuvre recorded during a measurement campaign on the M86 motorway section in Hungary is used to evaluate the radar sensor model output data using the DGT-SMV *Dynamic Ground Truth Sensor - Model Validation* method to illustrate the performance of the radar sensor model[63]. Taking into account the number of available potential target vehicles, a tailor-made manoeuvre catalogue was created, comprising a total of 17 manoeuvres, 12 of which are designed for measurement runs on a motorway section of the M86 and five on the dynamic platform of the Zala-Zone automotive test site[98].

The selected driving scenario is the *Range test target leaving*, which can be defined as a combination of the subsets shown in Fig. 3.2 as follows. Scenario (*S*), intended to be performed on a closed public road (*CPL*), involving a moving (*DYD*), complex (*CTS*) and single (*STR*) target, which performs receding drive (*RED*) from the EGO vehicle. The scenario is meant to be performed in daylight (*DYL*) on a dry (*DYW*) road surface.

$$S = [CPL, DYD, CTS, STR, RED, DYL, DYW] \quad (3.1)$$

The initial conditions for this driving manoeuvres are set as follows. The ego vehicle follows the target vehicle in the same lane at a constant set speed in Adaptive Cruise Control mode, system is already in steady state condition. When the initial conditions are met, the manoeuvre begins, the target vehicle accelerates to increase speed and leaves the ego vehicle behind. The manoeuvre ends when the relative distance has reached the maximum defined value. For more details please refer to Section 5.

#### 3.2.3. Identifying Radar Detection Phenomena

Based on previous research [37] we decided to implement the following observations in the radars sensor model, Fig. 3.1, where such phenomena can be related to the *target and environment*, the *signal processing*, the *radar hardware*:

- i **Radar detections** can be assigned to three distinct area inside the gating window.

### 3. Development process flow and procedure of the radar sensor model approach

Location	Dynamic	Target Structure	Num. of Targets	Type of Scenario	Weather	Lighting
- Proving Gnd. (PGL) - Public Road (PRL) - Urban (U) - Interurban (IU) - Highway (H) - ... - Closed PR (CPL) - Urban (U) - Interurban (IU) - Highway (H) - ... - Tunnel (TUL) - ... - ...	- Static (STD)  - Dynamic (DYD)	- Simple (STS) - Met. Plate (M) - Sphere (S) - Cor.Refl. (CR) - Complex (CTS) - Ped. (P) - Bicycle (B) - Mot. B. (MB) - Car (C) - Truck (T)	- Single (STR)  - Multiple (MTR)	- Free-Drive (FRD) - Follow-Drv. (FOD) - Approach-Drv. (APD) - Receding-Drv. (RED) - Overtake-Drv. (OVD) - Oncom.-Drv. (OND) - Crossing-Drv. (CRD) - ...	- Dry (DYW) - Wet (WTW) - Spalsh (S) - Mud (M) - ... - Rain (RIW) - Heavy (H) - Med (M) - Light (L) - Snow (SNW) - ...	- Daylight (DYL) - Early-Morning - Morning - Midday - Afternoon - Late Afternoon - Evening - Night - Gloom - Artificial - ...

Figure 3.2.: Parameters to define driving manoeuvres

- Around the closest point defined by the shortest radial distance between radar sensor and target vehicle.
  - Around wheel mounting positions (moderately scattered).
  - Under vehicle body (strongly scattered).
- ii **The RCS measurement** carried out according to the Euro-NCAP Global Vehicle Target (GVT) Validation procedure [23] shows a characteristic fluctuation pattern of the signal strength.
  - iii **Detection of occluded targets** is also possible without a direct line of sight to the second or even multiple occluded target vehicle ahead. Signal attenuation by the vehicle directly in front depends on the installation position of the radar sensor above the road surface, the distance to the preceding and the first occluded target vehicle, the ground clearance and the height of the vehicle directly in front of the radar sensor.
  - iv The **speed signal** recorded in the area of the wheel mounting positions deviates from the speed signal measured on the vehicle body. The phenomenon results from the rotational movement of the wheels and can be described with a Micro-Doppler effect, as described in [111].
  - v **Speed signals** referenced to radar detections on the body of the target vehicle as well as under body reflections exhibit prediction algorithm error-like deviations when the relative acceleration (jerk) changes rapidly.
  - vi The detection boundaries referred often as **Sensor Field of View** of the radar sensors in terms of range and azimuth angle coverage as well as resolution and separability are as specified in the data-sheet.

Those detected phenomena led to the definition of the modeling approach and the related parameter identification as described in the next sections.

### 3. Development process flow and procedure of the radar sensor model approach

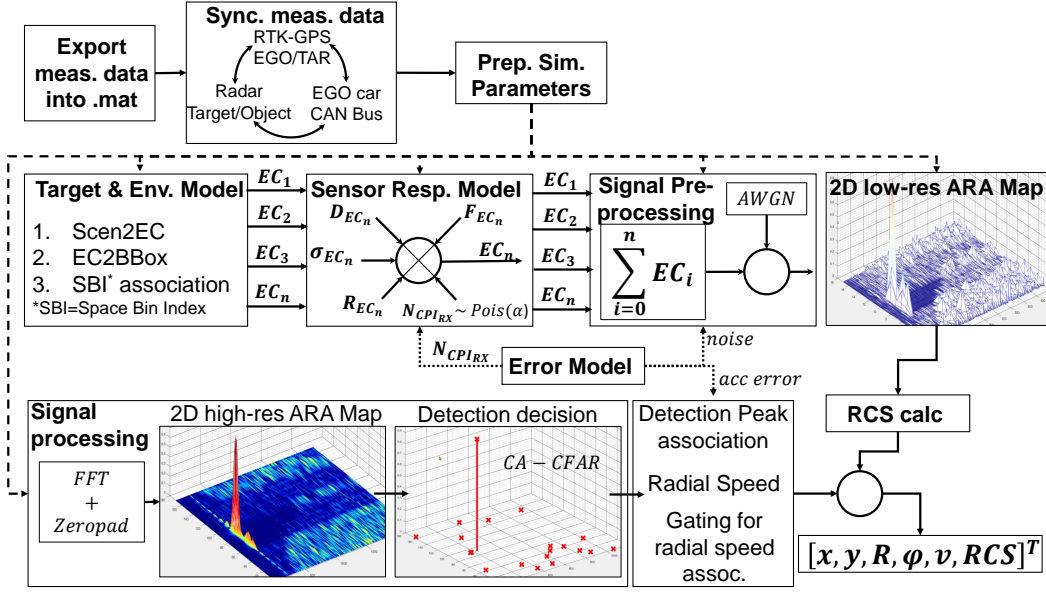


Figure 3.3.: Implementation of the model

#### 3.2.4. Implementation in Matlab

In this paper we use Matlab/Simulink as a modeling, simulation and implementation platform. Figure 3.3 shows the schematic representation of the implementation of the radar sensor model according to the higher-level model described in detail in the previous chapter.

The implementation starts with the export of the recorded data from the ego and the target vehicle. Followed by the synchronisation of the asynchronous data sets based on the timestamp of the Real Time Kinematics/Global Positioning System (RTK-GPS). In this processing step, the measurements of the dynamic state of the ego and the target vehicle are synchronised with the controller area network (CAN) bus signals of the ego vehicle and the outputs of the radar sensors, which provide target information in the form of radar point cloud data and object information in the form of object lists, both recorded via the CAN bus. From this, the simulation parameters for the radar sensor model and for the virtual replay of the experimental data in simulation is prepared. The remainder of Fig. 3.3 follows the methodology of the sensor model approach divided in *Target and Environment Model*, sec. 4.2.3, the *Sensor Response Model*, sec. 4.2.3, the *Signal Processing* module, sec. 4.2.3, as well as the *Error Model*, sec. 4.2.3 that affects both *signal Processing* and *Sensor Response Model* modules. The block *2D low-res ARA (Amplitude Range Azimuth) Map* visualizes the results of the low resolution detection from which the RCS is calculated and associated with the results from the *Signal Processing* module.

The final result is the simulated output vector  $[x, y, R, \phi, v, RCS]^T$ , which is compared with the corresponding quantities of the real radar sensor obtained by the measurement in the next section, where  $x, y, R, \phi$  are coordinates of the radar point cloud in the (Cartesian and polar) sensor coordinate system,  $v$  the radial velocity and  $RCS$  the Radar Cross Section.

#### 3.2.5. Calibration

The presented radar sensor modeling approach is aimed to generate synthetic radar sensor outputs, comparable with its real sensor counterpart, called radar-under-simulation (RUS). As only limited knowledge available of the HW/SW components of the real sensor, test drives were carried out to characterize the sensor features and capabilities in terms of environment sensing, see Section 4.2.

Observations and identified behaviors to be implemented are already listed in Section 3.2.3. The driving scenarios and the exact driving manoeuvres were generated on a basis of the combination of the underling parameters defined to each pillar as shown in Fig. 3.2.

According to the definition, a scenario consists of at least one driving manoeuvre, which is characterized by the exact definition of the start, execution and end state with regard to e.g. position, target/set speed of ego and target vehicle, driver tasks etc.

In addition to our own driving scenarios, we also used a standardized measurement procedure to calibrate the synthetic RCS output of the sensor model. The RCS measurement method we adopted is described in detail in the Technical Bulletin TBo25 [23], which was defined by the Euro-NCAP consortium for the verification of GVT soft-targets, being used for official Euro-NCAP tests. In agreement with the measurement results reported in TBo25, our own RCS measurement results also follow a characteristic fluctuation pattern, which could be due to the effect of small-scale multipath propagation of the EM waves, described in [76, p. 139]. Considering the installation geometry of the RUS, which in our case was mounted 0.5 m above the road surface, the effect of multipath propagation is inherent. More detail about the test vehicle and measurement setup can be found in [63].

The effect of multi-path propagation is implemented with the propagation factor  $F(r_s, \theta_s, \phi_s)$  see Section 4.2.3. According to the authors in [76, p. 70], the local average value of the received signal energy for mobile radio systems is calculated by averaging the measured signal over an evaluation distance with a length of 5-40 times the wavelength. We have adopted this method with the modification that the local average is calculated not on a wavelength-based evaluation range, but on the set of occupied resolution cells. The output RCS value is then the local average of the simulated signal power calculated over the corresponding space bins assigned to the target vehicle, normalised to one and scaled by the factor  $u$ . After rearranging the radar equation, the RCS value can be calculated by substituting the local average of the synthetic generated received energy Power  $P_{Rx}$ , see (4.2).

#### 3.2.6. Assessment Method and Benchmark

Sensor models with different complexity in relation to the applied simulation method, with varying accuracy or realism can legitimately be used through the entire vehicle development process,[62]. In order to meet the different modelling requirements, it must be evaluated whether a sensor model with its tailored skills can sufficiently represent the real world with the required accuracy to validate the functional safety of ADAS/AD systems accordingly. In the literature several assessment methods with its own advantages and disadvantages can be found

### 3. Development process flow and procedure of the radar sensor model approach

---

for specific application areas, see [30, 84, 15, 72, 71, 78, 19] and a comprehensive summary in a tabular form can be found in [80, p. 42 ff].

Taking in to account the research objectives and the available HW resources, a novel approach called Dynamic Ground Truth-Sensor Model Validation has been developed for the performance evaluation of active environmental sensor models. A detailed description of the evaluation process including the technical specification of the test vehicle, the measurement system and the sensor cluster, can be found in [63], which is briefly summarized in Section 4.3.1.

The method allows the statistical comparison of synthetic and measured point cloud data, which in our case is equivalent with the target list, see Fig. 4.3, and aims to provide a quantifiable assessment of the tested sensor model. The DGT-SMV approach is depicted in Figure 4.10.

The evaluation process starts with the definition of a specific driving scenario in terms of the selected phenomena to be implemented in the modelling process. In the following phase, the measurement is performed with the test vehicle according to the driving manoeuvre catalogue described above, equipped with the RUS and a ground truth reference system. The GT system is used to associate the output data from the RUS by means of measurement data labeling. In the next step, the real driving scenario is implemented in the virtual environment with the help of the digital twin of the measurement location, which allows the driving manoeuvres to be replayed while maintaining the relations measured in the real environment. The evaluation is based on the comparison of two or more discrete probability distributions quantified by calculating the Jensen-Shannon Divergence (JSD).

## 4. Methodology

### 4.1. Experimental methodology

#### 4.1.1. Vehicle Set-Up and Measurement System

The procedure for evaluating the performance of the sensor model described in section 4.3 is essentially based on the comparison of low-level sensor point cloud data obtained from measurements of real automotive radar sensors declared as reference with synthetic point cloud data simulated by their virtual counterpart. Due to the stochastic properties of radar detection output, the two data sets are not directly compared, but related to the measured and virtually reproduced ground truth. This requires highly accurate reference data of the environment, including static and dynamic objects, and a reproduction accuracy of the scenario that is below the measurement accuracy of the real sensor. By precisely measuring position, velocity and acceleration, the corresponding pitch, roll and yaw angles as well as angular velocities in all three-dimensional axes, the current state of an object can be considered fully defined at each measurement period. Given in a Cartesian frame as  $x = [x, y, z, \phi, \theta, \psi]$  along with  $\dot{x} = [\dot{x}, \dot{y}, \dot{z}, \dot{\phi}, \dot{\theta}, \dot{\psi}]$  and  $\ddot{x} = [\ddot{x}, \ddot{y}, \ddot{z}, \ddot{\phi}, \ddot{\theta}, \ddot{\psi}]$ , as well as  $\ddot{x}$  when also considering jerk. The schematic representation of the measurement setup for synchronised acquisition of the ground truth, the sensor output data and the via radio-link connected reference vehicle can be seen in Figure 4.1.

The basic measurement setup used to collect ground truth and sensor data for the DGT-SMV approach, consists of:

- i **Two test vehicles** defined as ego, equipped with the sensor cluster consisting of four radar and one LIDAR sensor, and target as a subject of detections of interest.
  - *Ego-Vehicle*: The configuration of the ego-vehicle and the sensors used to generate sensor and GT data is shown in Figure 4.2(a). Figure 4.2(b) shows the antenna setup on the roof, consisting of the GPS, GSM, Car2Car and WiFi antenna, with the ego-vehicle connected to the target vehicle. In the basic configuration of the measurement system, only one target vehicle is considered, but measurements with up to 4 connected vehicles have also been carried out.
  - *Target-Vehicle*: In the schematic representation of the measurement setup, it can be seen that the number of components required to set up the basic configuration of the measurement setup in the target vehicle was deliberately reduced to an RTK-GPS <sup>1</sup> based Inertial Measurement Unit

---

<sup>1</sup>for more explanation see text bellow

(IMU) and a Data Acquisition Unit. This design consideration allows for flexibility in the selection of the road user defined as the target vehicle.

ii **Ground truth** measurement system.

The essential part of the entire measurement system is the determination of relative and absolute vehicle positions and dynamic behaviour in terms of providing the ground truth information. The Dewetron CAPS [10] measurement system was selected to provide online GT information from both ego and target vehicles equipped with a DEWE-CAPS Data Acquisition Unit and the most advanced Automotive Dynamic Motion Analyzer (ADMA-G-Pro+) for high precision measurements of the vehicle's states. The output of the Inertial Measurement Unit is corrected with Global Navigation Satellite System (GNSS) data by sensor fusion. To achieve sub-centimetre measurement accuracy, the integrated differential-GPS (DGPS) receiver [73] incorporates correction data provided by a base station or country-specific data provider. In the basic two-vehicle measurement arrangement presented here, the RTK-GPS correction data is received from a service provider via a Global System for Mobile Communications (GSM) RTK mobile data modem mounted in the ego-vehicle. The correction data is transmitted to the target vehicle via the WiFi connection. The special feature of the measurement system is that the selected data can be sent from the target vehicle to the ego vehicle using the same WiFi connection. The DAU system calculates online, based on the GPS time stamp, the temporal relationship of the individual data packets as well as the relative position and speed information. Part of this data can be displayed so that the user can visualise the measurement process during the measurement. All these data are recorded together with auxiliary data from the vehicle, analogue and digital input signals, video data as well as radar point cloud data provided via the CAN bus.

- *ADMA-G-Pro+ RTK-GPS/IMU*: The ADMA-G-Pro+ gyro system from GeneSys Offenburger GmbH. is the most sophisticated ADMA variant that has no moving parts and is therefore extremely robust and resistant against shock and vibration. The system consists of three fibre-optic gyro sensors for detecting rotational movements, three servo acceleration sensors for determining acceleration and an internal DGPS receiver for accurate position updates with RTK-GPS corrections. The ADMA-G-Pro+ gyro system allows measurements to determine relative position with a high accuracy of up to  $\pm 2$  cm [73] and velocity measurements with an accuracy of less than  $\pm 0.01$  m/s as well as the determination of the heading angle with an accuracy of  $\pm 0.05^\circ$  [25]. The ADMA is mounted via a rack in the boot of the vehicle. To configure the device, the mounting offset between its measurement centre and the GNSS antenna and to the virtual measurement point is needed. For the measurement setup used to create the GT, the reference point was defined and measured at the centre of the rear axle of each vehicle. The advanced Kalman-filter combines internal and external sensor data to achieve a high frequency output of up to 100 Hz. In addition, the GPS-PPS-based (pulse per second)

synchronisation technology makes it possible to use the ADMA system as a stand-alone device as well as in combination of two or more ADMAs synchronised with the GPS-PPS time synchronisation signal. Since the GPS synchronisation works independently in two or more vehicles and all data is time tagged, the data transmission between the vehicles can be done via asynchronous WLAN. [10]

- *Data Acquisition Unit:* The basic configuration of the Dewetron CAPS measurement system was designed for the setup of two vehicles. The included DAU developed by Dewetron, is equipped with sensor interfaces and time synchronisation hardware components which are also developed by Dewetron. The Sync-Clock technology is used to derive the measurement time from the high-precision synchronisation signal PPS, which runs absolutely synchronously on each GPS receiver. In addition, based on the Sync-Clock technology, a precise 80 MHz system clock is generated within the CAPS measuring computer and synchronised with the atomic clock reference signal of the GPS satellites. The division of the system clock into slower, multi-phase sync clocks ensures that all recorded data is perfectly synchronous, even with asynchronously running data with different sampling rates, such as signals at analogue inputs, CAN data or video images. [10]

#### iii **Environment perception sensors**, with open data interface.

The main sensor used in this work is the ARS 308-2C/21 HS/AO automotive radar. However, the test vehicle was also equipped with other environmental perception sensors to serve as a platform for data collection. The setup allows for both performance analysis and practical test drives to support the development and validation of various perception sensor models that have been and are being developed at the Institute of Automotive Engineering at Graz University of Technology. In order to capture as much information as possible from the test vehicle's surroundings, the ego car was additionally equipped with two industrial FMCW radar sensors ARS 308-2C/21 HS/AO from Continental AG, with a 16-beam LIDAR sensor from Robosense Ltd., with a front camera module of the type ME-630 from MobilEye, a Car2Car communication development platform of type MK4 from Choda Wireless and a video camera used for documentation purposes.

- The ARS-308 radar sensor operates in the 76–77 GHz frequency band and applies Frequency Modulated Continuous Wave (FMCW) technology, modulated by fast chirped sequences [61], as the basic principle for estimating relative distance and speed. In this modulation method, the carrier signal is modulated with a saw-tooth waveform whose frequency varies linearly with time. The mechanically scanning antenna provides two independent scans in the range of 0.25–200 m for long range detection and 0.25–60 m for short range detection [88]. The radar sensor output is configurable between two modes according to the level of data processing: target and object list. In object mode, only the tracked objects are displayed as the result of calculations carried out over several scans,



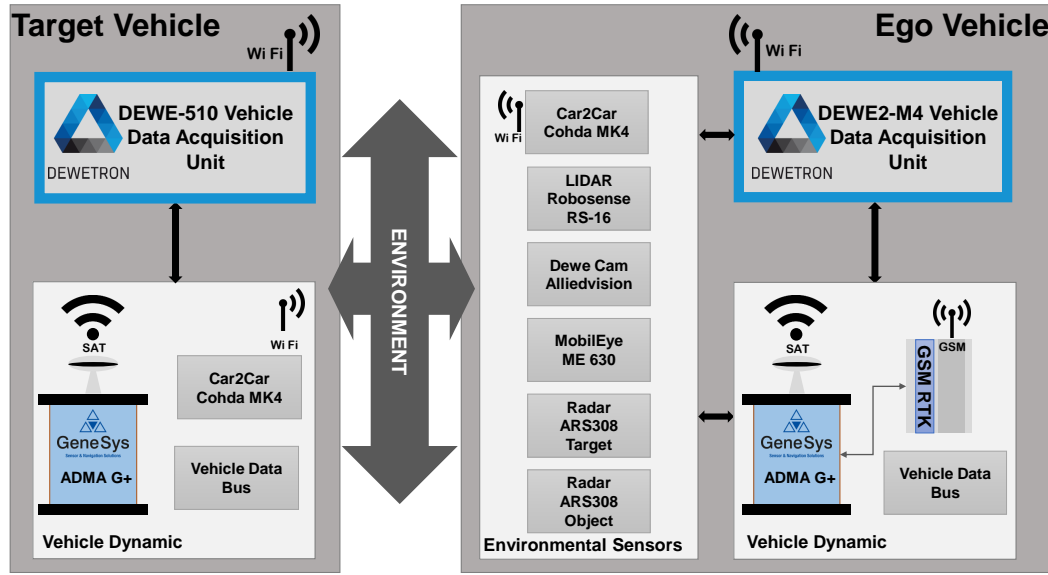


Figure 4.1.: Schematic diagram of the measurement setup.

while in target mode all detections are displayed calculated individually for each scan. In target mode, which was used for the experiments presented here, twelve parameters are available per target, the most important of which are range, azimuth angle, speed and RCS.

- The Robosense RS-16 LIDAR sensor is mounted in the centre of the vehicle roof and provides 3D point cloud data of the 360° sensor field of view that represents depth information relating to the vehicle surrounding environment.
- MobilEye ME-630 front camera module mounted behind the windscreen of the test vehicle in the centre, aligned with a longitudinal vehicle axis and provides information on traffic signs, road users, lane markings etc. measured in the sensor FOV.
- MK4 Car2Car wireless communication development platform from Cohda Wireless configured according to the ETSI ITS-G5 standard.
- Video Camera, provides visual information of the driving scenarios, used during post processing.

The developed test vehicle body had to be able to provide stable sensor data recordings in all weather conditions as well as the required electrical power not only for the additionally mounted sensors but also for the data acquisition unit. The sensor setup is waterproof and the boot where the DAU and IMU are mounted together with the power box is cooled by the vehicle's own air conditioning. The base vehicle is a BMW640i Coupé, which is appropriately equipped with various driver assistance functions and environmental perception sensors.



Figure 4.2.: Test vehicle measurement setup. (a) Front view of the test vehicle with the additionally mounted sensors. (b) Top view of the test vehicle with the antennas required.

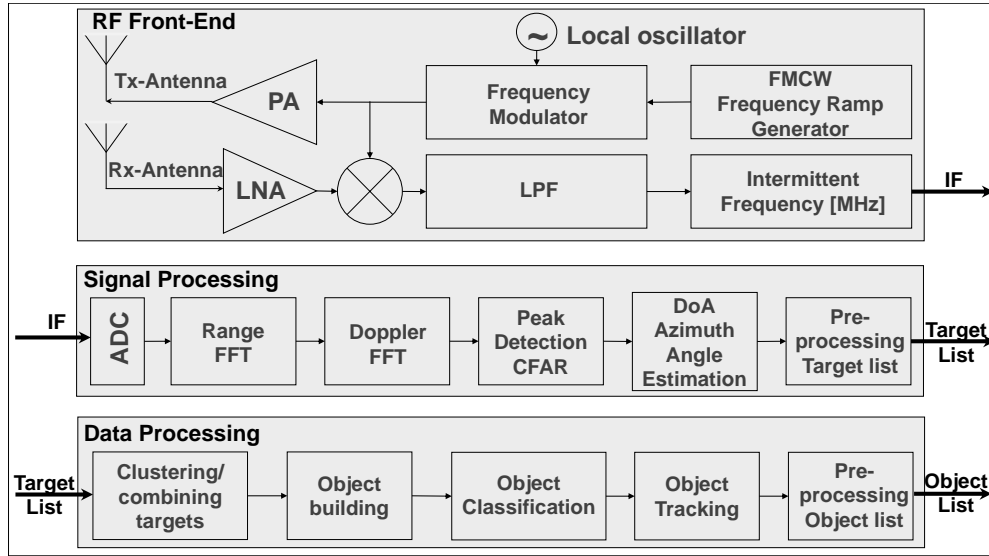


Figure 4.3.: Block diagram of an FMCW radar processing flow

## 4.2. Sensor modelling

### 4.2.1. Operating Principle of Frequency Modulated Continuous Wave Radar Detectors

Modern radar sensors used in the automotive industry are based on the know-how of the radar sensor suppliers, which means that little or no information is available about the inner workings of the device. In [107], the FMCW radar principle applied for Range Doppler detection (RD) are presented, using the Fast Fourier Transform (FFT) as the basic computational step. Figure 4.3 shows a typical block diagram of an FMCW radar processing flow:

The HF front-end contains the analogue Receiver/Transceiver (Rx/Tx) components of the radar transceiver, and the output is the frequency difference between the received and transmitted signals. The bandwidth of this down-converted beat or

intermittent frequency is small compared to the modulation bandwidth, allowing the radar detector to operate with Analog-Digital-Converter (ADC) sampling rates as low as a few megahertz. By performing an FFT from the sampled beat frequency, the resulting frequency peaks in the range spectrum are proportional to the radial distance of the illuminated objects. To determine the speed of the detected objects, the phase change of the beat signal can be evaluated over a series of range samples by performing a second FFT for each range bin. The resulting peaks in the Doppler spectrum correspond to the relative velocity between the detector and the detected objects.

The result of this two-stage FFT processing is the RD spectrum, which is a 2D distance-velocity image or an FFT heat map. After estimating the distance and velocity of the received signal, the next processing step is to make a detection decision by applying different Continuous False Alarm Rate (CFAR) algorithm. In the phased array antenna system, a third FFT is applied to the detected objects to estimate the angle of arrival of the detected objects. Since the radar detector used in our experiments is equipped with a mechanically scanned antenna, this third FFT processing stage can be replaced by the positioning sensor output of the beam steering mechanism. The detection peaks obtained at the output of this processing stage can be sorted into a detection list with the corresponding radial range, azimuth angle, velocity and signal strength. This is called the target list.

The target list contains a number of static and dynamic reflection points, but also some unwanted detections in the form of clutter noise. Depending on the intended vehicle function, the target list can be further processed in the data processing module. After clustering or combining the individual reflection points, a larger object can be defined based on the selected attributes. The ARS-308 radar detector is able to determine the width and length of the clustered reflections, which enables object classification. In the final processing step, a tracking algorithm is applied to the object information resulting from the hypotheses about the object made by measurements and estimations in the previous steps. The result of this processing step is the object list.

### 4.2.2. Modular Structure

In view of the modelling considerations defined above and our observations selected for implementation, in combination with the high-level functional structure of an FMCW radar, radar theory in terms of antenna characteristics and electromagnetic wave propagation, a modular structure see Fig. 4.4 has proven to be the most appropriate modelling structure. The modular framework ensures the flexibility to easily include additional effects and allows the simulation engineer to adapt the model to the complexity of the simulation during the development process.

### 4.2.3. Functional model / design philosophy

With respect to our modelling objectives, the radar sensor model simulates detections represented in a 2D range azimuth (RA) map to be comparable with the low-level data output of the signal processing block. According to the terminology

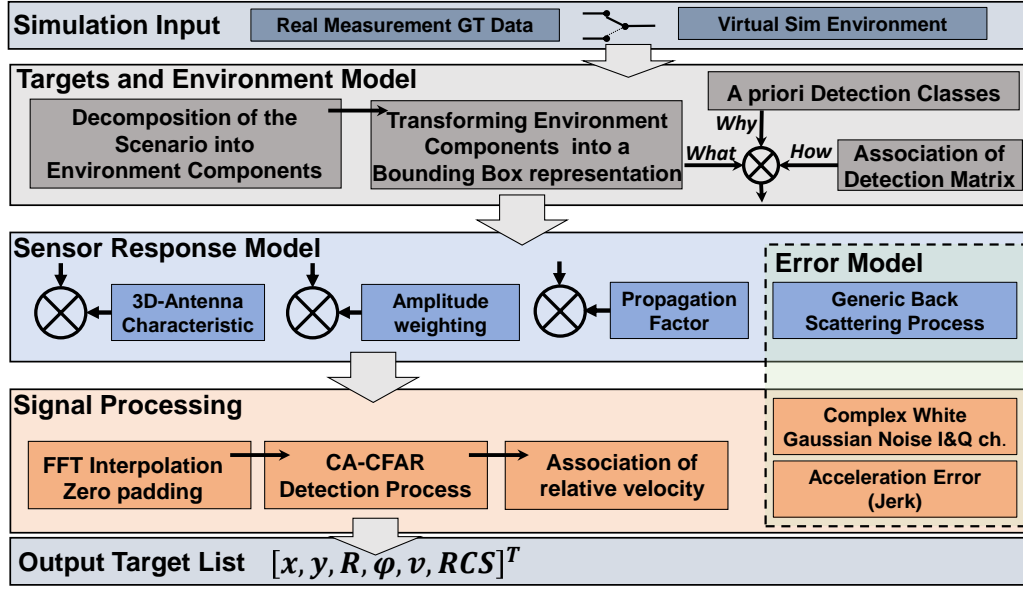


Figure 4.4.: Modular structure of the radar sensor model

used in the data sheet provided with the real radar sensor [13], the low-level data output in Fig. 4.3 is referred to as the target list. With regard to the complex and highly sophisticated signal processing chain in a real sensor, the model synthesizes a squared law detector like output. Accordingly, the distribution of the power of the back scattered signal is assumed to have an exponential shape for each resolution bin. Since the only information of a real radar sensor related to the received signal strength is the radar cross section expressed in dB, the basic radar equation for calculating the RCS value is applied to the synthetic radar data. The effect of shadowing by preceding traffic objects is incorporated by calculating the local signal attenuation which is a function of the radial distance to radar and the 3D dimension of the shadowing object. The 2-way propagation channel is characterized by small and large scale fading to represent the effects caused by multi-path wave propagation combined with range dependent free-space signal attenuation.

The modular structure of the sensor model depicted in Fig. 4.4 is described in the following. Basis of the modeling approach is **simulation input** coming either from a commercial virtual simulation environment or from a replay of real measurements. The following modular sensor components are:

- I **Targets and Environment Model.** This modelling step start with the **decomposition of the scenario into environment components (EC)**. Despite the projection of the real sensor FOV into a 2D representation we assume that the scenario is measured in all three dimensions. The virtual sensor FOV is then extended in elevation direction by the same number of receiver channels as defined in the real radar's data sheet for the azimuth direction. The scenario from a real measurement or from a virtual test drive are transformed into the 3D virtual sensor FOV with reduced resolution in all three dimensions. At this processing stage the virtual sensor FOV is divided into  $17 \times 17 \times 450$

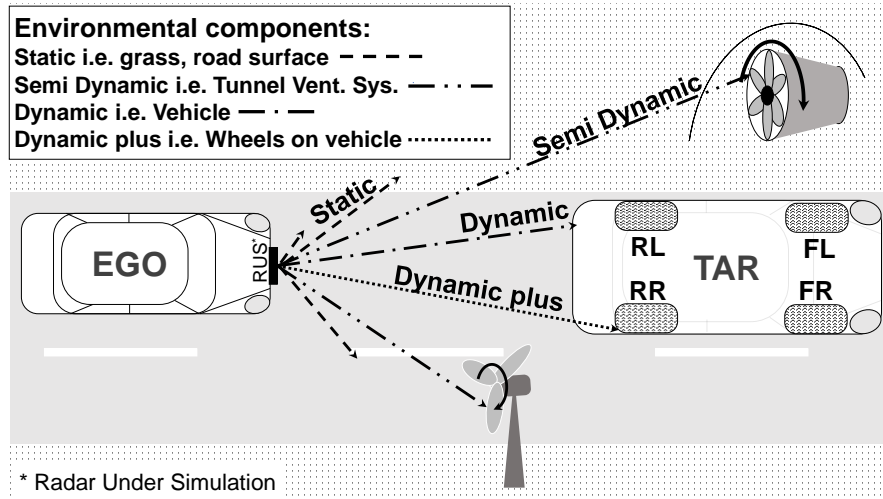


Figure 4.5.: Environment classes for the sensor model

space bins (SB) labelled with the space bin indicator (SBI), which corresponds to an angular resolution in both azimuth and elevation direction of  $1.0625^\circ$  and  $0.45\text{m}$  in range direction. This low-resolution spatial representation allow us to **transform the environment components into a bounding-box representation**.

- **Environment Components (“What”)** Based on our observations describing the environmental components relevant for radar detection, we have defined the following general environmental classes, see Fig. 4.5:
  - \* **Static components** with fixed position in the global coordinate system: road surface, terrain, guard rail, etc.
  - \* **Semi dynamic** components like static components with fixed position in the global coordinate system but with moving parts on it ( $\mu\text{Doppler}$ ): i.e. tunnel ventilation system
  - \* **Dynamic components** or road users, they can change position in the global coordinate system introducing relative velocity, also defined as object classes in the radar data sheet: Targets in target mode, Pedestrian, Bicycle, Car and Truck in object mode.
  - \* **Dynamic plus environment components** beside the ability to change position in the global coordinate system with given relative velocity, additionally can have other speed components due to its rotatory movement ( $\mu\text{Doppler}$ ). i.e.: Wheels
- **A priori Detection Classes (“Why”)** After defining the environmental classes, in the next step we also defined different detection-related classes based on the observation of the modality of the radar detections in order to generalise the virtual radar detection behaviour:
  - \* **Simple detections:** Environment components are in line of sight, detection is expected on signal strength being above a detection threshold (i.e. guard rail, traffic lamp, etc.).

- \* **Scattered detections** related to environment components are not in line of sight such as detection of obstructed vehicles via under body reflections.
  - \* **Doppler detection:** Environment components with relative speed different to speed of ego vehicle.
  - \*  **$\mu$ Doppler detections** related to environment components with rotatory movement relative its own body, such as wheels but also tunnel ventilation system.
- **Association of Detection matrix (“How”)** To implement the virtual detection method, a detection matrix combining the environmental components and detection features was defined, taking into account the FMCW principle and its powerful frequency analysis capability. This matrix maps all environmental components to a possible detection:
- \* Static environment components  $\rightarrow$  Simple detection
  - \* Semi-dynamic components  $\rightarrow$  Simple +  $\mu$ Doppler detection
  - \* Dynamic components  $\rightarrow$  Simple + Scattered+ $\mu$ Doppler detection
  - \* Dynamic Plus components  $\rightarrow$  Scattered+ $\mu$ Doppler detection.

The assignment of the environmental components to the detection modalities makes it possible to realise detections based on either the signal amplitude level or the relative velocity or in combination of both signals, as in the case of the real sensor. At the same time, this method allows the model to be extended to include the separability function, which also uses the signal amplitude and/or velocity signals.

## II Sensor Response Model

The sensor response model, Fig. 4.4, represents in simplified form the processes that belong to the HF front-end of a real radar sensor. The result of this module is the superposition of the observed, but also partly suspected effects that could have an influence on the received signal strength. As mentioned before, the RUS is completely unknown with respect to the internal HW/SW parts responsible for the detection function, which allows us to consider the system as a black box. To describe the desired system behaviour, our modelling approach implies that linear time-invariant (LTI) signal processing theory can be adopted. An LTI system can be represented by its impulse response function, which is the system output when the input is an impulse. If the impulse response function is known, the output of an LTI system can be calculated deterministically for each input. The impulse response of a radar system is the sum of the back-scattered signals returning from each scatterer in the sensor’s field of view. For the derivation of the system impulse response function, which is characterised by the statistical superposition of several scattering objects, an approach defined in the spatial domain was used [75]. The transition from the time domain to the spatial domain means that frequency-dependent quantities are not represented as a function of time but as a function of location by converting the time axis into the spatial axis via the speed of light [75].

In automotive radar applications, the propagation of EM waves can be characterised by the basic effects of reflection and scattering. The EM wave is reflected when the irradiated object has a dimension much larger than the wavelength of the radar's carrier frequency, while scattering occurs on large rough surfaces consisting of irregularities that have a small dimension compared to the wavelength. Considering a typical mounting geometry for an automotive radar sensor and assuming that the sensor transmits only in the horizontal plane of polarisation, the impulse response  $g_s$  of a point scatterer  $s$  located at a distance  $r_s$  at any angular position  $\vartheta_s$  for elevation and  $\phi_s$  for azimuth can be defined as follows:

$$g_s(r_s, \vartheta_s, \phi_s) = D(r_s, \vartheta_s, \phi_s) \cdot R(r_s, \vartheta_s, \phi_s) \cdot F(r_s, \vartheta_s, \phi_s) \cdot e^{-i \cdot 2k_\lambda \cdot r_s}, \quad (4.1)$$

where  $D(r_s, \vartheta_s, \phi_s)$  represents the effect of the directional characteristic of the antenna considering also the sidelobe reflections,  $R(r_s, \vartheta_s, \phi_s)$  represents the amplitude response (amplitude decay/path loss) as a function of radial distance to the scatterer,  $F(r_s, \vartheta_s, \phi_s)$  represents the impact of propagation effects, and  $e^{-i \cdot 2k_\lambda \cdot r_s}$  the phase term of the back scattered signal with  $k_\lambda$  the wave number.

According to the authors in [75], the radar equation can be determined from the quotient of the transmitted and received power  $\frac{P_{Rx}}{P_{Tx}}$ , by forming the absolute square of the impulse response function w.r.t. power  $g_{sP}(r_s, \vartheta_s, \phi_s)$ ,

$$|g_{sP}(r_s, \vartheta_s, \phi_s)|^2 = \frac{P_{Rx}}{P_{Tx}} = \frac{\lambda_c^2 \cdot G_{Tx}(\vartheta_s, \phi_s) \cdot G_{Rx}(\vartheta_s, \phi_s) \cdot \sigma_s}{(4\pi)^3 \cdot r_s^4} \cdot F(r_s, \vartheta_s, \phi_s)^4, \quad (4.2)$$

where  $\lambda_c$  is wavelength of the carrier frequency,  $G_{Tx}$  and  $G_{Rx}$  the gain of transmitter and receiver antenna, and  $\sigma_s$  is the reflection coefficient of the point scatterer.

As we are interested to express the amplitude  $A$  of the impulse response  $g_s(r_s, \vartheta_s, \phi_s)$  in terms of the transmitted power, (4.2) can be rewritten according to [55] into

$$g_s(r_s, \vartheta_s, \phi_s) = \frac{1}{4\pi r_s^2} \sqrt{\frac{2P_{Tx} \cdot G_{Tx}(\vartheta_s, \phi_s) \cdot \sigma_s}{\varepsilon_0 \cdot c}} \cdot e^{-i \cdot 2k_\lambda \cdot r_s} \cdot |1 + \Gamma \cdot e^{i \cdot k_\lambda \Delta r_s}|^2, \quad (4.3)$$

where  $\varepsilon_0$  is the permittivity of the vacuum,  $k_\lambda$  is the wavenumber,  $c$  the speed of light, and  $\Gamma \cdot e^{i \cdot k_\lambda \Delta r_s}$  is the Fresnel reflection coefficient.

- \* **Amplitude weighting** as a function of distance. In radar theory, the power of the received signal is expected to be proportional to the fourth power of the distance to the scatterer or target. Due to the many simplifications applied for the simulation, this rule does not fit our *radar link budget* [76, p. 102] compared to the real sensor

output, so we introduced a new amplitude weighting function in the form of an exponential decay. The new exponential amplitude decay  $R(r_s, \vartheta_s, \phi_s)$  is still the function of the range and can be expressed by definition as follows,

$$R(r_s, \vartheta_s, \phi_s) = R_0 e^{-\tau \cdot r_s}, \quad (4.4)$$

where  $R_0$  is the minimum detection range of the radar under simulation (RUS),  $\tau$  is the rate constant and if it is less than zero, it represents a decay.

\* **3D-Antenna Characteristic** The antenna is the coupler that transfers the EM waves of the propagation channel into the electronic HF components of the radar sensor. Radar antennas are characterized by its directional beams that can be described with the antenna diagram or antenna radiation pattern. The three main characteristic of the radiation or directivity pattern, we consider in the simulation is the half-power or -3dB beam-width, the peak level of the first sidelobe relative to mainlobe and the realized antenna gain  $G_0$ . The ARS-308 industrial radar sensor is built with a unique mechanically scanning antenna concept as found in [7]. In [88], the authors presented a high-resolution imaging radar sensor prototype for vehicle applications with a similar antenna concept. The antenna scans over the sensor's FOV and the output power is given as a function of the scan position. For the model design, we used the functional principle presented there as a basis. According to [94, p. 228] to achieve an operational antenna performance with narrow mainlobe width and a low sidelobe level different type of aperture antennas can be considered. Based on the angular parameters with regard to the antenna beam width in azimuth and elevation direction found in the datasheet in accordance with published antenna parameters in [88], the radar antenna can be considered as a fan-shaped beam antenna. A two-dimensional planar array in a form of a rectangular aperture or radiation surface [77, p. 316] with cosine shaping aperture tapering [95] can be used to realize a kind of fan-shaped antenna radiation pattern [94, p. 55, p. 279]. According to our modeling consideration, we simulate the received power, which is a contribution of the main- and sidelobe reflections collected over the integration period during a scanning interval. In the simulation to generate a synthetic antenna pattern we used the equations given in [95]. Figure 4.6 shows the simulated antenna radiation pattern in azimuth direction (blue/solid) and in elevation direction (red/dashed) on a logarithmic scale, while Fig. 4.7 shows the 3D antenna gain pattern in a 3D plot.

\* **Propagation factor**

The link between the environmental components and the radar sensor is the transmission path through which the EM waves propagate. The characteristics of the EM propagation channel can vary from di-



## 4. Methodology

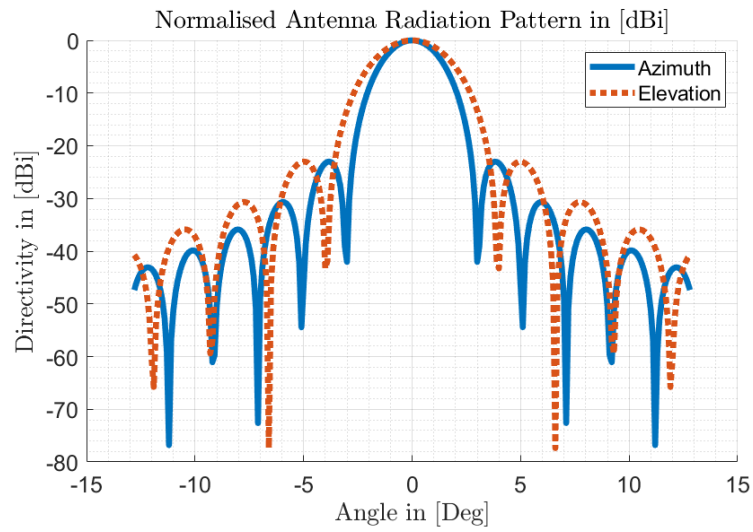


Figure 4.6.: Synthetic Antenna Radiation Pattern

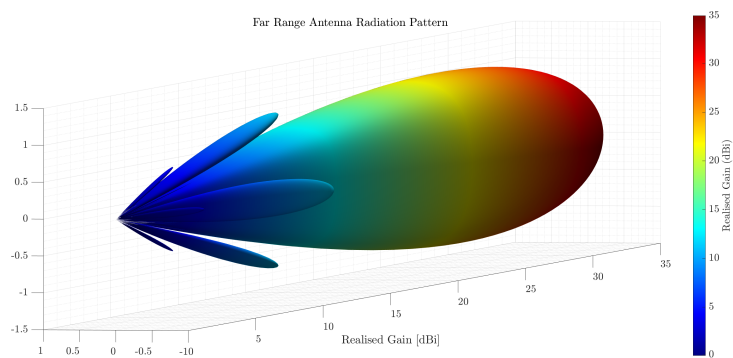


Figure 4.7.: Synthetic Antenna Pattern in 3D plot

rect line-of-sight to partially or completely obscured environmental components caused by other road users under influence of different weather conditions, hence it can be described as extremely random. In general, the behavior of the propagation channel is the combination of the impacts of a number of physical effects described by the propagation factor  $F$ , see [77, p. 118]. Modelling of the EM wave propagation channel is the subject of many research works, but it is usually done on a statistical basis [76, p. 69]. Radar detection is generally characterized by the processing of back scattered EM waves in our case under consideration of a monostatic radar geometry. Since we decided to use only the real radar sensor subject of the simulation, the propagation channel was analyzed empirically using the real radar output without applying any high-frequency reference measurement equipment. The experiment was performed following the Euro-NCAP Global Vehicle Target validation procedure [23, App. A3, Fig. A8, p. 21], and resulted in a so-called multipath fading pattern. Detailed description about the measurement process and results can be found in [63]. In [77, p. 142] a detailed description of multipath EM wave propagation with respect to radar detection can be found. For the simulation, we consider the road surface, side barriers or guard rails and other vehicles for the indirect reflection path only if the necessary geometric, position and distance requirements are fulfilled. In order to be able to reproduce the resulting signal strength or RCS pattern, two basic propagation phenomena, namely reflection and scattering mechanism were incorporated in the model. According to the authors in [76, p.70], the signal strength can vary by three or four orders of magnitude even if a situation changes by only a small fraction of the wavelength. Therefore, the propagation channel is usually characterized by the local average signal power measured over a distance of 5-40 times the wavelength. In the presented simulation the 2-ray ground reflection model is applied to every range bin and receiver channel defined by the bounding box calculated to represent the ground clearance geometry under the vehicle body. The simulated received signal strength is averaged over the physical length of the target vehicle and receiver channels. The two-way propagation factor for a monostatic radar geometry is given by (4.5), [77, p. 143].

$$F^4 = |1 + 2 \cdot \Gamma \cdot \cos(k_\lambda \Delta R) + (\Gamma \cdot \cos(k_\lambda \Delta R))^2|^2, \quad (4.5)$$

Where  $\mathbf{1}$  is the magnitude of the E-field in the direct path,  $\Gamma$  the complex Fresnel reflection coefficient of the surface,  $k_\lambda$  is the wave number and  $\Delta R$  is the difference in range between the direct path and the reflected path. The reflection coefficient  $\Gamma$  is a function of the boundary admittance and the angle of incidence, it depends on the carrier frequency of transmitted signal, expressed to vertical and horizontal E-field polarization to the plane of incidence. [76,

p. 79]. The Fresnel reflection coefficient  $\Gamma$  we incorporated into the simulation is given according to [77, p. 148],

$$\Gamma = \Gamma_0 \cdot (\rho_s + \rho_d) , \quad (4.6)$$

where  $\Gamma_0$  is a smooth earth reflection coefficient,  $\rho_s$  represents the specular while  $\rho_d$  the diffuse roughness factor. A detailed description of theoretical background and derivation of equations can be found in [77, ch. 4, p. 117].

The backscattered signal in a radar image is composed of many small scatterers whose positions are distributed across the field of view. As defined in the Section 4.2.3, the sensor's field of view is divided into spatial areas that represent the resolution cells. The resolution cell is then the smallest area in which the contribution of (finitely) many, interfering scatterers is combined into one amplitude value. According to [21] the backscattering process in one resolution cell, can be defined by calculating the sum of the contribution of the particular scatterer located at  $x, y$  in the sensor's coordinate system. The reflection coefficient  $\sigma_{SBI}$  for every resolution cell can then be written as:

$$\sigma_{SBI} = Pois_{SBI} \cdot \sum_{i=1}^N b_i \delta(x - x_i) \delta(y - y_i) , \quad (4.7)$$

where  $b_i$  is a random number, and  $\delta$  is the impulse of the scatterer. Since FMCW signal processing is characterized by the coherent process interval (CPI) in terms of the number of the integrated phase-locked chirps required for a given velocity resolution  $N_{CPI_{Tx}}$ , we extend equation 4.7 by the random variable  $Pois_{SBI}(r, \alpha)$ ,

$$Pois_{SBI}(r, \alpha) = \frac{\alpha^r}{r!} \cdot e^{-\alpha} , \quad (4.8)$$

with

$$\alpha = N_{CPI_{Tx}} / 2 . \quad (4.9)$$

We define the sum of the individual scatterers for each  $N$  and  $b_i$  as 1 and assume that the backscattering process is a random sequence within a CPI and can be described as a Poisson distribution. With this simplification, the amplitude of the backscattered signal is a function of a statistical Poisson random process representing the number of coherently received chirps from each resolution cell labelled with the space-bin indicator (SBI), see section 4.2.3. After calculating the signal amplitude in each SB for all environment components, the joint RA map is calculated by summing the individual amplitude values.

### III Signal Processing

The output of the RUS can be described by its detections in the sensor FOV, which may be the result of some sophisticated detection algorithms unknown

to us, without tracking and classification. The detection is an automatically performed decision, comparing the received signal with a threshold value, whether the target of interest exist in the antenna beam. The detection process is performed on the preprocessed signal by predicting the detection threshold signal level under the influence of external noise, internal receiver thermal noise, clutter and noise jamming of other traffic participant equipped with radar sensor operates in a same frequency band. As the noise level can change rapidly, the adaptive threshold setting is automatically adjusted to the current noise level while maintaining the predefined CFAR [77, Ch. 15, p. 547, ].

- **FFT Interpolation with Zero padding** In our modelling approach, the data is preprocessed before applying the CFAR detector by generating a denser set of spatial frequencies. In digital signal processing, a better approximation of the peak frequency position can be achieved by quadratic interpolation or by zero padding the data acquired at a lower sampling rate and performing a higher-points FFT, see [77, p. 519]. According to [55, p. 24], in the practice for an input sequence of sampled signal the frequency spectra can be calculated by applying the Discrete Fourier Transform (DFT). However in micro controllers, the DFT is performed using the fast Fourier transform algorithm. In the hardware implementation of the FFT algorithm, especially in older realisations, the length of the input sequence applied to the FFT, had to be a power of two. If this condition was not met for the input sequence, zeros were appended to the data set to increase the length of the input sequence to a power of two. According to the authors in [77, p. 654], a less computationally intensive method is to implement a quadratic interpolation by fitting a parabola through each apparent peak and the two adjacent samples, without introducing unwanted frequencies.

To reproduce the accuracy of the data output in terms of the azimuth angle and radial range measurement of the real radar sensor, an FFT interpolation with zero-padding is applied on a spatial domain. We choose zero-padding instead of quadratic interpolation because zero-padding smooths the spectrum with a  $\text{sinc}(x)$  function, which leads to introducing falsified frequency peaks that may not be present in the original input data, see [55, p. 75]. We use this effect to increase the uncertainty of the received signal before estimating the detection threshold.

- **CA-CFAR Detection Process** In the last processing step, in order to reduce the amount of unwanted detections, an automatic detection threshold detector is applied. According to the authors in [77, p. 589] for a given statistical back scattering process, a CFAR algorithm can be applied to evaluate the presence of targets. The evaluation is done by the comparison of signal power in every resolution cell compared to the local average of the adjacent cells. According to the properties of different CFAR algorithms given in [77, p. 532], [79] we implemented the 1D Cell Averaging (CA) and 1D Ordered Statistic (OS) CFAR models for

automatically setting the detection threshold for radar target extraction based on the RA map. Although the 1D CA-CFAR performed well in distance measurement and the 1D OS-CFAR performed well in azimuth detection in accordance with theory, the latter was computationally too expensive. This led to the implementation of a modified 2D-FFT based realization of a well-known CA-CFAR algorithm in [79].

- **Association of relative velocity** signal. FMCW radar technology is characterized by its ability to analyze the frequency spectra of the backscattered signal in a very advanced way. The frequency analysis is performed in two stages, see Fig. 4.3. The first FFT frequency analysis of each received pulse or “chirp” determines the distance bin number, which is directly related to the radial distance. The second FFT frequency analysis is applied to a set of range-related frequencies received at the target vehicle during the dwell time period defined by the coherent processing interval, which determines the Doppler frequency shift caused by a moving vehicle. There may be additional Doppler modulation in the frequency spectrum generated by the oscillating or rotating moving parts on the target vehicle, defined as a micro-Doppler ( $\mu$ Doppler) effect, [14, 104].

According to the environment component classes defined in Section 4.2.3, four different speed signals can be distinguished to represent the speed signals measured by the real sensor.

The relative velocity measured by the radar sensor is the result of the frequency analysis of the Doppler-shifted signal, which is determined by the vector component of the velocity vectors of the target vehicle acting along the line of sight in radial direction to the radar sensor. In real radar application the resulted speed vector is a function of the azimuth and elevation angle in a radar coordination system. As shown in the schematic representation of the model in Fig. 4.5, the relative velocities are calculated on a 2D plane and assigned to the high-resolution data set, taking only the azimuth angle into account.

Consequently, the relative velocity for static environment components with respect to the azimuth angle can be defined as a function of the velocity of the EGO vehicle. The relative speed of the Dynamic EC-s can be determined by calculating the difference between the radial speed components of the EGO and the target vehicle. The relative speed of Dynamic-plus EC-s are characterized by the  $\mu$ Doppler Effect resulted from the rotational motion of the wheels. The  $\mu$ Doppler effect extends the target attribute with some characteristic information about rotating or vibrating parts of the target vehicle, which also allows target classification, [104]. In the simulation, speed signals related to the wheels are calculated according to our observations in the real radar measurement shown in Fig. 4.8, which are characterized by the deviation of the RCS and speed values compared to the vehicle body.

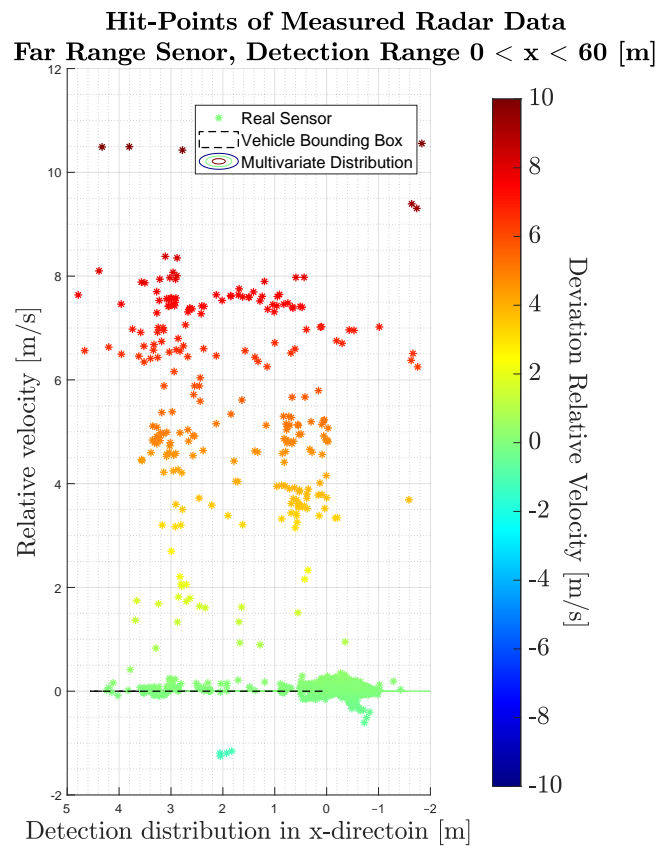


Figure 4.8.: Measured Relative Velocity on the Wheels, with a Far-range sensor in Target Mode

#### IV Error Model

In order to include some uncertainty in the synthetic radar point cloud data generation and at the same time increase the fidelity to the real radar sensor, the error model shown in Fig. 4.4, can be defined according to Fig. 4.9.

- **Generic Back Scattering Process** The error model can be defined based on the schematic drawing of the virtual sensor. The generic backscattering mechanism related to the smallest evaluation area is assumed to be a random process that can be described by the statistical superposition of a finite number of uniformly distributed isotropic and uncorrelated point scatterers. Fast chirp modulation FMCW radars use multi pulse processing to evaluate the Doppler shift of moving targets and improve the signal-to-noise ratio with the number of detected pulses in a CPI or dwell time. With a mechanically scanning radar such as the ARS-308, the target may only be in the centre of the antenna beam for a few pulses in a processed CPI, resulting in a loss of beam shape, [77, p. 69]. To incorporate the influence of the number of pulses received in a CPI on detection in combination with the stochastic nature of EM wave propagation into the modelling, we simulate the sum of backscattered pulses for a non-fluctuating target as a Poisson random variable. This simplification can be made assuming a large number of isotropic scatterers, all of which have a similar reflection coefficient. According to the author in [55, p. 81], for a real target consisting of a large number of scatterers with nearly the same reflection coefficient, the superposition of the phase term is nearly zero. Thus, the total reflection coefficient can be given by the sum of the reflection coefficients of the individual isotropic scatterers.
- **Complex White Gaussian Noise In-phase and Quadrature (I/Q Phase Channel).** The active components of the radar sensor, including the antenna, emit EM waves at almost all frequencies. This thermal noise is always present, so the backscattered signal received from the target vehicle or background at the receiver output is always a combination of the noise and the target signal. The ratio of the target signal power to noise power is referred to as the signal-to-noise ratio (SNR). The power spectral density of the thermal noise is constant, the noise power is uniformly distributed over the range of frequencies in which the radar operates defined by the receiver bandwidth  $B$ . Since in our sensor model we consider the coherent integration of a received pulse, the SNR for a CPI consisting of  $N_{CPI_{RX}}$  pulses can be calculated as the SNR of one pulse times the number of pulses  $N_{CPI_{RX}}$  [55, p. 77]. The power of the thermal noise  $P_n$  in one pulse is given by [77, p. 65], and reads

$$P_n = k \cdot T_0 \cdot F \cdot B , \quad (4.10)$$

where  $k$  is the Boltzmann's constant,  $T_0$  is the ambient temperature (290 K), and  $F$  is the *receiver noise figure* of the radar subsystem. The noise figure is a system parameter in which all thermal noise power contributions of the individual radar receiver subsystems or receiver

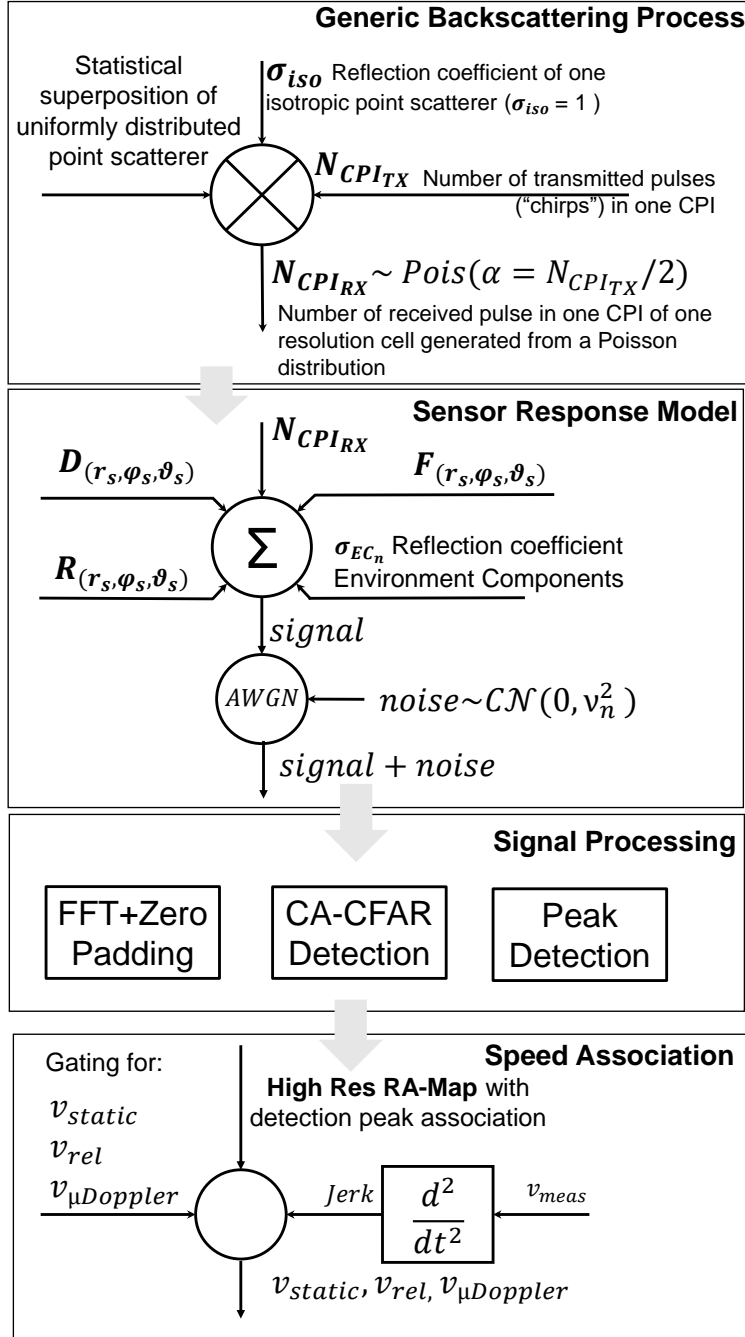


Figure 4.9.: Error Model



stages are summarized. For more details please refer to [77, p. 404] or [76, p. 565]. In the simulation, the practical value of  $F = 4.5 \text{ dB}$  was used for the noise figure as defined for a real system in [88], and the thermal noise is modelled as additive complex white Gaussian noise. Caution should be taken when specifying this, as the letter  $F$  is also used for the propagation factor in radar literature.

- **Acceleration error (Jerk)** To extract the radial target velocity a second Fourier analysis can be done to every range bin signal. A target vehicle with a constant speed will introduce a linear phase shift between the consecutive pulses in a CPI, caused by the changes in target range between pulses [77, p. 292]. The generated frequency spectrum consists of equally spaced frequencies, which can be easily converted to radial velocities. In ideal case, a moving target produces a sharp peak at its Doppler frequency but in the reality this peak spreads out over several frequency bins [55, p. 77]. The acceleration or jerk of the target vehicle inducing an unsteady Doppler signals resulting in Doppler frequency migration [77, p. 841]. Since a linear phase change is assumed, an error occurs due to the abrupt changes in vehicle movement. The radial speed estimation error was observable in the measurement data of the RUS with respect to target vehicle's radial acceleration and jerk.

### 4.3. Evaluation methodology

#### 4.3.1. Dynamic Ground Truth Sensor Model Validation approach

The DGT-SMV approach is depicted in Figure 4.10. The process starts with the definition of driving scenarios (*scenario definition*), which are related to a specific radar detection phenomena of the evaluated sensor, such as multipath propagation and separation capability [36, 101]. In the next step, the tests are performed on a proving ground or in public traffic (*real test drive*), including an accurate measurement equipment.

The measurement data is used to label the recorded low-level radar point cloud sensor output data (*measurement data labelling*). In order to provide a method for the evaluation of synthetically generated radar point clouds data compared to its real counterpart, the test drives are replayed in a detailed virtual representation using a digital twin (*virtual sensor replay*). The sensor then produces the virtual low-level sensor output that is finally compared with the measured sensor output (*performance evaluation*) with statistical methods. The individual steps in the DGT-SMV process are described in detail in the next sections.

#### 4.3.2. On-Road Measurements

Virtual testing can be conducted on a road section edited with a simple road editor in the initial development phase; however, commercially available simulation programs can be also used to re-simulate the real-world measurements of specific testing sites. Ultra-High-Definition Maps [101] often also referred to as Digital-

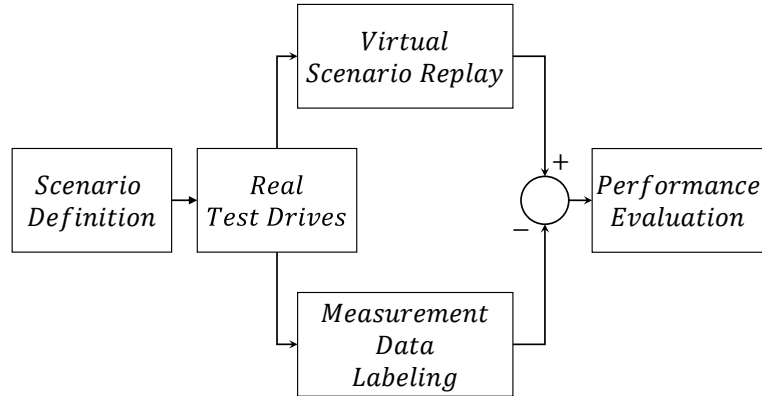


Figure 4.10.: Process flow for the sensor model benchmark method DGT-SMV

Twins allow the simulation of existing real road geometries, thus, facilitating the realistic modelling of the virtual environment. This method allows the analysis of the complete functional chain of an ADF, starting with the detection performance of environment perception sensors up to the actuators of the intervention subsystems.

On the digital map, one can accurately measure the position, direction and movement of the test vehicles, as well as the reference distance to static objects, such as lane markings, guardrails and curbs using a high precision inertial measurement unit.

Driving manoeuvres are an essential part of the assessment methodology, especially with regard to the availability of the Digital-Twin of the road section or test site on which the measurements are taken. It should be mentioned here that reproducing measurements in a virtual world based on highly accurate positional data provided by a suitable ground truth system may represent the state of the art in the modelling community. However, there are also digital twins of commonly used test sites, but these represent a highly controlled environment.

The driving manoeuvres used to develop the presented evaluation methodology and to demonstrate the performance of the radar sensor model presented in this paper were acquired in a measurement campaign in joint collaboration with the Department of Automotive Engineering of the Budapest University of Technology and Economics. [101] The special feature of the measurement campaign is not only the high number of participating test vehicles equipped with the high-precision GT system, but also in addition to the fact that it took place on a section of motorway not yet opened to public traffic, the Digital-Twin was also provided.

The availability of a Digital-Twin of a real road section, which has since been released for public use, allows sensor models to be developed and evaluated in a real traffic environment, leading to more reliable generation of synthetic radar point cloud data for subsequent perception algorithms.

### 4.3.3. Re-Simulation of Experiments

When the on-road measurements are taken, it is possible to simulate exactly the same scenarios in the virtual simulation by using the recorded trajectories of the vehicles provided by the GT reference measurement system and the Digital Twin. IPG CarMaker<sup>®</sup> was selected for the simulation environment, as this software package provides a Virtual Vehicle Environment (VVE), which represents a Multi-Body-Simulation Environment of a vehicle. This includes, among other mathematical formulae, the equations for calculating e.g. movements and kinematics, but also the models of the perception sensors used to generate the input for ADAS applications are included here. For the implementation of the Digital-Twin of the test site, Joanneum Research Forschungsgesellschaft, also a partner in the measurement campaign, provided a detailed Ultra High-Definition (UHD) map [101]. This map represents a highly accurate reproduction of the test site, in an OpenDRIVE file format. As the road geometry in IPG CarMaker<sup>®</sup> [49] is defined in a RD5 file format, the UHD map in in OpenDRIVE format has to be converted.

The virtual map includes the following road geometry items [101]:

- lane borders and markings,
- lane centre lines,
- curbs and barriers,
- traffic signs and light pole and
- road markings.

This detailed description of the environment makes it possible to reduce deviations between the real and virtual world to a minimum. In addition to the preparation of the virtual environment, the recorded trajectories must be transformed from the geodetic WGS-84 coordinate system to a metric coordinate system, which is used in the simulation. Since the operating radius of the experiments is smaller than 50 km, the curvature of the earth can be neglected, and the transformation can be performed on a plane metric coordinate system, which is spanned relative to a reference point [10].

The IPG CarMaker simulation tool [49] distinguishes between two categories of vehicles, the ego vehicle and traffic vehicle. The first one represents the Vehicle Under Test (VUT), including a multi-body representation where all sub-systems can be changed by the user, e.g., mounting ADAS sensors to the vehicle, whereas the traffic vehicle only represents a motion model, which is, in our case, a single-track model. In order to make the traffic vehicle follow the previously recorded and afterwards transformed trajectory, the exact position in  $x$ - and  $y$ -direction was given to the vehicle at every time step.

The ego vehicle is controlled via the IPG Driver, a mathematical representation of the behavior of a human. This Driver performs any interaction to the car, e.g., steering or accelerating/braking. If the ego vehicle is now given a target trajectory, this would be approximated by the IPG Driver, just as a human driver would do. However, since in our case, an exact following of the recorded trajectories is absolutely necessary for the evaluation of the sensor model, a by-pass has to be performed on the driver model. This was done with a modification in the C-Code

interface provided by the software vendor IPG. With this adaptation, the ego vehicle is now able to reproduce the same trajectory in the virtual environment as it was measured in the real world, ignoring any intervention by the IPG driver and thereby deactivating the dynamic vehicle simulation.

For the replay of the scenarios, a standard IPG-Car parameter set was used, including models of powertrain, tires, chassis, steering, aerodynamics and sensors. Since the ego vehicle exactly follows the recorded trajectory, no detailed parameter setting is required. The simulation software offers a number of different sensor models, which operate at different levels, ranging from ideal sensors to phenomenological sensors and to raw signal interfaces.

Since the presented thesis focuses on the development and validation of radar sensor models providing low-level radar point clouds data, the commercial RSI radar-sensor model from IPG CarMaker V 8.1.1<sup>®</sup>[49] is considered. The use of CarMaker's RSI radar sensor model is intended for both the development of the assessment method and the comparison of the presented model and described in detail.

### 4.3.4. Commercial Radar Sensor Model

This sensor model provided by IPG CarMaker imitates the physical wave propagation by an optical ray-tracing approach. It includes the major effects of wave propagation, e.g.,

- Multipath/repeated path propagation.
- Relative Doppler shift.
- Road clutter.
- False positive/negative detections of targets.

Using this ray tracing based sensor model in a virtual environment requires the modelling of material properties of objects, such as the relative electric permittivity for electromagnetic waves and scattering effects. These parameters have a significant influence on the reflected direction and field strength of the reflected wave. The reflections are created by a detailed 3D surface in the visualisation. In the used set-up, the default values provided by the simulation tool for a 77 GHz radar were used.

### 4.3.5. Parameter Setting of the Sensor Model

Radar sensors are influenced by a multitude of parameters, which makes the parameter setting of such models complex. To ensure the comparability of the sensor model, the real hardware was treated like a black box so the sensor model was set with those parameters given in the data sheet provided by the manufacturer of the Radar sensor. To set the parameters for the atmospheric environment, temperatures and in particular the data sheet based parameters: Field of View, Range, Cycle time, Max. Channels, Frequency, Separability Distance, Separability Azimuth, Separability Elevation, and Separability Speed was used.

With the additionally offered two "design" parameters and scattering effect, CarMaker<sup>®</sup> gives users the possibility to fine tune the sensor model. However,

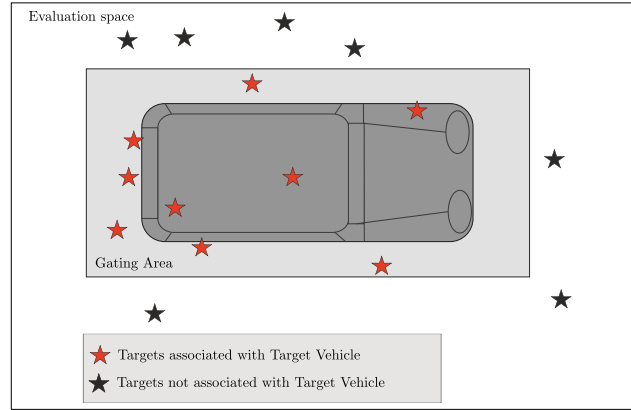


Figure 4.11.: Gating area of the target vehicle with and with not associated reflection points according to [105].

one parameter given in the data sheet of the real hardware was not adjustable in the software package. The inaccuracy depending on the distance of the detected object was afterwards superimposed to the simulation results, as this leads to more robust results. To make this modified data visible in the results, this data is marked as *modified data* in [105, 49].

### 4.3.6. Labelling of Radar Measurement Data

In order to assign the individual reflection points of the radar sensor to the dynamic targets, a method that is already known in the field of object tracking is used, namely the gating technique. Using the ground truth information of the dynamic objects, target points only in a specific shaped area around an object of interest are considered. Figure 4.11 represents the gating area with the associated and not associated target points. The shape of the gating area can be variously designed, such as rectangular or elliptical [110].

In accordance with the shape of an average car, we used a rectangular shape. In this case, only dynamic objects are considered, as no static object information is available in the virtual map, e.g., bridge heads or overhead traffic signs. This means that the evaluation is limited to moving objects where the ground truth is measured with the RTK-GPS IMU measurement equipment but is also applicable to static objects, given that the ground truth is referenced.

### 4.3.7. Evaluation Procedure

Different evaluation metrics are given in literature, such as comparison of occupancy grid maps, statistical hypothesis testing, confidence intervals, correlation measurements and the generation of probability density functions [83, 74, 54, 1]. In contrast to object list based deterministic sensor models, physical non-deterministic sensor models do not allow a direct comparison between experimental observations and simulation models. To make the stochastic process of the physical radar sensor model comparable, including the physical attributes, e.g., the relative velocity or

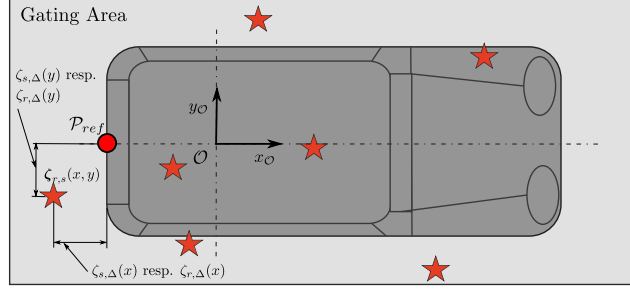


Figure 4.12.: Reference point  $\mathcal{P}_{ref}(x, y)$  on the dynamic object ; Deviation target points real sensor to reference point  $\zeta_{r,\Delta}(x, y)$  and deviation target points simulation to reference point  $\zeta_{s,\Delta}(x, y)$  according to [105].

RCS value, statistical evaluation methods are best suited to describe the distribution of parameters in space and time.

Using previously labelled data, it is possible to evaluate them by statistical means in such a way that a quantitative statement can be made about the quality of the sensor model used in comparison to the real hardware. Introducing a reference point  $\mathcal{P}_{ref}(x, y)$  on the target vehicle enables the calculation of the deviation on every radar detection point to the ground truth of the dynamic object, see Figure 4.12. The radar point clouds data are represented by the vector  $\zeta_r$  for the measured sensor data and  $\zeta_s$  for the simulated data. The deviation is calculated with

$$\zeta_{s,\Delta}(x, y) = \zeta_s(x, y) - \mathcal{P}_{ref}(x, y), \quad (4.11)$$

$$\zeta_{r,\Delta}(x, y) = \zeta_r(x, y) - \mathcal{P}_{ref}(x, y). \quad (4.12)$$

where  $\zeta_{s,\Delta}$  representing the deviation of the simulation data and  $\zeta_{r,\Delta}$  representing the deviation of the real sensor data to the reference point.

Assuming radar sensors are subject to a highly stochastic process, the detection points can be treated as realizations of a distribution function [94, p. 26]. Using methods, including kernel density estimation (KDE), a probability density function (PDF) can be generated from the large number of realizations.

#### 4.3.8. Validation Metrics for Comparing Probability Distributions

The validation of simulation models is based on the numerical comparison of data sets from experimental observations and the computational model output for a given use case. To quantify the comparison, validation metrics can be defined to measure the difference between the physical observation and the simulated output. Whether comparing measured physical quantities or virtual simulations, observed values contain uncertainties. In the presence of uncertainties, the observed values subject to validation are samples from a distribution of possible measured values, which are usually unknown.

To optimally quantify the difference or the similarity between distributions, we need the actual distributions. For the empirical data sets resulting from the experimental observations (real radar sensor) and the output of the computational model (radar sensor model), we do not know the actual distribution or even its

shape. Although one can always make assumptions (parametric) or kernel density estimates, in practice these are not quite ideal as their analysis is limited to certain types of distributions or kernels used. To stay as close as possible to the data, we therefore consider a non-parametric divergence measure. Non-parametric models are extremely useful when moving from discrete data to probability functions or distributions.

Non-parametric approaches are another way to estimate distributions. Such methods can be used to map discrete distributions of any shape. The simplest implementation of non-parametric distribution estimation is the histogram. Histograms benefit from knowledge of the data sets to be estimated and require fine-tuning to achieve optimal estimation results. In our application, this knowledge is available, since the bin width of the histogram can be determined according to the real sensor data sheet.

As stated above, a metric is a mathematical operator that gives a formal measure of the difference between experimental and model results. The metric plays a central role as it can be used to describe the fidelity of sensor models used to validate ADAS/AD systems. A low metric value means a good match and vice versa. According to [1] the metric can be defined by the following criteria: it must be intuitively understandable, applicable to both deterministic and non-deterministic data, a good metric defines a confidence interval as a function of the number of measured data and meet the mathematical properties of the metric.

The variables measured by perception sensors are usually non-parametric due to the highly stochastic nature of the output data [36]. Based on these properties, one possible description of the correspondence between synthetic and real perceptual data could be the comparison of their probability distribution functions. In the context of validating perception-sensor models, the most useful characterization appears to be the comparison of the distributions of random variables and the shapes of the corresponding observations. Random variables whose distribution functions are the same are called "distribution inequalities".

If the shapes of the distributions are not exactly the same, the difference can be measured using several possible measures. The authors have described in [66] some validation metrics for deterministic and probabilistic data that are used to validate computational models by quantifying the information from physical and simulated observations. In the context of this study, the use of the Jensen-Shannon divergence (JSD) [56] is proposed as it provides a quantified measure of the results of a comparison between two or more discrete probability distributions in a normalised manner.

The JSD, is a smoothed version of the Kullback-Leibler Divergence (KLD) described in detail in [1, 66]. The JSD is symmetric, bounded, and provides a true metric in the sense of the mathematics. We consider a true discrete probability distribution  $\mathcal{P}$  and its approximation  $\mathcal{Q}$  over the values taken on by the random variable. The Jensen-Shannon Divergence calculated with

$$DJS(\mathcal{P}||\mathcal{Q}) = \frac{1}{2}DKL(\mathcal{P}||\mathcal{M}) + \frac{1}{2}DKL(\mathcal{Q}||\mathcal{M}) \quad (4.13)$$

where  $\mathcal{M}$  is the mean distribution for  $\mathcal{P}$  and  $\mathcal{Q}$ , as given by

$$\mathcal{M} = \frac{\mathcal{P} + \mathcal{Q}}{2} \quad (4.14)$$

The Jensen–Shannon Divergence uses the Kullback–Leibler Divergence to calculate a normalized measure. If  $\mathcal{P}$  and  $\mathcal{Q}$  describe the probability distribution of two discrete random variables, the KL divergence is calculated according to Equation 4.15.

$$DKL(\mathcal{P}||\mathcal{Q}) = \sum_{i=1} \mathcal{P}_i(x) \log\left(\frac{\mathcal{P}_i x}{\mathcal{Q}_i x}\right) \quad (4.15)$$

Since the JS Divergence is a smoothed and normalised measure from the KL Divergence, it provides a more suitable measure. Furthermore JSD is upper-bounded and symmetric facilitating it can be easily integrated into development processes. By definition, the square root of the Jensen–Shannon divergence describes the Jensen–Shannon distance.

$$DistJS(\mathcal{P}||\mathcal{Q}) = \sqrt{DJS(\mathcal{P}||\mathcal{Q})} \quad (4.16)$$

As both the divergence  $DJS(\mathcal{P}||\mathcal{Q})$  and the distance  $DistJS(\mathcal{P}||\mathcal{Q})$  are symmetric with respect to the arguments  $\mathcal{P}$  and  $\mathcal{Q}$  and the JS-Divergence is always non-negative and also upper bounded, the value of  $DJS(\mathcal{P}||\mathcal{Q})$  is always a real number in the closed interval of  $[0; 1]$ .

$$0 \leq DJS(\mathcal{P}||\mathcal{Q}) \leq 1 \quad (4.17)$$

If the value is 0, the two distributions  $\mathcal{P}$  and  $\mathcal{Q}$  are the same, if the value is 1, the two distributions are as different as possible. For better interpretation we present JSD in percentage values in the following. As  $DistJS(\mathcal{P}||\mathcal{Q})$  fulfils the mathematical properties of a true metric [22], such as symmetry, triangle inequality and identity, the Jensen–Shannon Distance is a valid metric distance.



## 5. Results and discussion

This thesis essentially addresses three related but separately developed overarching problems closely related to virtual V&V testing activities and offers a solution by identifying the factors that hinder or prevent widespread adoption.

Accordingly, this chapter presents the results of the literature review in the form of a proposal for a new classification procedure and the online availability of the database as well as the simulation results of the radar sensor model presented in this thesis, which inherently also demonstrate the applicability and efficiency of the DGT-SMV approach for evaluating perceptual sensor models also presented in this thesis.

### 5.1. Survey on Modelling of Automotive Radar Sensors and Modelling Approaches

This section presents the outcomes of the literature review on the state-of-the-art of radar sensor modelling methods. Section 2 summarises the various models and simulation approaches described in the literature as well as their classifications. Based on the findings Section 2.7 presents a new classification method with regard to its use in the vehicle development process. The new classes are defined in ascending order of complexity and use along the V-Model integration approach as *operating models*, *functional models*, *technical models* and *individual models* respectively. The association of the different models in relation to the V-Model is already shown in Figure 2.2. Further all those different approaches and the classifications were summarised in a comprehensive table that combines previous classifications with a newly introduced approach. Finally, a web link was provided to the full classification data, presented as a dynamic spreadsheet that is available to the public at: <https://doi.org/10.3217/kgg17-wq710>.

According to this extensive literature review, the novel contributions of the presented research was deduced, see Section 2.8.

### 5.2. Process chain for implementing the sensor model development method

This section presents the final results of the model development procedure introduced in this thesis, using the evaluation method described in Section 4.3 to demonstrate the ability of the sensor model developed in Section 4.2 to synthetically reproduce the characteristics of real radar point cloud data obtained by performing driving scenarios as defined in Section 3.2.2 with the measurement setup defined in Section 4.1. An overview of the process chain is shown in Figure 5.1

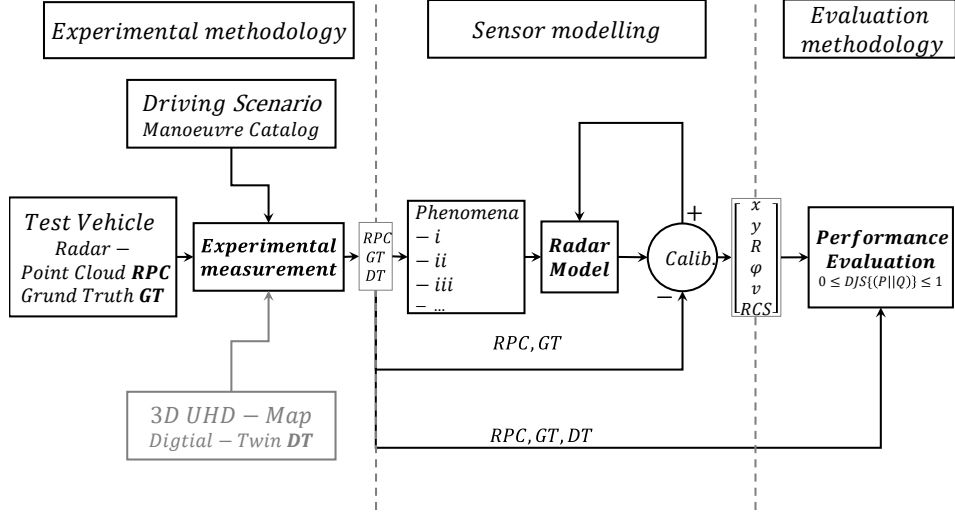


Figure 5.1.: Summary diagram for the realisation of the sensor model development method.

The **experimental methodology** includes the definition, implementation and calibration of the measurement system as well as the definition of the driving manoeuvres and finally the interpretation of the measurement results. The measurement provides the data on which the observation was based and contributes to the definition of the phenomena associated with radar detection. The importance of measurement in terms of the quality of the recorded measurement data can be further increased by considering its own contribution to the assessment process in the form of the assessment result as shown in Figure 5.1

Several phenomena have been identified in **Sensor modeling** that are related either to the radar targets and driving environment (i–iii), to the radar signal processing (iv–v), or to the characteristics of the hardware architecture of the radar sensor (vi). Since the sensor model developed in this work aims to synthetically generate radar point cloud data to reenact real measured radar detections, the superposition of all these phenomena were considered.

In the **Evaluation methodology** the assessment and demonstration of the translation of all observations into a radar sensor model by developing a novel semi-physical modelling method is presented using the DGT-SMV evaluation method also developed in this thesis. The potential and performance of both the radar sensor modelling and the assessing method are illustrated using one selected driving manoeuvre—the *Range test target leaving*, which is depicted in Figure 5.2.

### 5.3. Driving manoeuvre definition

The selected driving scenario defined as a combination of the subsets shown in Fig. 3.2 as:

$$S = [CPL, DYD, CTS, STR, RED, DYL, DYW] \quad (5.1)$$

This driving scenario contains four driving manoeuvres with varying target vehicle speed parameters. The initial state is defined as follows. Both vehicles with activated FSRA (Stop and Go ACC) and follow time set to the minimum reached the initial speed, which was set to 30 km/h for this manoeuvre. The distance to the TARGET vehicle controlled by the FSRA system of the EGO vehicle is in steady state condition. After the initial conditions are reached, the driver of the target vehicle changes the set speed of the FSRA system from the initial 30 km/h to  $v_{\text{set\_TAR}} = v_{1-4\_TAR}$  and leaves the EGO vehicle.

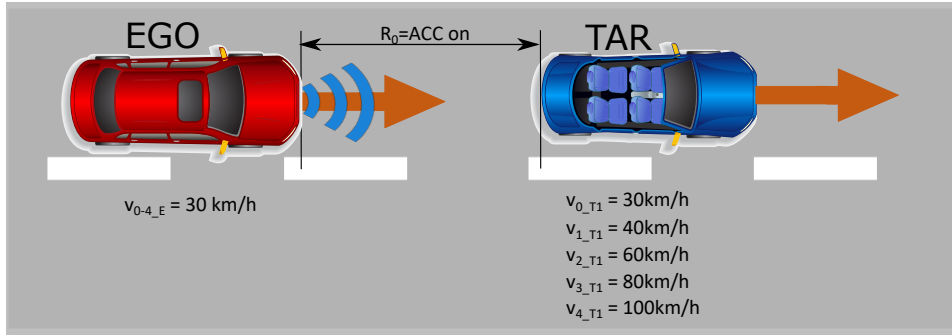


Figure 5.2.: Target leaving with constant delta speed.

The measurement is considered complete when the distance between the vehicles has reached 250 m. To obtain the best measurement result, the angular orientation deviation (with respect to the direction of movement of the sensor) of the vehicles tested shall be kept below 1 degree. Unfortunately, the highway section used in this joint research project had a slightly curved characteristic, and therefore the angular orientation deviation continuously changes during the test runs and increases over 1 degree. This road geometry will lead to that the reflection points on a cumulative representation are shifted.

In the following subsections, the results of the statistical analysis showing the behaviour and differences between the radar sensor model developed in this work and a sensor model available for commercial applications are presented and a final comparison of the two models is made. The point cloud data of the real and virtual radar sensor were divided into a close range (0-60 m) and a far range (60-200 m) for the commercial sensor model and (60-202.5 m) for the model of this work, according to the real radar characteristics. The radar sensor used can provide point cloud data in the near range between 0 and 60 m in both near and far range configuration modes, resulting in an overlap of the two sensor modes. For this reason, the far range was further subdivided into the 0 to 60 m and 60 to 200 m data for a detailed analysis.

#### 5.4. Evaluation of modelling approach of the presented radar sensor model

Figure 5.3 shows the spatial distribution of the measured (a) and synthetically generated (b) radar point cloud data for a near-range detection sector, on a 2D plane in the sensor coordinate system related to the dynamic target vehicle. The colour code of each radar detection point (Hit-point) indicates its velocity deviation with respect to the measured radial velocity provided by the GT reference measurement system. The dashed line shows the boundary line of the target vehicle, and the contour lines in this diagram represent the multivariate distribution of the radar point cloud. Figure 5.3(a) is a top view of Fig. 4.8. These figures facilitate to understand that, in addition to the obvious radar detections at the rear of the vehicle, there are also detections that can be attributed to the installation position of the wheels. Figure 5.4 shows the PDF's of the divergence from the reference point  $\mathcal{P}_{ref}(x, y)$  in  $x$ - and  $y$ -direction of the measured and simulated radar point cloud. The reference point  $\mathcal{P}_{ref}(x, y)$  is provided by the GT reference system, for more details please refer to [63]. The probability distribution can not only be used to qualitatively assess the distribution of the reflections, but also serves as a basis for calculating the Jensen-Shannon Divergence. Figure 5.4(a) shows the divergence in the **longitudinal direction** and Fig. 5.4(b) the divergence in the **transverse direction**. Figure 5.5 shows a PDF of the divergence of the **radial velocity** of each radar detection point compared to the GT relative velocity of the target vehicle.

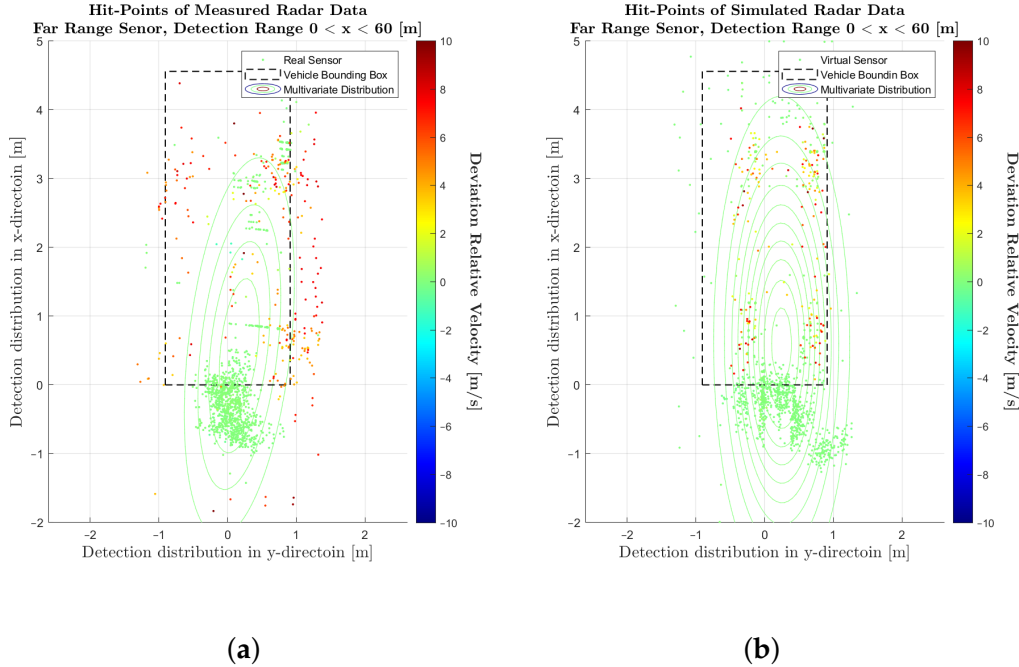


Figure 5.3.: Visualisation of the measured and simulated radar point cloud data, accumulated over the entire measurement time, in the near-range detection sector. (a) Scatterplot of detections for the real sensor. (b) Scatterplot of detections for the sensor model.

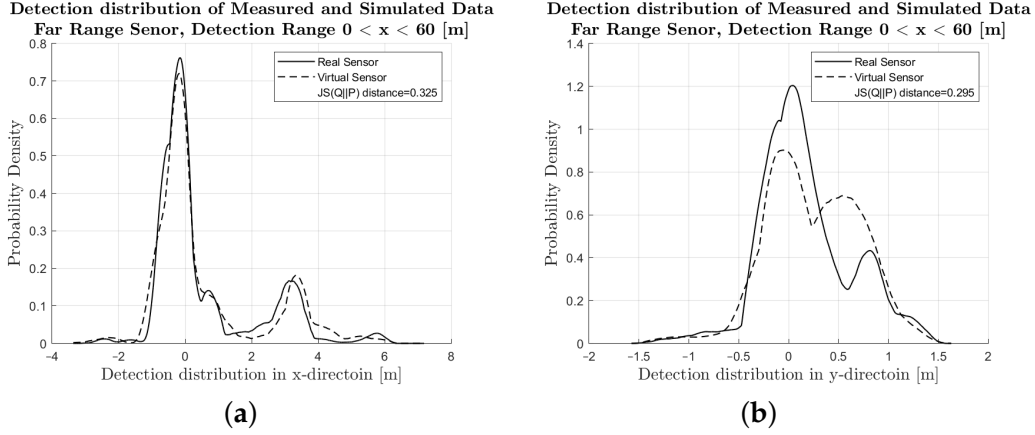


Figure 5.4.: Visual comparison and evaluation of the PDF of the deviation of the measured and simulated radar point clouds with respect to the reference point in the near-range detection sector. (a) PDF of the deviation in the  $x$ -direction from  $\mathcal{P}_{ref}(x, y)$  of the real sensor and sensor model. (b) PDF of the deviation in the  $y$ -direction from  $\mathcal{P}_{ref}(x, y)$  of the real sensor and sensor model.

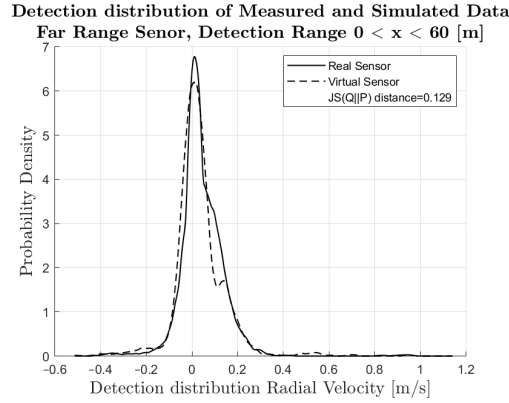


Figure 5.5.: Visual comparison and evaluation of the probability distribution function (PDF) of the deviation of the measured and simulated radar point clouds with respect to the reference point  $\mathcal{P}_{ref}(x, y)$  in the near-range detection sector: PDF of the radial velocity deviation from the reference velocity.

#### 5.4.1. Performance assessment of the presented radar sensor model

To quantitatively evaluate the performance of the sensor model in terms of its accuracy or fidelity, the Jensen-Shannon Divergence (JSD) can be calculated, which is the core part of the DGT-SMV method introduced in Section 3.2.6. The Jensen-Shannon Divergence (JSD) measures the distance between the discrete distribution of the real sensor point cloud data and the synthetic radar data both of them referenced to the GT system, by comparing their shape. It is a real mathematical metric that always returns the value of  $\text{DistJS}(\mathcal{P}||\mathcal{Q})$  as a scalar number in the closed interval between 0 and 1. If the result of  $\text{DistJS}(\mathcal{P}||\mathcal{Q}) = 0$ , the two distributions  $\mathcal{P}$  and  $\mathcal{Q}$  are equal; otherwise, if the result of  $\text{DistJS}(\mathcal{P}||\mathcal{Q}) = 1$ , they differ as much as possible. For better readability, the JSD in the Tables 5.1 and 5.2 is expressed as a

percentage, where  $\zeta_{s,r\Delta}$  representing the deviation of the simulated and measured real sensor data to the reference point  $\mathcal{P}_{ref}(x, y)$ .

Table 5.1.: Numerical result obtained by calculating the JSD to express the divergence between the PDF's with respect to the simulated and measured radar data, for the near-range detection sector, detection range  $0 < x < 60$  [m].

Evaluated Variable	JS-Distance in [%]
Relative distance in $x$ $\zeta_{s,r\Delta}(x)$	32.5
Relative distance in $y$ $\zeta_{s,r\Delta}(y)$	29.5
Radial velocity $v$ $\zeta_{s,r\Delta}(v)$	12.9

Table 5.2.: Numerical result obtained by calculating the JSD to express the divergence between the PDF's with respect to the simulated and measured radar data, for the far-range detection sector, detection range  $60 < x < 202.5$  [m].

Evaluated Variable	JS-Distance in [%]
Relative distance in $x$ $\zeta_{s,r\Delta}(x)$	40.1
Relative distance in $y$ $\zeta_{s,r\Delta}(y)$	23.6
Radial velocity $v$ $\zeta_{s,r\Delta}(v)$	1.8

#### 5.4.2. RCS performance assessment of the presented radar sensor model

This section shows the simulation result of the synthetically generated RCS output signal. The evaluation of the simulated RCS output as well as the measurement and measurement evaluation of the real sensor output already mentioned in Section 4.2.3 was based on the method presented in [23] and is briefly summarised here. The RCS value measured over the radial distance of a target vehicle is subject to fluctuation in signal amplitude due to the constructive and destructive interference caused by multipath propagation of EM waves. This fluctuation can lead to very low RCS values at certain distances compared to the typical or expected RCS value. To incorporate this phenomenon into the Euro-NCAP target validation process, the assessment is performed by setting an upper and lower limit based on the curve fitting function applied to the measured RCS data.

The lower plot in Fig.5.6 shows the results of the RCS measurement, the upper plot shows the synthetic RCS data simulated with the radar sensor model presented in this paper. For evaluation purposes, the result of curve fitting applied to both the measured and simulated RCS data is also shown with the solid line, while the dashed lines represent the lower and upper limits of acceptable fluctuation.

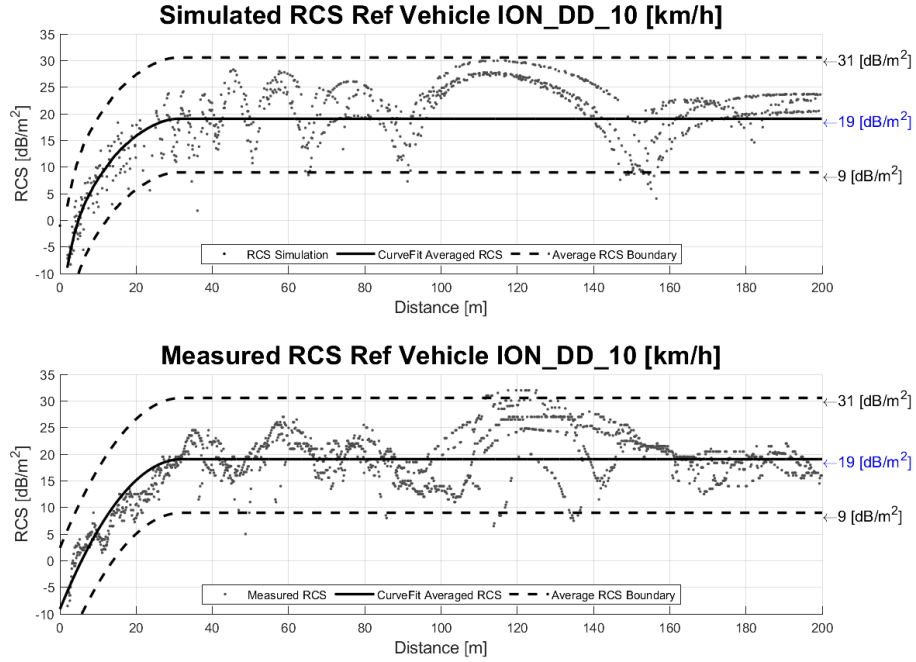


Figure 5.6.: Evaluation of the synthetically generated (top) and the measured real radar point cloud (bottom) in terms of the radar cross-section signal (RCS), following the procedure described in [23].

The results of the far range detection sector (60 to 202.5 m) with the corresponding plots can be found in Fig. B.1–B.3.

### 5.5. Evaluation of modelling approach IPG-RSI

In this section, the results of the sensor model evaluation of the selected radar sensor model are presented to demonstrate the modelling performance and capabilities of a commercially available radar sensor model. The evaluation of the model is done in the same way as in the previous section to facilitate comparison. The statistical analysis shows the detection characteristics of the sensor model compared to the GT and the real sensor. The results are obtained by applying the DGT-SMV method using the same driving manoeuvre. It should be mentioned that the evaluated sensor model follows a physical modelling approach using the ray-tracing method. In this work, the default values for the model parameters of the commercial sensor were used, as a sensitivity study showed that adjusting the parameters does not change the results significantly.

Figure 5.7 shows the spatial distribution of the measured (a) and synthetically generated (b) radar point cloud data for a near-range detection sector, on a 2D plane in the sensor coordinate system related to the dynamic target vehicle. The colour code of each radar detection point (Hit-point) indicates its velocity deviation with respect to the measured radial velocity provided by the GT reference measurement

system. The dashed line shows the boundary line of the target vehicle, and the contour lines in this diagram represent the multivariate distribution of the radar point cloud. Figure 5.7(a) is a top view of Fig. 4.8. These figures facilitate to understand that, in addition to the obvious radar detections at the rear of the vehicle, there are also detections that can be attributed to the installation position of the wheels. Figure 5.8 shows the PDF's of the divergence from the reference point  $\mathcal{P}_{ref}(x, y)$  in  $x$ - and  $y$ -direction of the measured and simulated radar point cloud. The reference point  $\mathcal{P}_{ref}(x, y)$  is provided by the GT reference system, for more details please refer to [63]. The probability distribution can not only be used to qualitatively assess the distribution of the reflections, but also serves as a basis for calculating the Jensen-Shannon Divergence. Figure 5.8(a) shows the divergence in the **longitudinal direction** and Fig. 5.8(b) the divergence in the **transverse direction**. Figure 5.9 shows a PDF of the divergence of the **radial velocity** of each radar detection point compared to the GT relative velocity of the target vehicle.

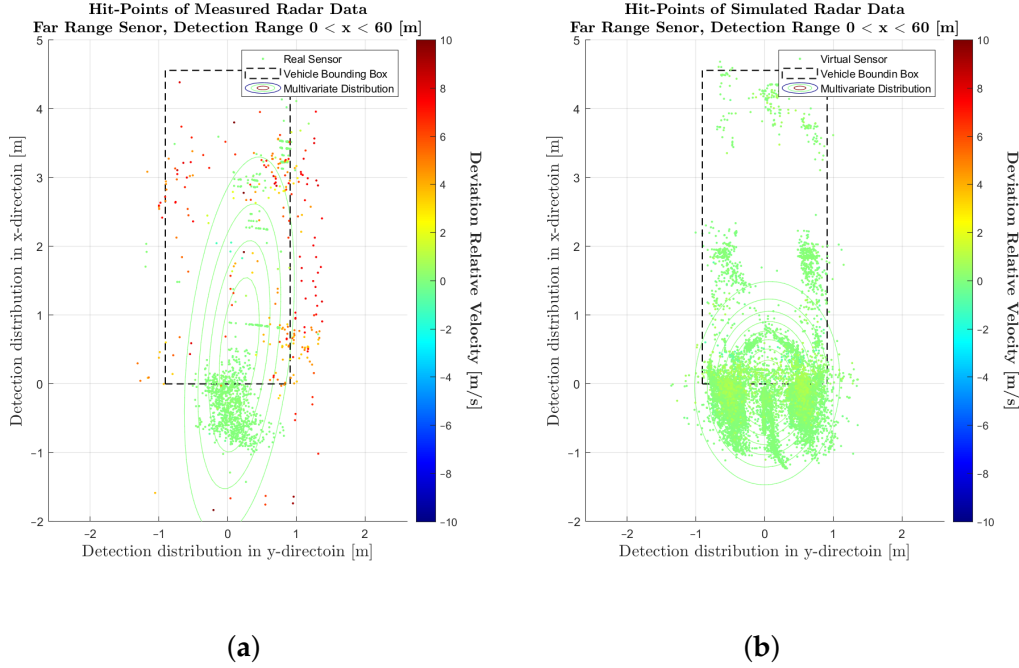


Figure 5.7.: Visualisation of the measured and simulated radar point cloud data, accumulated over the entire measurement time, in the near-range detection sector. (a) Scatterplot of detections for the real sensor. (b) Scatterplot of detections for the sensor model.



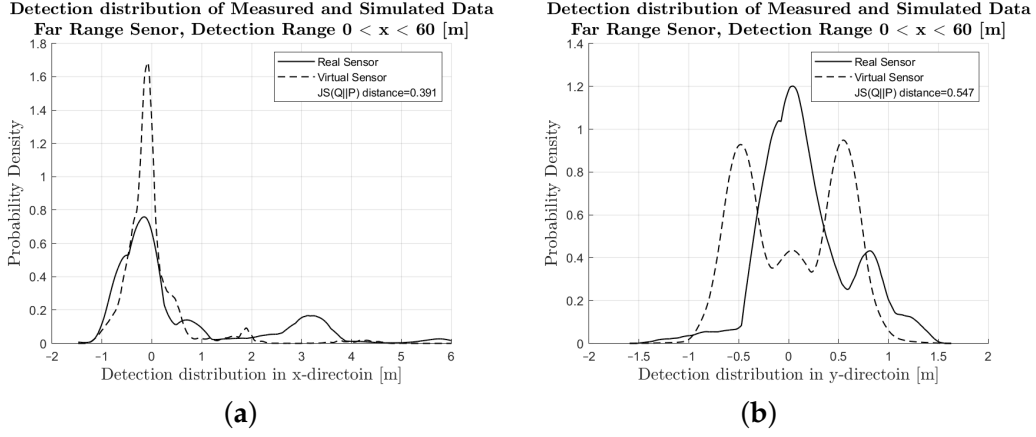


Figure 5.8.: Visual comparison and evaluation of the PDF of the deviation of the measured and simulated radar point clouds with respect to the reference point in the near-range detection sector. (a) PDF of the deviation in the  $x$ -direction from  $\mathcal{P}_{ref}(x, y)$  of the real sensor and sensor model. (b) PDF of the deviation in the  $y$ -direction from  $\mathcal{P}_{ref}(x, y)$  of the real sensor and sensor model.

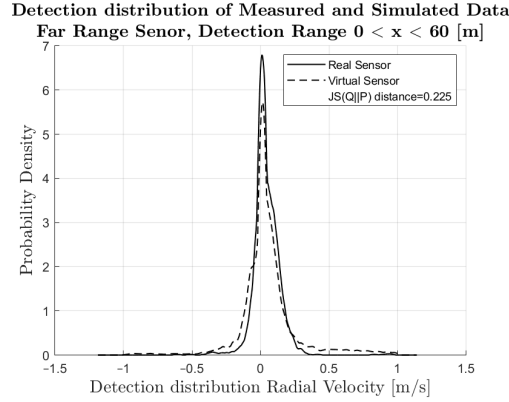


Figure 5.9.: Visual comparison and evaluation of the probability distribution function (PDF) of the deviation of the measured and simulated radar point clouds with respect to the reference point  $\mathcal{P}_{ref}(x, y)$  in the near-range detection sector: PDF of the radial velocity deviation from the reference velocity.

### 5.5.1. Performance assessment - IPG-RSI

For better readability, the JSD in the Tables 5.3 and 5.4 is expressed as a percentage, where  $\zeta_{s,r\Delta}$  representing the deviation of the simulated and measured real sensor data to the reference point  $\mathcal{P}_{ref}(x, y)$ .

Table 5.3.: Numerical result obtained by calculating the JSD to express the divergence between the PDF's with respect to the simulated and measured radar data, for the near-range detection sector, detection range  $0 < x < 60$  [m].

Evaluated Variable	JS-Distance in [%]
Relative distance in $x$ $\zeta_{s,r\Delta}(x)$	39.1
Relative distance in $y$ $\zeta_{s,r\Delta}(y)$	54.7
Radial velocity $v$ $\zeta_{s,r\Delta}(v)$	22.5

Table 5.4.: Numerical result obtained by calculating the JSD to express the divergence between the PDF's with respect to the simulated and measured radar data, for the far-range detection sector, detection range  $60 < x < 202.5$  [m].

Evaluated Variable	JS-Distance in [%]
Relative distance in $x$ $\zeta_{s,r\Delta}(x)$	26.1
Relative distance in $y$ $\zeta_{s,r\Delta}(y)$	50.2
Radial velocity $v$ $\zeta_{s,r\Delta}(v)$	21.1

The results of the far range detection sector (60 to 200 m) with the corresponding plots can be found in Fig. B.4–B.6.

The next section discusses the presented results and compares the findings between the radar sensor model presented in this thesis with the selected commercial radar sensor model.

## 5.6. Discussion

Efficient validation and verification of ADSs is a complex problem in terms of statistical proof of functional safety based on on-road testing. Combined real and simulation-based testing can significantly reduce validation efforts [97], but needs a suitable proof of prognosis quality of the virtual perception sensors. The application of simulation in different phases of vehicle development requires different modelling approaches of sensor models that can vary greatly ranging from simple geometric modelling to complex models for simulating the semiconductor components of radar sensors. The choice of the modeling approach depends on the intended use at different stages of the development process and needs to be validated accordingly [72]. Currently, there are no standardised evaluation criteria or requirements for the automotive industry to evaluate the performance of a radar sensor model against its real-world counterpart. Rosenberger [80, p.42 ff] provides a comprehensive collection about different evaluation metrics reported in the literature. They can be distinguished by the level of signal processing of the input data, but also by the range of values of the output metrics from good to poor. Based on the observation of the measured point cloud of the real radar sensor, detections around the target vehicle as well as under the target vehicle, especially from the wheels, were registered in a stochastic way. According to the authors in

[66], both the measured and the synthetically generated non-deterministic data sets can be evaluated in terms of uncertainties by comparing the PDFs or after applying the gating function of the empirical distribution functions (EDF). Combined with the findings presented by the authors in [72] that although a sensor model may be inaccurately assessed in a direct comparison, the connected algorithm may still show a high level of compliance, and the methodology used in this work to identify phenomena, led to the introduction of visual or intuitive assessment of the simulated radar point cloud data. Proper documentation for repeatability and traceability of the sensor model used, with varying complexity and accuracy at each stage of development, requires a simple and intuitive metric as a result of quantitative assessment processes. Taking into account the metric selection considerations, the calculation of the Jensen-Shannon distance shows appropriate properties, since it provides a quantified expression of the results of a comparison between two or more discrete probability distributions in a normalised manner. The Jensen-Shannon distance is the square-root of the JS-Divergence and is bounded by 1 for two probability distributions, given that one uses the base 2 logarithm. Although the JS-Divergence is not linear, the results obtained in a closed interval allows intuitively to understand what counts as a "good" or "unacceptable" value of the metric [66], which explains the choice of JSD in this thesis.

Inspecting the results of the **presented radar sensor model**, a quick overview on the performance of the virtual sensor can immediately be achieved by the JSD metrics, where the deviations  $\zeta_{s,r\Delta}$  calculated for 0% represents the perfect and 100% the worst performance accordingly. In the presented example, it can be seen that, in the far range detection sector, the virtual sensor is more accurate in reproducing the relative velocity than in the near detection sector. For the radial velocity, the JSD of  $\zeta_{s,r\Delta}(v)$  is 12.9% up to 60 m and 1.8 % up to 202.5 m.

For the relative distance, the better performance is seen in the  $y$  direction. The JSD of  $\zeta_{s,r\Delta}(y)$  is 29.5% in the near range detection sector up to 60 m and 23.6% up to 202.5 m. In the  $x$  direction, the related JSD values of  $\zeta_{s,r\Delta}(x)$  are 32.5%, and 40.1%, respectively.

This result is confirmed by visual inspection of the PDF illustrated in Figures 5.4, 5.5, B.2 and B.3 as well as the scatter plots in Figures 5.3 and B.1. Comparing the shape of the PDFs, the strengths and shortcomings of the sensor model can be assessed, providing recommendations for parameter tuning and drawing conclusions on the validity of the results.

As with the results discussed earlier, a quick overview of the performance of the **commercial radar sensor model** can also be obtained by looking at the numerical values calculated by the JSD metrics. The deviation calculated for  $\zeta_{s,r\Delta}$ , 0% represents a perfect, whereas the deviation calculated for 100% the worst performance. In the presented example, it can be seen that, in the far range detection sector, as well as in the near range detection sector the commercial virtual sensor is nearly equally accurate in reproducing the relative velocity. For the radial velocity, the JSD of  $\zeta_{s,r\Delta}(v)$  is 22.5% up to 60 m and 21.1 % up to 200 m.

For the relative distance, the better performance is seen in the  $x$  direction. The JSD of  $\zeta_{s,r\Delta}(x)$  is 39.1% in the near range detection sector up to 60 m and 26.1% up to 200 m. In the  $y$  direction, the related JSD values of  $\zeta_{s,r\Delta}(y)$  are 54.7%, and 50.2%,

respectively.

This result is confirmed by visual inspection of the PDF illustrated in Figures 5.8, 5.9, B.5 and B.6 as well as the scatter plots in Figures 5.7 and B.4. Comparing the shape of the PDFs, the strengths and shortcomings of the sensor model can be assessed, providing recommendations for parameter tuning and drawing conclusions on the validity of the results.

Applying the same assessment methodology by using the same driving manoeuvre to compare the sensor models, even with different modelling approaches, allows a direct comparison of the assessment results.

In Fig. 5.10 the related results for the radar point clouds are observable. It can be clearly seen that the radar point clouds of the commercial sensor differs strongly from the measurements and are concentrated around the rear of the vehicle. The same holds for the comparison of the PDF's, Figures 5.11, 5.12, 5.13 show a rather divergent result for the commercial sensor model. The visual impression is also supported by the JSD metrics provided in Tab. 5.5 and 5.6 where the presented model outperforms the commercial in almost all aspects but the relative distance in  $x$  in the far range. This can be explained that some reflections points are observable in the presented model which did not appear in the measurement. Results for the RCS cannot be compared since the commercial model does not deliver those, which is a major drawback for subsequent perception algorithms that lead to object lists. Hence perception algorithms cannot be applied for the commercial model in a realistic manner.

The explanation for the results and deviations lies in the specific modelling approach of the selected commercial radar sensor model, where the radar effects are simulated on the physical basis by applying the built-in ray tracing engine.

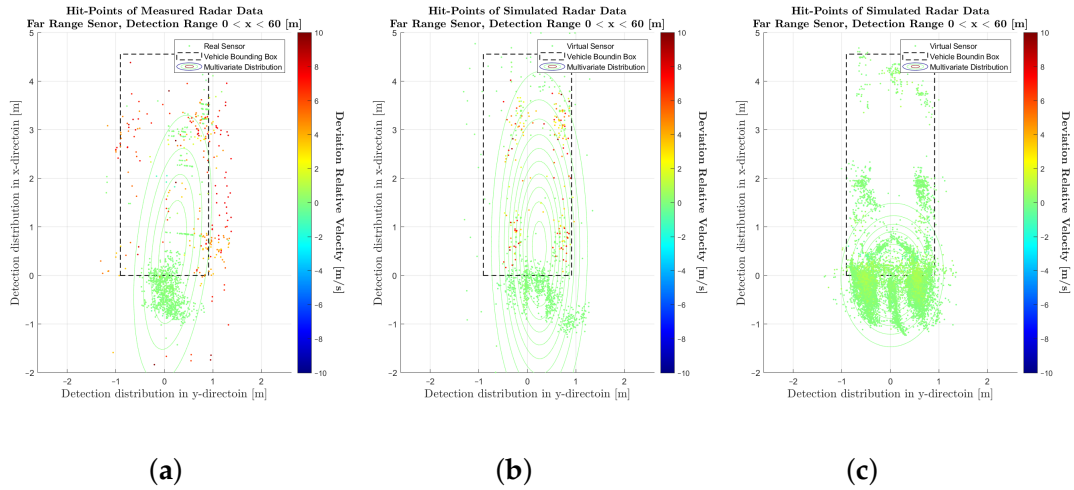


Figure 5.10.: Visualisation of the measured and simulated radar point cloud data, cumulated over the entire measurement time, in the near-range detection sector. (a) Scatterplot of detections for the real sensor. (b) Scatterplot of detections for the sensor model presented in this paper. (c) Scatterplot of detections for the sensor model of commercial application.

## 5. Results and discussion

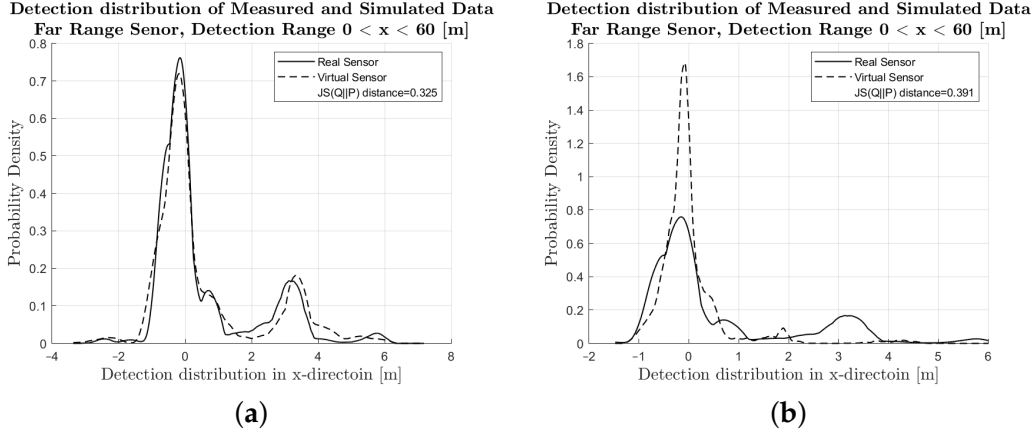


Figure 5.11.: Visual comparison and evaluation of the probability distribution function (PDF) of the deviation of the measured and simulated radar point clouds with respect to the reference point in the near-range detection sector. (a) PDF of the deviation in the  $x$ -direction from  $\mathcal{P}_{ref}(x, y)$  of the real sensor and sensor model presented in this paper. (b) PDF of the deviation in the  $x$ -direction from  $\mathcal{P}_{ref}(x, y)$  of the real sensor and sensor model for commercial applications.

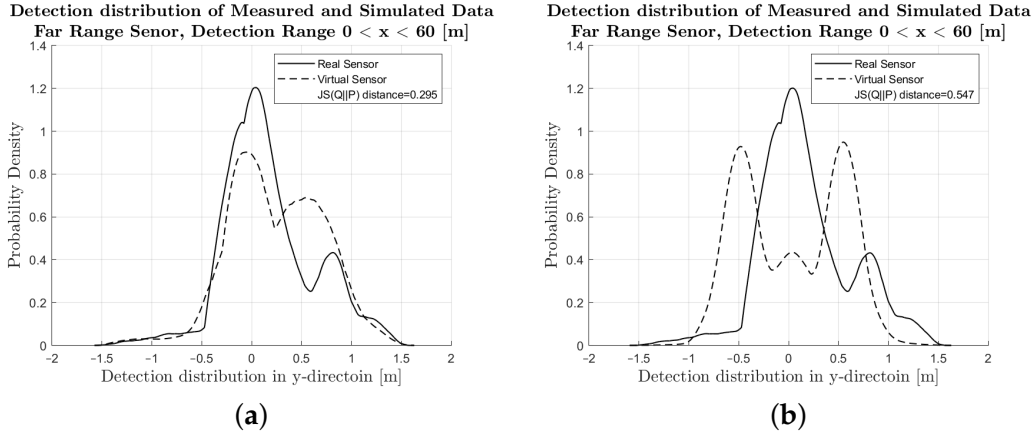


Figure 5.12.: Visual comparison and evaluation of the probability distribution function (PDF) of the deviation of the measured and simulated radar point clouds with respect to the reference point in the near-range detection sector. (a) PDF of the deviation in the  $y$ -direction from  $\mathcal{P}_{ref}(x, y)$  of the real sensor and sensor model presented in this paper. (b) PDF of the deviation in the  $y$ -direction from  $\mathcal{P}_{ref}(x, y)$  of the real sensor and sensor model for commercial applications.

## 5. Results and discussion

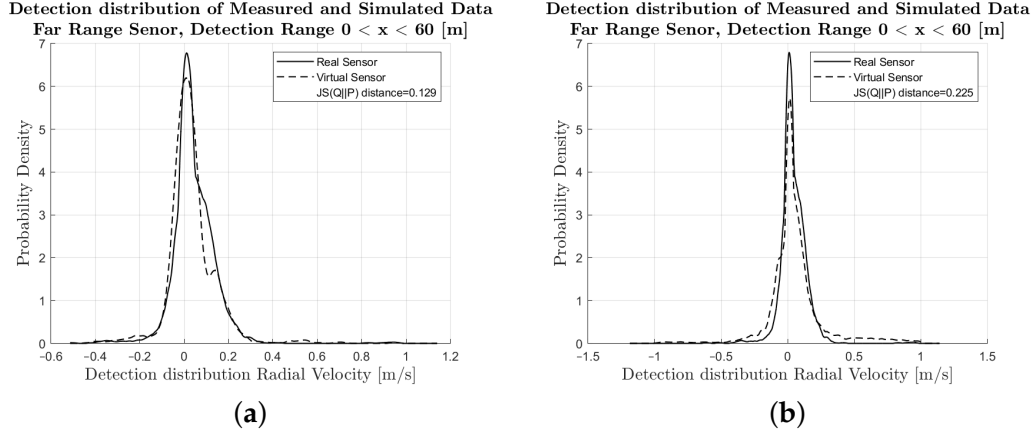


Figure 5.13.: Visual comparison and evaluation of the probability distribution function (PDF) of the deviation of the measured and simulated radar point clouds with respect to the reference point  $\mathcal{P}_{ref}(x, y)$  in the near-range detection sector. (a) PDF of the radial velocity deviation from the reference velocity of the real sensor and sensor model presented in this paper. (b) PDF of the radial velocity deviation from the reference velocity of the real sensor and sensor model for commercial applications.

The results of the far range detection sector (60 to 202.5 m) with the corresponding plots can be found in Fig. B.7–B.10.

Table 5.5.: Comparison of the numerical results of the JSDs calculated for the presented sensor model and for a commercial sensor model, for the near-range detection sector, detection range  $0 < x < 60$  [m].

Evaluated Variable	JS-Distance in [%]	JS-Distance in [%]
	Current sensor model	Commercial sensor model
Relative distance in $x$ $\zeta_{s,r\Delta}(x)$	32.5	39.1
Relative distance in $y$ $\zeta_{s,r\Delta}(y)$	29.5	54.7
Radial velocity $v$ $\zeta_{s,r\Delta}(v)$	12.9	22.5

Table 5.6.: Comparison of the numerical results of the JSDs calculated for the presented sensor model and for a commercial sensor model, for the far-range detection sector, detection range  $60 < x < 202.5$  [m].

Evaluated Variable	JS-Distance in [%]	JS-Distance in [%]
	Current sensor model	Commercial sensor model
Relative distance in $x$ $\zeta_{s,r\Delta}(x)$	40.1	26.1
Relative distance in $y$ $\zeta_{s,r\Delta}(y)$	23.6	50.2.7
Radial velocity $v$ $\zeta_{s,r\Delta}(v)$	1.8	21.1

## 6. Summary

This chapter provides a summary of the present thesis.

### **Chapter 1: Introduction.**

In this chapter the main drivers for the increasing demand of development and integration of Advanced Driver Assistance Systems (ADAS), SAE level 0-2, and higher level Automated Driving functions (ADF), SAE level 3-5, in modern vehicles were discussed. Despite the advantages of automated driving technologies with respect to road safety, driver comfort, efficiency in energy consumption and traffic flow, as well as introducing new mobility concepts, only driver assistance systems of SAE levels 0 to 2, with the first applications in SAE L3, are on the market. One of the main reasons is the lack of proof in functional safety, which is due to the immense efforts required in real world testing. The need for virtual development for safety validation of ADAS and AD functions, have come along with the drastic increase in on-road testing kilometres. Among others, Kalra et al [53] quantified the total amount of testing kilometres needed for safety validation and, depending on how the statistical questions is raised, mentioned values between 1.6 million to 11 billion miles. Hence, the required integration of virtual models into the vehicle development process has led to the systematic use of simulation techniques that allow for virtual-based verification and validation (V&V) to prove the correctness of the system concept already in the requirements analysis phase. A key issue in virtual V&V of driving automation is the implementation of machine perception, which demands virtual sensor models of sufficient prognosis quality.

The demand for a scalable, realistic radar sensor model and a practicable evaluation tool led to the formulation of the research objectives, which are also presented in this chapter.

**Chapter 2: State of the Art.** In this chapter, considerable attention has been paid to the acquisition and understanding of the state-of-the-art radar sensor models and its modelling approaches. Since the basic task of modelling is to support the vehicle design process according to the V-model, the test processes that are carried out during the vehicle life cycle were examined first. As a result of the study, three phases were identified that run through the life cycle in a chronologically staggered sequence. It was also found that the test tasks described in each of the three areas are based on different national and international legal regulations and that legally different bodies are responsible for their implementation. However, in order to increase reliability and road safety, these test procedures are partially or fully integrated into the first phase of the life cycle, i.e. the design phase of the vehicle. Based on this knowledge this chapter provides a comprehensive overview of the heterogeneous state of the art in radar sensor modelling. Instead of a technology-based classification, this thesis summarises the practical methods described in the literature and introduces a novel classification method based on how these

models can be used in vehicle development using the V-model. Since X-in-the-loop based approaches ultimately support the goal of whole vehicle level development, the available modelling approaches are divided into *models* based on how they are or can be used in the development process in ascending order of complexity. The application and usability of these models along the development process are summarised in a comprehensive tabular overview that combines previous classifications with the new approach introduced in this chapter. Thus, the output of this chapter provides a quick overview and helps to select a suitable modelling method for further use. Finally, the novel contributions of the presented research is summarised, which are the specific experimental setup to identify radar phenomena, the specific semi-physical modelling approach, the applicability of the model in different vehicle development phases, its real time capability and minimum amount of needed information from the sensor supplier.

**Chapter 3: Overall goals and scope of the thesis/Development Process.** In this chapter, the entire development process of the radar sensor model was discussed and presented. Based on the knowledge gained in the previous section, guidelines for the modeling process development was determined as follows:

- a Real measurement data acquired on the test track and synthetic data simulated on the digital twin should be transferable and interchangeable.
- b Modular design of the model structure that enables the implementation of third party sub-modules.
- c Simplified model parameter derivation, based on data sheet information and some characterising measurements with a real sensor.
- d Flexibility in terms of complexity and fidelity according to the V-model.

Following the guidelines under consideration the available hardware resources in terms of data acquisition and environment perception sensor with a required open data interface the process flow to derive the radar sensor model was developed and discussed. Following this process flow, the further work packages were identified, divided into the development of a suitable measurement setup, the definition of the driving scenarios, the identification of the phenomena relevant for radar detection, the definition of a suitable modelling approach, the implementation of the radar sensor model in a simulation environment, the calibration and parameterisation of the model and finally the performance evaluation.

The measurement setup used was designed on the basis of the advanced vehicle dynamics measurement system, which is mounted on the ego and target vehicle and connected via a wireless link. With this measurement system, the relative position between the ego and target vehicle was measured with an accuracy of a few centimetres. The developed advanced data synchronization technology allowed the simultaneous acquisition of two open data interface radar sensors.

The driving scenarios and the driving manoeuvres they contain, were defined primarily to challenge the radar sensor, defined as Radar under Test (RUS), in various traffic situations with regard to sensor technology and functional safety. The driving scenarios were defined according to the parameter list introduced in this chapter.



With the execution of the driving manoeuvres and recording of the radar data with the measuring system defined in this chapter, several phenomena were identified that are related either to the radar targets and driving environment, to the radar signal processing, or to the characteristics of the hardware architecture of the radar sensor.

Those detected phenomena led to the concept definition of the semi-physical modeling approach developed and described in detail in Chapter 4. and the related parameter identification.

The virtual radar sensor model was coded, implemented and executed in Matlab/Simulink. The implementation starts with the export and synchronisation of real measurement data, followed by the Target and Environment Module, the Sensor Response Module, the Signal Processing Module as well as the Error Module.

The same driving scenarios were used to calibrate the model as were used to determine the phenomena related to radar detection. In addition, a standardised measurement procedure was also used to calibrate the synthetic RCS output of the sensor model, which was adopted from Technical Bulletin TBo25 [23] defined by the Euro-NCAP consortium.

Finally, an evaluation method was developed and applied to the model. To assess the quality of the model, Jensen-Shannon divergence was used to calculate the metrics.

**Chapter 4: Methodology.** In this chapter, special attention was given to introduce and describe the three main themes on which the radar sensor modelling process is built.

In the experimental methodology part the development and implementation of the overall measurement setup consisting of two test vehicles both of them equipped with high accuracy localisation system to provide Ground Truth information and the environment perception sensor with open data interface were explained. Those two test vehicles were defined as ego-, equipped with the radar under simulation, and target vehicle as a subject of detections of interest. A precise commercial measurement system was selected to provide online Ground Truth information in terms of relative and absolute vehicle positions and dynamic behaviour. Both vehicle were equipped with the same data acquisition unit and an accurate measurement system for vehicle state measurements based on the combination of precise GPS and vehicle motion data from an accurate Inertial Measurement Unit. An advanced time synchronization technology implemented in the data acquisition unit allowed for the recording of multiple asynchronous data streams from the connected open data interface sensors synchronised with the GPS time stamp. The radar sensor used in this work was an automotive radar sensor with open interfaces to retrieve the radar point cloud and object lists. In addition, the test vehicle was equipped with other perception sensors for data collection: two additional FMCW radar sensors of a more recent type, a 16-beam LIDAR sensor, a front camera module, a Car2Car communication development platform and a video camera used for documentation purposes.

In the sensor modelling methodology part the main contribution of this work was developed and described in detail. In order to achieve the most realistic sensor

performance possible, the operating principle of the FMCW radar was first analysed and the functions relevant to the radar detection process were classified according to the processing level into RF front-end, signal and data processing. In the functional model and design philosophy part, the modular structure was developed and introduced in accordance with the modelling considerations, observations in the measurement data and the FMCW operating principle. The basis of the modular structure is the simulation input, prepared for both virtually and real measured Ground Truth data. Functions were developed in order to rearrange the scenario into environment classes, which were converted into a bounding box representation. This was followed by the definition of detection classes derived from the observed radar detection characteristics. Finally a detection matrix was defined to associate the detection classes to the environment components. Algorithms were developed to incorporate the presumed root causes of the observed detection phenomena. Assuming that the detection process of the radar sensor can be considered as a linear time-invariant system. The output of this module was considered as a superposition of the effect of the directional characteristic of the antenna, the free-space attenuation or path-loss and the propagation factor represents the multipath interference. In the signal processing module functions were developed to incorporate further effects resulting of FFT processing as well of the characteristic of the Continuous False Alarm Rate detection algorithms. Finally an error module was considered consisting of the functions to incorporate the effects regarded to the basic reflection process considered as a Poisson process, the additive white Gaussian noise and the acceleration of the vehicles.

In the evaluation methodology part a perception sensor model evaluation method was developed and described. The Dynamic Ground Truth Sensor Model Validation (DGT-SMV) approach allows firstly the visual inspection of the synthetically generated and recorded sensor output, secondly the transformation of this data with statistical methods based on probability distribution functions to show the main performance of the virtual sensors, and finally, for a quick quantitative comparison by calculating the Jensen-Shannon divergence.

### **Chapter 7: Results and discussion**

In this chapter the overall outcomes of the modelling development process and the result of the simulation the selected automotive radar sensor using the developed assessment method were presented.

In order to demonstrate the capability and performance of the developed methods for the synthetic generation of realistic radar point cloud data and their evaluation, the developed evaluation method was applied to a commercial sensor model as well as to the radar sensor model developed in this thesis. The use of the same evaluation method and driving manoeuvres allowed a direct comparison of the simulation results.

The visual inspection of the accumulated radar point clouds for the sensor model introduced in this thesis shows a qualitatively good comparability of the real and simulated radar point cloud data, both for the position of reflections in  $x$  and  $y$  and radial velocity. The attribution of PDF's to these data reveals the nice correlation of the simulation in longitudinal direction as well as for the radial velocity; for

the lateral direction the comparability is still acceptable. This visual impression is confirmed by calculating a quantitative performance number using the JSD metric.

For the Radar Cross Section values, the visual inspection revealed good correlations between measurement and simulation. It is worth to notice that the accuracy of the GT referencing system does not influence the results, since the comparison is drawn directly between the experiment and the simulation.

The presented research introduced a novel radar sensor model that, due to its real-time performance and remarkable accuracy compared to commercial sensor models closes existing gaps in validation and verification of automated vehicles.

# Bibliography

- [1] Alexander Schaermann. "Systematische Bedatung und Bewertung umfelderfassender Sensormodelle." Doctoral dissertation. Technische Universität München, München, Germany, 2019 (cit. on pp. 51, 53).
- [2] M. E. Asghar et al. "Radar Target Simulator and Antenna Positioner for Real-Time Over-the-air Stimulation of Automotive Radar Systems." In: *2020 17th European Radar Conference (EuRAD)*. IEEE, 2021, pp. 95–98. ISBN: 978-2-87487-061-3. DOI: \url{10.1109/EuRAD48048.2021.00035} (cit. on p. 11).
- [3] Emna Bel Kamel, Alain Peden, and Patrice Pajusco. "RCS modeling and measurements for automotive radar applications in the W band." In: *2017 11th European Conference on Antennas and Propagation (EUCAP)*. IEEE, 2017, pp. 2445–2449. ISBN: 978-8-8907-0187-0. DOI: \url{10.23919/EuCAP.2017.7928266} (cit. on p. 17).
- [4] Stefan Bernsteiner et al. "Radar Sensor Model for the Virtual Development Process." In: *ATZelektronik worldwide* 10.2 (2015), pp. 46–52. DOI: \url{10.1007/s38314-015-0521-1} (cit. on pp. 10, 15).
- [5] R. Bhalla and Hao Ling. "Three-dimensional scattering center extraction using the shooting and bouncing ray technique." In: *IEEE Transactions on Antennas and Propagation* 44.11 (1996), pp. 1445–1453. ISSN: 0018-926X. DOI: \url{10.1109/8.542068} (cit. on p. 10).
- [6] Eckard Bringmann and Andreas Kr. "Model-Based Testing of Automotive Systems." In: *2008 International Conference on Software 2008-09-04 - 2008-11-04*, pp. 485–493. DOI: \url{10.1109/ICST.2008.45} (cit. on p. 13).
- [7] C. Waldschmidt, J. Hasch, and W. Menzel. "Automotive Radar — From First Efforts to Future Systems." In: *IEEE Journal of Microwaves* 1.1 (2021), pp. 135–148. DOI: \url{10.1109/JMW.2020.3033616} (cit. on p. 38).
- [8] Peng Cao. "Modeling Active Perception Sensors for Real-Time Virtual Validation of Automated Driving Systems." PhD thesis. Darmstadt, Germany: Technische Universität Darmstadt, 2017. URL: %5Curl%7Bhttps://d-nb.info/1162621664/34?msclkid=38e29c5cc0a611eca63b2d3ee53bb5c6%7D (visited on 04/20/2022) (cit. on p. 10).
- [9] Peng Cao, Walther Wachenfeld, and Hermann Winner. "Perception sensor modeling for virtual validation of automated driving." In: *it - Information Technology* 57.4 (2015), pp. 243–251. ISSN: 1611-2776. DOI: \url{10.1515/itit-2015-0006} (cit. on p. 11).
- [10] Caps-acc Technical Reference Guide. In: *Available online: (accessed on 12 (2013), p. 2022. URL: %5Curl%7Bhttps://ccc.dewetron.com/dl/52af1137-c874-4439-8ba0-7770d9c49862%7D* (cit. on pp. 29, 30, 49).

- [11] Jing-Jun Cheng et al. "An Indoor Rapid Testing Platform for Autonomous Vehicles Using Vehicle-in-the-Loop Simulation." In: *CICTP 2020*. Ed. by Heng Wei et al. Reston, VA: American Society of Civil Engineers, 2020, pp. 411–422. ISBN: 9780784483053. DOI: \url{10.1061/9780784483053.035} (cit. on p. 11).
- [12] Woo Young Choi, Jin Ho Yang, and Chung Choo Chung. "Data-Driven Object Vehicle Estimation by Radar Accuracy Modeling with Weighted Interpolation." In: *Sensors (Basel, Switzerland)* 21.7 (2021). DOI: \url{10.3390/s21072317} (cit. on p. 15).
- [13] Continental Engineering Services GmbH. *Standardized ARS Interface. Technical Documentation. ARS 308-2C/-21*. Ed. by Continental Engineering Services GmbH. 2012 (cit. on pp. 22, 34).
- [14] D. Kellner et al. "Wheel extraction based on micro doppler distribution using high-resolution radar." In: *2015 IEEE MTT-S International Conference on Microwaves for Intelligent Mobility (ICMIM)*. 2015, pp. 1–4. DOI: \url{10.1109/ICMIM.2015.7117951} (cit. on p. 43).
- [15] Ulrich Dahmen and Jürgen Roßmann. "Simulation-based Verification with Experimentable Digital Twins in Virtual Testbeds." In: *Tagungsband des 3. Kongresses Montage Handhabung Industrieroboter*. Ed. by Thorsten Schüppstuhl, Kirsten Tracht, and Jörg Franke. Berlin, Heidelberg: Springer Berlin Heidelberg, 2018, pp. 139–147. ISBN: 978-3-662-56714-2 (cit. on pp. 7, 27).
- [16] Thomas Dallmann, Jens-Kristian Mende, and Stefan Wald. "A Radar Target Simulator for Complex Traffic Scenarios ATRIUM." In: *2018 IEEE MTT-S International Conference on Microwaves for Intelligent Mobility (ICMIM)*. IEEE, 2018, pp. 1–4. ISBN: 978-1-5386-1725-0. DOI: \url{10.1109/ICMIM.2018.8443515} (cit. on p. 11).
- [17] Axel Diewald et al. "Radar Target Simulation for Vehicle-in-the-Loop Testing." In: *Vehicles* 3.2 (2021), pp. 257–271. DOI: \url{10.3390/vehicles3020016} (cit. on p. 11).
- [18] Thomas Doms et al. *Highly Automated Driving – The new challenges for Functional Safety and Cyber Security: White Paper*. Ed. by TÜV Austria holding AG and Virtual Vehicle Research and Test Center GmbH. 2018. URL: %5Curl%7Bhttps://www.v2c2.at/wp-content/uploads/2018/11/tuv-austria-white-paper-iv-highly-automated-driving\_web.pdf%7D (visited on 04/26/2022) (cit. on pp. 5, 6).
- [19] Riccardo Dona and Biagio Ciuffo. "Virtual Testing of Automated Driving Systems. A Survey on Validation Methods." In: *IEEE Access* 10 (2022), pp. 24349–24367. DOI: \url{10.1109/ACCESS.2022.3153722} (cit. on p. 27).
- [20] M. Dudek et al. "Millimeter wave FMCW radar system simulations including a 3D ray tracing channel simulator." In: *2010 Asia-Pacific Microwave Conference*. 2010, pp. 1665–1668 (cit. on p. 17).

- [21] E. Fishler et al. "Spatial Diversity in Radars—Models and Detection Performance." In: *IEEE Transactions on Signal Processing* 54.3 (2006), pp. 823–838. ISSN: 1941-0476. DOI: \url{10.1109/TSP.2005.862813} (cit. on p. 41).
- [22] D. Endres and J. A. Schindelin. "new metric for probability distributions." In: *IEEE Trans. Inf. Theory* 2003 (), pp. 1858–1860. DOI: \url{10.1109/TIT.2003.81350610.1109/TIT.2003.813506} (cit. on p. 54).
- [23] EuroNCAP. *Technical Bulletin TBo25 Global Vehicle Target Specification v1.0*. Ed. by European New Car Assessment Programme. 2018. URL: %5Curl%7Bhttps://cdn.euroncap.com/media/39159/tb-025-global-vehicle-target-specification-for-euro-ncap-v10.pdf%7D (visited on 10/28/2022) (cit. on pp. 24, 26, 40, 60, 61, 71).
- [24] Michael E. Gadringer et al. "Virtual reality for automotive radars." In: *e & i Elektrotechnik und Informationstechnik* 135.4-5 (2018), pp. 335–343. ISSN: 0932-383X. DOI: \url{10.1007/s00502-018-0620-9} (cit. on p. 11).
- [25] GeneSys Elektronik GmbH. *ADMA 3.0 Technical Documentation: ADMA G ADMA-Speed ADMA-Slim*. Ed. by GeneSys Elektronik GmbH. Offenburg, Germany, 2020 (cit. on p. 29).
- [26] Sreehari Buddappagari Jayapal Gowdu et al. "System architecture for installed-performance testing of automotive radars over-the-air." In: *2018 IEEE MTT-S International Conference on Microwaves for Intelligent Mobility (ICMIM)*. IEEE, 2018, pp. 1–4. ISBN: 978-1-5386-1725-0. DOI: \url{10.1109/ICMIM.2018.8443490} (cit. on p. 11).
- [27] Michael Gschwandtner et al. "BlenSor: Blender Sensor Simulation Toolbox." In: *Advances in Visual Computing*. Ed. by George Bebis et al. Berlin, Heidelberg: Springer Berlin Heidelberg, 2011, pp. 199–208. ISBN: 978-3-642-24031-7. DOI: \url{10.1007/978-3-642-24031-7\textunderscore{20}} (cit. on p. 10).
- [28] Jiao Guo et al. "A Novel Method of Radar Modeling for Vehicle Intelligence." In: *SAE International Journal of Passenger Cars - Electronic and Electrical Systems* 10.1 (2017), pp. 50–56. ISSN: 1946-4622. DOI: \url{10.4271/2016-01-1892} (cit. on p. 10).
- [29] T. Hanke et al. "Generic architecture for simulation of ADAS sensors." In: *Generic Architecture for Simulation of ADAS Sensors*. Ed. by Hanke T. et al. IEEE, 2015, pp. 125–130. ISBN: 978-3-9540-4853-3. DOI: \url{10.1109/IRS.2015.7226306} (cit. on p. 10).
- [30] Timo Hanke et al. *Generation and validation of virtual point cloud data for automated driving systems: 20th International Conference on Intelligent Transportation Systems : Mielparque Yokohama in Yokohama, Kanagawa, Japan, October 16-19, 2017*. Piscataway, NJ: IEEE, 2017. ISBN: 9781538615263. URL: %5Curl%7Bhttp://ieeexplore.ieee.org/servlet/opac?punumber=8307147%7D (cit. on p. 27).

- [31] Maike Hartstern et al. "Simulation-based Evaluation of Automotive Sensor Setups for Environmental Perception in Early Development Stages." In: *2020 IEEE Intelligent Vehicles Symposium (IV)*. IEEE, 2020, pp. 858–864. ISBN: 978-1-7281-6673-5. DOI: [10.1109/IV47402.2020.9304771](https://doi.org/10.1109/IV47402.2020.9304771) (cit. on pp. 12, 14).
- [32] Martin Herrmann and Helmut Schön. "Efficient Sensor Development Using Raw Signal Interfaces." In: *Fahrerassistenzsysteme 2018*. Ed. by Torsten Bertram. Proceedings. Wiesbaden: Springer Fachmedien Wiesbaden, 2019, pp. 30–39. ISBN: 978-3-658-23750-9. DOI: [10.1007/978-3-658-23751-6\\_textunderscore3](https://doi.org/10.1007/978-3-658-23751-6_textunderscore3) (cit. on p. 12).
- [33] N. Hirsenkorn et al. "A non-parametric approach for modeling sensor behavior." In: *2015 16th International Radar Symposium (IRS)*. IEEE, 2015, pp. 131–136. ISBN: 978-3-9540-4853-3. DOI: [10.1109/IRS.2015.7226346](https://doi.org/10.1109/IRS.2015.7226346) (cit. on pp. 10, 15).
- [34] Nils Hirsenkorn et al., eds. *A ray launching approach for modeling an FMCW radar system: 28-30 June 2017*. The 18th International Radar Symposium IRS 2017, June 28-30, 2017, Prague, Czech Republic: IEEE, 2017. ISBN: 9783736993433. URL: [5Curl%7Bhttp://ieeexplore.ieee.org/servlet/opac?punumber=8001662%7D](https://ieeexplore.ieee.org/servlet/opac?punumber=8001662) (cit. on pp. 10, 17).
- [35] Nils Hirsenkorn et al. "Virtual sensor models for real-time applications." In: *Advances in Radio Science* 14 (2016), pp. 31–37. DOI: [10.5194/ars-14-31-2016](https://doi.org/10.5194/ars-14-31-2016) (cit. on pp. 10, 15).
- [36] M. Holder et al. "Measurements revealing Challenges in Radar Sensor Modeling for Virtual Validation of Autonomous Driving." In: *Proceedings of the 2018 21st International Conference on Intelligent Transportation Systems (ITSC)*. HI, USA, pp. 2616–2622: Maui, 2018, pp. 4–7 (cit. on pp. 47, 53).
- [37] M. F. Holder et al. *Measurements revealing Challenges in Radar Sensor Modeling for Virtual Validation of Autonomous Driving: November 4-7, Maui, Hawaii*. Piscataway, NJ: IEEE, 2018. ISBN: 9781728103235. URL: [5Curl%7Bhttp://ieeexplore.ieee.org/servlet/opac?punumber=8543039%7D](https://ieeexplore.ieee.org/servlet/opac?punumber=8543039) (cit. on p. 23).
- [38] Martin Holder et al. "Data-driven Derivation of Requirements for a Lidar Sensor Model." In: *Graz Symposium Virtual Vehicle 2018*. Ed. by Virtual Vehicle Research and Test Center. Virtual Vehicle Research and Test Center, 2018, pp. 1–10. URL: [5Curl%7Bhttps://tuprints.ulb.tu-darmstadt.de/7548/1/2018\\_GSVF\\_Lidarfeatures.pdf%7D](https://tuprints.ulb.tu-darmstadt.de/7548/1/2018_GSVF_Lidarfeatures.pdf) (visited on 06/23/2022) (cit. on p. 10).
- [39] Martin Holder et al., eds. *The Fourier Tracing Approach for Modeling Automotive Radar Sensors*. 20th International Radar Symposium (IRS): IEEE, 2019. ISBN: 9783736998605. URL: [5Curl%7Bhttp://ieeexplore.ieee.org/servlet/opac?punumber=8764049%7D](https://ieeexplore.ieee.org/servlet/opac?punumber=8764049) (cit. on pp. 11, 17).
- [40] Martin F. Holder. "Synthetic Generation of Radar Sensor Data for Virtual Validation of Autonomous Driving." PhD thesis. TU Darmstadt, 2021. DOI: [10.26083/tuprints-00017545](https://doi.org/10.26083/tuprints-00017545) (cit. on pp. 11, 17).

- [41] Allan C. Hutchinson, ed. *Cryptocurrencies and the Regulatory Challenge*. London: Routledge, 2021. ISBN: 9781003222071. DOI: \url{10.4324/9781003222071} (cit. on p. 6).
- [42] International Standard of Organisation. *ISO 11270:2014: Intelligent transport systems — Lane keeping assistance systems (LKAS) — Performance requirements and test procedures*. Geneva, Switzerland, 2012. URL: %5Curl%7Bhttps://www.iso.org/standard/50347.html%7D (visited on 05/18/2022) (cit. on p. 6).
- [43] International Standard of Organisation. *ISO 15622:2018: Intelligent transport systems — Adaptive cruise control systems — Performance requirements and test procedures*. Geneva, Switzerland, 2019. URL: %5Curl%7Bhttps://www.iso.org/standard/71515.html%7D (visited on 05/18/2022) (cit. on p. 6).
- [44] International Standard of Organisation. *ISO 17361:2017: Intelligent transport systems — Lane departure warning systems — Performance requirements and test procedures*. Geneva, Switzerland, 2017. URL: %5Curl%7Bhttps://www.iso.org/standard/72349.html%7D (visited on 05/18/2022) (cit. on p. 6).
- [45] International Standard of Organisation. *ISO 17387:2008: Intelligent transport systems — Lane change decision aid systems (LCDAS) — Performance requirements and test procedures*. Geneva, Switzerland, 2018. URL: %5Curl%7Bhttps://www.iso.org/standard/43654.html%7D (visited on 05/18/2022) (cit. on p. 6).
- [46] International Standard of Organisation. *ISO 21202:2020: Intelligent transport systems — Partially automated lane change systems (PALS) — Functional / operational requirements and test procedures*. Geneva, Switzerland, 2020. URL: %5Curl%7Bhttps://www.iso.org/standard/70072.html%7D (visited on 05/18/2022) (cit. on p. 6).
- [47] International Standard of Organisation. *ISO 22733-1:2021: Road vehicles — Test method to evaluate the performance of autonomous emergency braking systems — Part 1: Car-to-car*. Geneva, Switzerland, 2021. URL: %5Curl%7Bhttps://www.iso.org/standard/73761.html%7D (visited on 05/18/2022) (cit. on p. 6).
- [48] International Standard of Organisation. *ISO 26262 Part 1-12: Road vehicles — Functional safety*. Geneva, Switzerland (cit. on pp. 5, 7).
- [49] IPG Automotive. *IPG CarMaker Reference Manual(V 8.1.1)*. IPG Automotive GmbH: Karlsruhe, Germany, 2019 (cit. on pp. 12, 49–51).
- [50] *ISO/PAS 21448:2019 Road Vehicles—Safety of the Intended Functionality*. URL: %5Curl%7Bhttps://www.iso.org/standard/70939.html%7D (visited on 04/26/2022) (cit. on p. 8).
- [51] Michal Jasinski. *A Generic Validation Scheme for real-time capable Automotive Radar Sensor Models integrated into an Autonomous Driving Simulator*. Piscataway, NJ: IEEE, 2019. ISBN: 9781728109336. URL: %5Curl%7Bhttp://ieeexplore.ieee.org/servlet/opac?punumber=8854467%7D (cit. on p. 10).



- [52] Zhan Jun et al. "New modeling method of millimeter-wave radar considering target radar echo intensity." In: *Proceedings of the Institution of Mechanical Engineers, Part D: Journal of Automobile Engineering* 235.10-11 (2021), pp. 2857–2870. ISSN: 0954-4070. DOI: \url{10.1177/09544070211004501} (cit. on p. 9).
- [53] N. Kalra and S. M. Paddock. "Driving to Safety: How Many Miles of Driving Would It Take to Demonstrate Autonomous Vehicle Reliability?" In: *Transportation Research Part A: Policy and Practice* 2016 (2016), pp. 182–193. DOI: \url{10.1016/j.tra.2016.09.010} (cit. on pp. 1, 69).
- [54] C. Keimel. *Design of Video Quality Metrics with Multi-Way Data Analysis - A data driven approach*. Springer: Berlin/Heidelberg, Germany, 2015 (cit. on p. 51).
- [55] Don Koks. *How to create and manipulate radar range-Doppler plots: DSTO-TN-1386*. Ed. by DSTO Defence Science and Technology Organisation. Edinburgh (Australia), 2014. URL: %5Curl%7Bhttps://apps.dtic.mil/sti/citations/ada615308%7D (cit. on pp. 37, 42, 45, 47).
- [56] J. Lin. "Divergence measures based on the Shannon entropy." In: *IEEE Trans. Inf. Theory* 1991 (), pp. 145–151. DOI: \url{10.1109/18.6111510.1109/18.61115} (cit. on p. 53).
- [57] H. Ling, R.-C. Chou, and S.-W. Lee. "Shooting and bouncing rays: calculating the RCS of an arbitrarily shaped cavity." In: *IEEE Transactions on Antennas and Propagation* 37.2 (1989), pp. 194–205. ISSN: 0018-926X. DOI: \url{10.1109/8.18706} (cit. on p. 10).
- [58] Clemens Linnhoff et al. "Highly Parameterizable and Generic Perception Sensor Model Architecture." In: *Automatisiertes Fahren 2020*. Ed. by Torsten Bertram. Proceedings. Wiesbaden: Springer Fachmedien Wiesbaden, 2021, pp. 195–206. ISBN: 978-3-658-34751-2. DOI: \url{10.1007/978-3-658-34752-9\textunderscore16} (cit. on p. 14).
- [59] Belinda J. Lipa and Donald E. Barrick. *FMCW Signal Processing*. Ed. by Mirage Systems, Sunnyvale, California. 1990. URL: %5Curl%7Bhttp://www.codar.com/images/about/1990LipaBarr\_FMCW.pdf%7D (visited on 06/23/2022) (cit. on p. 9).
- [60] S. Lutz et al. "Target simulator concept for chirp modulated 77 GHz automotive radar sensors." In: *2014 11th European Radar Conference*. 2014, pp. 65–68. DOI: \url{10.1109/EuRAD.2014.6991208} (cit. on p. 12).
- [61] Steffen Lutz et al. "On fast chirp modulations and compressed sensing for automotive radar applications." In: *2014 15th International Radar Symposium (IRS)*. IEEE, 2014, pp. 1–6. ISBN: 978-617-607-470-0. DOI: \url{10.1109/IRS.2014.6869182} (cit. on p. 30).
- [62] Z. F. Magosi et al. "A Survey on Modelling of Automotive Radar Sensors for Virtual Test and Validation of Automated Driving." In: *Sensors* 22.15 (2022). ISSN: 14248220. DOI: \url{10.3390/s22155693}. URL: %5Curl%7Bhttps://www.scopus.com/inward/record.uri?eid=2-s2.0-85136767061&doi=10.

- 3390%2fs22155693&partnerID=40&md5=fbccb17367a2df0c73d2e199e1ceb79b%7D (cit. on p. 26).
- [63] Z. F. Magosi et al. "Evaluation Methodology for Physical Radar Perception Sensor Models Based on On-Road Measurements for the Testing and Validation of Automated Driving." In: *Energies* 15.7 (2022). ISSN: 19961073. DOI: \url{10.3390/en15072545}. URL: %5Curl%7Bhttps://www.scopus.com/inward/record.uri?eid=2-s2.0-85128024711&doi=10.3390/2fen15072545&partnerID=40&md5=c2b48e57782a260ce8b45b1471a7362b%7D (cit. on pp. 22, 23, 26, 27, 40, 58, 62).
- [64] F. Michael Maier, Vamsi P. Makkapati, and Martin Horn. "Environment perception simulation for radar stimulation in automated driving function testing." In: *e & i Elektrotechnik und Informationstechnik* 135.4-5 (2018), pp. 309–315. ISSN: 0932-383X. DOI: \url{10.1007/s00502-018-0624-5} (cit. on pp. 12, 17).
- [65] Adam Martowicz, Alberto Gallina, and Grzegorz Karpiel. *2019 24th International Conference on Methods and Models in Automation and Robotics (MMAR)*. Piscataway, NJ: IEEE, 2019. ISBN: 9781728109336. URL: %5Curl%7Bhttp://ieeexplore.ieee.org/servlet/opac?punumber=8854467%7D (cit. on p. 10).
- [66] K. Maupin, L. Swiler, and N. Porter. "Validation Metrics for Deterministic and Probabilistic Data." In: *J. Verif. Valid. Uncertain. Quantif* 2019 (). DOI: \url{10.1115/1.4042443} (cit. on pp. 53, 65).
- [67] Till Menzel, Gerrit Bagschik, and Markus Maurer. "Scenarios for Development, Test and Validation of Automated Vehicles." In: *2018 IEEE Intelligent Vehicles Symposium*. URL: %5Curl%7Bhttp://arxiv.org/pdf/1801.08598v3%7D (cit. on p. 13).
- [68] Stefan Muckenhuber, Eniz Museljic, and Georg Stettinger. "Performance evaluation of a state-of-the-art automotive radar and corresponding modeling approaches based on a large labeled dataset." In: *Journal of Intelligent Transportation Systems* (2021), pp. 1–20. ISSN: 1547-2450. DOI: \url{10.1080/15472450.2021.1959328} (cit. on pp. 14, 15).
- [69] Stefan Muckenhuber et al. *Object-based sensor model for virtual testing of ADAS/AD functions: The 8th IEEE International Conference on Connected Vehicles and Expo (ICCVE)*. Piscataway, NJ: IEEE, 2019. ISBN: 9781728101422. DOI: \url{10.1109/ICCVE45908.2019}. URL: %5Curl%7Bhttp://ieeexplore.ieee.org/servlet/opac?punumber=8952572%7D (cit. on p. 9).
- [70] Multiple Authors. *Safety First for Automated Driving*. Ed. by Daimler AG. 2019. URL: %5Curl%7Bhttps://www.mercedes-benz.com/content/dam/brandhub/innovation/safety-first-for-automated-driving/safety-first-for-automated-driving-withepaper\_en.pdf%7D (visited on 06/23/2022) (cit. on pp. 9, 13).

- [71] Anthony Ngo, Max Paul Bauer, and Michael Resch. *A Multi-Layered Approach for Measuring the Simulation-to-Reality Gap of Radar Perception for Autonomous Driving*. June 15, 2021. URL: <https://arxiv.org/pdf/2106.08372v2> (cit. on pp. 11, 27).
- [72] Anthony Ngo, Max Paul Bauer, and Michael Resch. *A Sensitivity Analysis Approach for Evaluating a Radar Simulation for Virtual Testing of Autonomous Driving Functions: ACIRS 2020 : July 17-19, 2020, Singapore*. Piscataway, NJ: IEEE, 2020. ISBN: 9781728198187. DOI: [10.1109/ACIRS49895.2020](https://doi.org/10.1109/ACIRS49895.2020). URL: <https://ieeexplore.ieee.org/servlet/opac?punumber=9154368> (cit. on pp. 11, 27, 64, 65).
- [73] NovAtel Inc., ed. *An Introduction to GNSS: GPS, GLONASS, BeiDou, Galileo and other Global Navigation Satellite Systems*. 2nd ed. Calgary, Alberta, Canada: NovAtel Inc., 2015. ISBN: 978-0-9813754-0-3. URL: <https://novatel.com/an-introduction-to-gnss/chapter-5-resolving-errors/real-time-kinematic-rtk> (visited on 11/15/2022) (cit. on p. 29).
- [74] W. Oberkampff and C. Roy. *Verification and Validation in Scientific Computing*. 2010. DOI: [10.1017/CB09780511760396](https://doi.org/10.1017/CB09780511760396) (cit. on p. 51).
- [75] Hanno Rabe. “Bildgebende Verfahren zur Steigerung der Ausfallsicherheit radarbasierter Füllstandsmesssysteme.” Doctoral dissertation. Gottfried Wilhelm Leibniz Universität Hannover, 2013. DOI: [10.15488/8144](https://doi.org/10.15488/8144). URL: <https://www.repo.uni-hannover.de/handle/123456789/8197> (cit. on pp. 36, 37).
- [76] Theodore S. Rappaport. *Wireless communications: principles and practice*. New Jersey: prentice hall PTR, 1996 (cit. on pp. 26, 37, 40, 47).
- [77] Mark A. Richards, James A. Scheer, and William A. Holm. *Principles of modern radar*. first published 2010, reprinted with corrections 2015. Vol. 1. Raleigh, NC: SciTech Publ, 2015. ISBN: 9781891121524. DOI: [10.1049/SBRA021E](https://doi.org/10.1049/SBRA021E) (cit. on pp. 38, 40–42, 45, 47).
- [78] Stefan Riedmaier et al. “Non-deterministic model validation methodology for simulation-based safety assessment of automated vehicles.” In: *Simulation Modelling Practice and Theory* 109 (2021), p. 102274. ISSN: 1569190X. DOI: [10.1016/j.simpat.2021.102274](https://doi.org/10.1016/j.simpat.2021.102274) (cit. on p. 27).
- [79] Hermann Rohling. “Radar CFAR Thresholding in Clutter and Multiple Target Situations.” In: *IEEE Transactions on Aerospace and Electronic Systems* AES-19.4 (1983), pp. 608–621. ISSN: 0018-9251. DOI: [10.1109/TAES.1983.309350](https://doi.org/10.1109/TAES.1983.309350) (cit. on pp. 42, 43).
- [80] Philipp Rosenberger. “Metrics for Specification, Validation, and Uncertainty Prediction for Credibility in Simulation of Active Perception Sensor Systems.” PhD thesis. Darmstadt, Germany: TU Darmstadt, 2022 (cit. on pp. 27, 64).

- [81] Philipp Rosenberger et al. "Towards a generally accepted validation methodology for sensor models-challenges, metrics, and first results." In: *Proceedings of 2019 Graz Symposium Virtual Vehicle*. Ed. by Virtual Vehicle Research and Test Center. 2019, pp. 1–13. URL: <https://tuprints.ulb.tu-darmstadt.de/8653/7/Towards%20a%20Generally%20Accepted%20Validation%20Methodology%20for%20Sensor%20Models.pdf> (visited on 06/23/2022) (cit. on p. 9).
- [82] Francisca Rosique et al. "A Systematic Review of Perception System and Simulators for Autonomous Vehicles Research." In: *Sensors (Basel, Switzerland)* 19.3 (2019). DOI: [10.3390/s19030648](https://doi.org/10.3390/s19030648) (cit. on p. 14).
- [83] Sargent, R. G. Verification and. "and validation of simulation models." In: *In Proceedings of the 2010* (2010), pp. 166–183. DOI: [10.1109/WSC.2010.5679166](https://doi.org/10.1109/WSC.2010.5679166) (cit. on p. 51).
- [84] Alexander Schaermann et al. "Validation of vehicle environment sensor models." In: *2017 IEEE Intelligent Vehicles Symposium (IV)*. IEEE, 2017, pp. 405–411. ISBN: 978-1-5090-4804-5. DOI: [10.1109/IVS.2017.7995752](https://doi.org/10.1109/IVS.2017.7995752) (cit. on p. 27).
- [85] Alexander Scheel and Klaus Dietmayer. "Tracking Multiple Vehicles Using a Variational Radar Model." In: *IEEE Transactions on Intelligent Transportation Systems* 20.10 (2019), pp. 3721–3736. ISSN: 1524-9050. DOI: [10.1109/TITS.2018.2879041](https://doi.org/10.1109/TITS.2018.2879041) (cit. on p. 10).
- [86] Birgit Schlager et al. "State-of-the-Art Sensor Models for Virtual Testing of Advanced Driver Assistance Systems/Autonomous Driving Functions." In: *SAE International Journal of Connected and Automated Vehicles* 3.3 (2020), pp. 233–261. ISSN: 2574-075X. DOI: [10.4271/12-03-03-0018](https://doi.org/10.4271/12-03-03-0018) (cit. on pp. 9, 10).
- [87] Simon Schmidt et al. "Configurable Sensor Model Architecture for the Development of Automated Driving Systems." In: *Sensors (Basel, Switzerland)* 21.14 (2021). DOI: [10.3390/s21144687](https://doi.org/10.3390/s21144687) (cit. on p. 7).
- [88] R. Schneider and J. Wenger. "High resolution radar for automobile applications." In: *Advances in Radio Science*. Copernicus GmbH, 2003, pp. 105–111. DOI: [10.5194/ars-1-105-2003](https://doi.org/10.5194/ars-1-105-2003). URL: <https://ars.copernicus.org/articles/1/105/2003/> (visited on 05/05/2003) (cit. on pp. 30, 38, 47).
- [89] Scott C. Schnelle et al. *Review of Simulation Frameworks and Standards Related to Driving Scenarios*. Dec. 1, 2019. URL: <https://rosap.ntl.bts.gov/view/dot/43621> (visited on 11/14/2022) (cit. on p. 9).
- [90] Hans-Peter Schoener. "Automotive Needs and Expectations towards Next Generation Driving Simulation." In: *Proceedings of the 2018 Driving Simulator Conference*. URL: [https://dsc2018.org/Docs/Keynotes/SCHOENER\\_KEYNOTE.pdf](https://dsc2018.org/Docs/Keynotes/SCHOENER_KEYNOTE.pdf) (visited on 05/19/2022) (cit. on p. 12).

- [91] Christian Schuesler et al. "A Realistic Radar Ray Tracing Simulator for Large MIMO-Arrays in Automotive Environments." In: *IEEE Journal of Microwaves* 1.4 (2021), pp. 962–974. DOI: \url{10.1109/JMW.2021.3104722} (cit. on p. 17).
- [92] Karin Schuler, Denis Becker, and Werner Wiesbeck. "Extraction of Virtual Scattering Centers of Vehicles by Ray-Tracing Simulations." In: *IEEE Transactions on Antennas and Propagation* 56.11 (2008), pp. 3543–3551. ISSN: 0018-926X. DOI: \url{10.1109/TAP.2008.2005436} (cit. on p. 10).
- [93] Barbara Schutt et al. "A Taxonomy for Quality in Simulation-Based Development and Testing of Automated Driving Systems." In: *IEEE Access* 10 (2022), pp. 18631–18644. DOI: \url{10.1109/ACCESS.2022.3149542} (cit. on p. 13).
- [94] Merrill I. Skolnik. *Introduction to radar systems*. 3. ed. McGraw-Hill electrical engineering series. Boston: McGraw-Hill, 2007. ISBN: 0072909803 (cit. on pp. 38, 52).
- [95] Benjamin J. Slocumb and Daniel L. Macumber. "Surveillance radar range-bearing centroid processing, part II: merged measurements." In: *Signal and Data Processing of Small Targets 2006*. Ed. by Oliver E. Drummond. SPIE Proceedings. SPIE, 2006, p. 623604. DOI: \url{10.1117/12.673521} (cit. on p. 38).
- [96] Jan Sobotka and Jiri Novak. *Digital Vehicle Radar Sensor Target Simulation: International Instrumentation & Measurement Technology Conference : May 25-29, 2020, Valamar Riviera, Dubrovnik, Croatia : 2020 conference proceedings*. Piscataway, NJ, USA: IEEE, 2020. ISBN: 9781728144603. DOI: \url{10.1109/I2MTC43012.2020}. URL: %5Curl%7Bhttps://ieeexplore.ieee.org/servlet/opac?punumber=9123988%7D (cit. on p. 11).
- [97] Stefan Jesenski et al. *Simulation-Based Methods for Validation of Automated Driving: A Model-Based Analysis and an Overview about Methods for Implementation: Auckland, New Zealand, 27-30 October 2019*. Piscataway, NJ: IEEE, 2019. ISBN: 9781538670248. URL: %5Curl%7Bhttps://ieeexplore.ieee.org/servlet/opac?punumber=8907344%7D (cit. on p. 64).
- [98] Z. Szalay, Z. Hamar, and P. A. Simon. "Multi-layer Autonomous Vehicle and Simulation Validation Ecosystem Axis: ZalaZONE." In: *Intelligent Autonomous Systems 15*. Springer: Berlin/Heidelberg, Germany, 2019, pp. 954–963 (cit. on p. 23).
- [99] Zsolt Szalay. "Next Generation X-in-the-Loop Validation Methodology for Automated Vehicle Systems." In: *IEEE Access* 9 (2021), pp. 35616–35632. DOI: \url{10.1109/ACCESS.2021.3061732} (cit. on pp. 5, 6).
- [100] Jorn Thieling, Susanne Frese, and Jurgen RoBmann. "Scalable and Physical Radar Sensor Simulation for Interacting Digital Twins." In: *IEEE Sensors Journal* 21.3 (2021), pp. 3184–3192. ISSN: 1530-437X. DOI: \url{10.1109/JSEN.2020.3026416} (cit. on p. 17).

- [101] V. Tihanyi et al. "Motorway Measurement Campaign to Support R&D Activities in the Field of Automated Driving Technologies." In: *Sensors* 2021 (). ISSN: 14248220. DOI: \url{10.3390/s2106216910.3390/s21062169} (cit. on pp. 47–49).
- [102] United Nations Economic Commission for Europe. *Regulation No 131 of the Economic Commission for Europe of the United Nations (UN/ECE) - Uniform provisions concerning the approval of motor vehicles with regard to the Advanced Emergency Braking Systems (AEBS)*. Geneva, Switzerland, 2014. URL: %5Curl%7Bhttps://eur-lex.europa.eu/legal-content/EN/TXT/?uri=CELEX:42014X0719(01)}%7D (visited on 05/18/2022) (cit. on p. 6).
- [103] United Nations Economic Commission for Europe. *UN Regulation No. 157 - Automated Lane Keeping Systems (ALKS)*. Geneva, Switzerland, 2021. URL: %5Curl%7Bhttps://unece.org/transport/documents/2021/03/standards/un-regulation-no-157-automated-lane-keeping-systems-alks%7D (visited on 05/18/2022) (cit. on p. 6).
- [104] V. C. Chen et al. "Micro-Doppler effect in radar: phenomenon, model, and simulation study." In: *IEEE Transactions on Aerospace and Electronic Systems* 42.1 (2006), pp. 2–21. ISSN: 0018-9251. DOI: \url{10.1109/TAES.2006.1603402} (cit. on p. 43).
- [105] C. Wellershaus. "Performance assessment of a physical sensor model for Automated Driving." Doctoral dissertation. Master's Thesis, Graz University of Technology, Graz, Austria, 2021 (cit. on pp. 51, 52).
- [106] Tim A. Wheeler et al. "Deep stochastic radar models." In: *2017 IEEE Intelligent Vehicles Symposium (IV)*. IEEE, 2017, pp. 47–53. ISBN: 978-1-5090-4804-5. DOI: \url{10.1109/IVS.2017.7995697} (cit. on p. 10).
- [107] Volker Winkler. *Range Doppler detection for automotive FMCW radars*. Piscataway, NJ: IEEE Service Center, 2007. ISBN: 2874870013 (cit. on p. 32).
- [108] Jeffrey Wishart et al. "Literature Review of Verification and Validation Activities of Automated Driving Systems." In: *SAE International Journal of Connected and Automated Vehicles* 3.4 (2020), pp. 267–323. ISSN: 2574-075X. DOI: \url{10.4271/12-03-04-0020} (cit. on p. 7).
- [109] World Forum for Harmonization of Vehicle Regulations. (GRVA) *New Assessment/Test Method for Automated Driving (NATM) - Master Document*. 2021. URL: %5Curl%7Bhttps://unece.org/transport/documents/2021/04/working-documents/grva-new-assessmenttest-method-automated-driving-natm%7D (visited on 05/19/2022) (cit. on p. 13).
- [110] Xuezhi Wang. "Challa, S.; Evans, R. Gating techniques for maneuvering target tracking in clutter." In: *IEEE Trans. Aerosp. Electron. Syst* 2002 (), pp. 1087–1097. DOI: \url{10.1109/TAES.2002.103942610.1109/TAES.2002.1039426} (cit. on p. 51).

- [111] Y. Li, L. Du, and H. Liu. "Hierarchical Classification of Moving Vehicles Based on Empirical Mode Decomposition of Micro-Doppler Signatures." In: *IEEE Transactions on Geoscience and Remote Sensing* 51.5 (2013), pp. 3001–3013. ISSN: 1558-0644. DOI: \url{10.1109/TGRS.2012.2216885} (cit. on p. 24).
- [112] Bing Zhu et al. "Millimeter-Wave Radar in-the-Loop Testing for Intelligent Vehicles." In: *IEEE Transactions on Intelligent Transportation Systems* (2021), pp. 1–11. ISSN: 1524-9050. DOI: \url{10.1109/TITS.2021.3100894} (cit. on p. 11).
- [113] Luoyan Zhu et al. "Measurement and Ray-Tracing Simulation for Millimeter-Wave Automotive Radar." In: *2021 IEEE 4th International Conference on Electronic Information and Communication Technology (ICEICT)*. IEEE, 2021, pp. 582–587. ISBN: 978-1-6654-3203-0. DOI: \url{10.1109/ICEICT53123.2021.9531101} (cit. on p. 17).

## Appendix A.

### Summary of Papers

This section contains the author's summary and contribution of the publications on which the thesis is based, already listed in chapter chapter .

#### A.1. Paper 1

Holder, M., Rosenberger, P., Winner, H., D'hondt, T., Makkapati, V. P., Maier, F. M., Schreiber, H., Magosi, Z. F., Slavik, Z., Bringmann, O., Rosenstiel, W. (2018). Measurements revealing Challenges in Radar Sensor Modeling for Virtual Validation of Autonomous Driving. in 2018 21st International Conference on Intelligent Transportation Systems (ITSC) (S. 2616 - 2622)

The aim of the present work was to identify open issues related to automotive radar sensor modelling, model validation and metrics definition. By reviewing existing radar sensor models with respect to their applicability for virtual validation and verification of automated driving functions (ADF), the authors concluded that neither generally accepted requirements nor standardised validation criteria for radar sensor models are known. The paper highlights the need for metrics for sensor fidelity for important phenomena with characteristic effects on detection capability. The solution presented is based on on-road measurements that highlight the importance of multipath propagation, separability and variation of RCS over azimuth angles, and combines the observations with modelling approaches provided by commercial simulation platforms. The paper concludes that more specific experimental design is required for the validation of synthetic and measured radar sensor data, as radar detections are highly stochastic.

The thesis author was responsible for setting up two test vehicles, each equipped with a highly accurate RTK-GPS IMU and the ego vehicle additionally with a commercially available radar sensor with an open communication interface. Furthermore, for the creation of the driving manoeuvre catalogue in cooperation with the project partners and their execution on both closed and open roads. Support by writing the "Radar sensor fundamentals" part, as well as editing and proofreading of the publication.

#### A.2. Paper 2

Tihanyi, V., Tettamanti, T., Csonthó, M., Eichberger, A., Ficzer, D., Gangel, K., Hörmann, L. B., Klaffenböck, M., Knauder, C., Luley, P., **Magosi, Z. F.**, Magyar,



G., Németh, H., Soós, G., Szántay, D., Reckenzaun, J., Remeli, V., Rövid, A., Ruether, M., ... Szalay, Z. (2021). Motorway measurement campaign to support RnD activities in the field of automated driving technologies. *Sensors*, 21(6), 1-35. [2169].

The aim of the presented work was to perform on-road measurements on a real motorway section in Hungary. High-precision data acquisition was carried out with both vehicle and infrastructure sensors, so that the data of all vehicles involved could be synchronised with the infrastructure data in a post-processing. Besides equipping the test vehicle with additional open-interface perceptual sensors and differential global navigation satellite systems (GNSS) for ground truth localisation, the main contribution of the present work was to introduce the method for creating an Ultra High Definition (UHD) map based on road geometry mapped with high precision measurement system. Specific test scenarios were defined, executed and recorded to demonstrate the viability of the collected data with access to ground truth labeling. The methodology presented in this paper, in combination with the recorded various perception sensor data, forms the basis for the sensor modelling and model evaluation approach presented in this thesis.

The author of the thesis was responsible for setting up the two test vehicles involved in the measurement campaign, with the appropriate high-precision positioning and open interface perception sensors. Preparation and coordination of the execution of specific driving scenarios, with particular attention to the selected radar sensor phenomena. Writing and editing the subchapter "TU Graz Vehicles and Sensors" and editing and proofreading the publication.

### A.3. Paper 3

**Magosi, Z. F.**, Li, H., Rosenberger, P., Wan, L., Eichberger, A. (2022). A Survey on Modelling of Automotive Radar Sensors for Virtual Test and Validation of Automated Driving. *Sensors*, 22(15), [5693].

The aim of the presented work was to comprehensively summarise the heterogeneous state of the art in radar sensor modelling. Instead of a technology-based classification, this work summarises the partitioning methods described in the literature and introduces a novel classification method based on how these models can be used in vehicle development using the V-model. Since X-in-the-loop based approaches ultimately support the goal of whole vehicle level development, the available modelling approaches are divided into *operational*, *functional*, *technical* and *individual* models based on how they are or can be used in the development process, set out in ascending order of complexity. The application and usability of these models along the development process are summarised in a comprehensive tabular overview that combines previous classifications with our new approach. Thus, the paper provides a quick overview and helps to select a suitable modelling method for further use. Finally, a link to a dynamic spreadsheet has also been provided, which is publicly available.

The thesis author was responsible for evaluating the state-of-the-art methods used to radar sensor model categorisation. Developing the novel classification method and assigning the reviewed sensor modelling approaches. Defining the structure of the paper, writing and editing the publication.

#### A.4. Paper 4

**Magosi, Z. F., Eichberger, A. (2022).** A novel approach for simulation of automotive radar sensors designed for systematic support of vehicle development. Submitted to journal *Energies* on 07.11.2022

This paper presents a novel method for the synthetic generation of radar point clouds, introducing a process flow consisting of observations of on-road measurements converted into a semi-physical modelling approach. The modelling was done by establishing guiding principles considering transferability and interchangeability of synthetic and real radar data, modularity through extensibility, accessibility of only a reduced set of parameters, and flexibility in terms of modelling complexity in relation to model fidelity. The development of the modelling method was made possible by the carefully designed measurement setup developed in Paper 1, introduced in Paper 2 and Paper 5. The continuously developed and refined post-processing technique applied to the recorded raw data has allowed the real radar point cloud data to be mapped not only spatially but also temporally to the reference vehicle. The observations to determine and select typical radar detection phenomena to be implemented have been conducted over thousands of measured kilometres accumulated while performing hundreds of driving manoeuvres that can be assigned to the different driving scenarios. The definition, design and documentation of these specific driving scenarios to challenge the real radar sensor is also part of the modelling process. The novel contribution of the modelling method presented, is to apply physical modelling where possible, otherwise mathematical approximations based on experimental data. The semi-physical modelling approach is used to generate the synthetic radar point clouds and simulate the Radar Cross Section (RCS) by taking into account the antenna characteristics, the radar equation and the calculation of the velocities using physical effects as determined by measurements. The model is real-time capable and can be used on various X-in-the-loop test benches. Its modular structure allows it to be used throughout the entire development process, from the concept phase to future virtual vehicle homologation.

The thesis author was responsible for the development of the overall modelling concept. Design and implement the measurement set-up, including the preparation of the test vehicles. Definition, design and documentation of radar sensor specific driving scenarios. Preparation, coordination and execution of driving manoeuvres. Development and implementation of a suitable post-processing technique, followed by the development and implementation of the semi-physical radar sensor model both in MATLAB. Simulation and evaluation of the sensor model using the method developed in Paper 5, as well as writing and editing the publication.

## A.5. Paper 5

**Magosi, Z. F.**, Wellershaus, C., Tihanyi, V., Luley, P., Eichberger, A. (2022). Evaluation methodology for physical radar perception sensor models based on on-road measurements for testing and validation of automated driving. *Energies*, 15(7), [2545].

This paper describes a novel sensor model evaluation procedure developed for the evaluation of sensor models simulating active perceptual sensors at a low level of signal processing. The presented assessment method that we call *Dynamic Ground Truth—Sensor Model Validation* (DGT-SMV), is based on a statistical comparison of simulated and measured radar point cloud data and aims to provide a quantifiable evaluation of the low-level radar-sensor model used. The presented method is suitable for the comparison of sensor models in virtual space even if the model defined as the reference sensor and the model to be evaluated only exist virtually, as well as in our case if the reference sensor data originate from real measurements. The evaluation method generally assumes that exactly the same driving manoeuvre is used to generate the synthetic radar data that was also recorded with a real sensor. This implies the quality requirements for the ground truth (GT) reference measurement system and the availability of an exactly identical replica, often referred to as a *Digital-Twin* of the real driving environment. For the method development the measurement data recorded with the measurement setup already presented in paper 2. is used to label the recorded low-level sensor output *measurement data labelling*. To provide a method for direct comparison, the test drives are then re-simulated in a detailed virtual representation with a digital twin, provided in Paper 2. and the virtual sensor under investigation *virtual sensor replay*, implemented in IPG CarMaker simulation framework. The virtual sensor then generates the low-level radar sensor point cloud data output, which is finally compared with the measured radar sensor output *performance evaluation* using statistical methods. In this paper, validation metrics are derived by comparing the probability distribution of selected signals and the shapes of the corresponding observations. A quantified expression for the difference between two or more discrete probability distributions is given by calculating the Jensen–Shannon Divergence (JSD).

The author of the thesis was responsible for defining the concept of the *Dynamic Ground Truth—Sensor Model Validation* method, developing the evaluation procedure, method development and implementation in MATLAB of the validation metric calculation (JSD), and writing and editing the corresponding parts including the following subsections: Driving Scenario, Vehicle Setup and Measurement System.

## A.6. Paper 6

Bernsteiner, S., **Magosi, Z. F.**, Lindvai-Soos, D., Eichberger, A. (2015). Radar Sensor Model for the Virtual Development Process. *ATZelektronik worldwide*, 10(2), 46–52 (2015).

This paper describes a radar sensor model that forms the basis for the semi-physical radar sensor model described in this thesis. The model follows a phenomenological approach and consists of three modules representing ground truth information, sensor properties and signal processing. The model output represents the highly processed data in terms of the level of signal processing so that it is comparable to the perceptual algorithm output of a real sensor. The performance evaluation of the presented phenomenological radar sensor model was performed indirectly by comparing the simulation results of the virtually executed ADAS function using the synthetic sensor data with its real counterpart undergoing the same driving scenario. This evaluation method requires the availability of models that sufficiently accurately describe the ADAS function under test, the real radar sensor and the dynamic behaviour of the real test vehicle.

The author of the paper was responsible for the development of the presented phenomenological radar sensor model, the implementation in MATLAB, the development of the measurement set-up, the preparation of test vehicles and for editing the publication.

### A.7. Paper 7

Eichberger, A., Markovic, G., **Magosi, Z. F.**, Rogic, B., Lex, C., Samiee, S. (2017). A Car2X Sensor Model for Virtual Development of Automated Driving. *International Journal of Advanced Robotic Systems*, 14(5).

In this work, two Car2X sensor models were developed, which differ in their scope of application. The first model (general model) was developed to handle general cases (e.g. two-way traffic, convoy or semi-static scenarios) in different areas (e.g. highway, rural, suburban, urban). The second model (intersection model) considers intersection scenarios by including some additional geometric inputs and exponents related to the geometry of a specific real world intersection. The modelling approach is based on modelling path loss by calculating free-space signal attenuation and on taking into account signal fluctuations caused by multipath wave propagation, which is accounted for by the two-beam ground reflection model. This work forms the basis for understanding specific wave propagation phenomena such as free space loss and signal cancellation in multipath propagation environments and gives a first impression of these effects, which are also included in the semi-physical model presented here.

The author of the dissertation was responsible for defining and implementing the measurement setup for two vehicles with range-extended data transmission channel, performing the measurements, preparing the measurement data for further processing, was involved as a consultant on the topic of wave propagation and editing these parts in the publication.

### A.8. Paper 8

Höber, M., Nalic, D., Eichberger, A., Samiee, S., **Magosi, Z. F.**, Payerl, C. (2020). Phenomenological Modelling of Lane Detection Sensors for Validating Perfor-

mance of Lane Keeping Assist Systems. 899-905. Beitrag in IEEE Intelligent Vehicle Symposium 2020, Virtual, Las Vegas, USA / Vereinigte Staaten.

In this paper, a phenomenological sensor model for the lane keeping assist system (LKAS) was presented. Using this model, a performance analysis of LKAS was performed in the virtual environment of IPG CarMaker. For the evaluation of the lane departure behaviour, the lane detection model was parameterised based on measured camera data collected on public roads. The presented approach allows to model image processing-based sensors for validation of ADAS functionalities in the simulation without considering and modelling physical effects that influence the sensor performance.

The author of the dissertation was responsible for defining and implementing the measurement setup, performing the measurements, preparing the measurement data for further processing, and editing the corresponding section in the publication.

## A.9. Paper 9

Babic, D., Babic, D., Fiolic, M., Eichberger, A., **Magosi, Z. F.** (2021). A Comparison of Lane Marking Detection Quality and View Range between Daytime and Night-Time Conditions by Machine Vision. *Energies*, 14(15), [4666].

The aim of this study was to investigate the differences in detection quality and field of view of a commercial visual perception sensor in dry day and night conditions. In order to determine and compare the detection quality and visual range of the Mobileye 630 vision system, tests were conducted on four rural road sections in Croatia.

The author of the dissertation was responsible for defining and implementing the measurement setup, performing the measurements, preparing the measurement data for further processing, and editing the corresponding section in the publication.

## A.10. Paper 10

Li, H., Kanuric, T., Arefnezhad, S., **Magosi, Z. F.**, Wellershaus, C., Babic, D., Babic, D., Tihanyi, V., Eichberger, A., Baunach, M. C. (2021). Phenomenological Modelling of Camera Performance for Road Marking Detection. *Energies*, 15(1), [194].

In this paper, a phenomenological lane departure detection (PLDM) model is presented to simulate the lane detection performance of a commercial front camera module. The presented approach uses the multi-layer perceptron (MLP) modelling technique, which belongs to the neural network (NN) class. To prepare the input training data for the presented PLD model, which consists of four hidden layers, on-road measurements were performed on a closed section of the M86 motorway in Hungary. The input data of the model includes vehicle dynamic signals (such as speed and acceleration, etc.) provided by the high accuracy ground truth (GT) measurement system. In addition, the difference between the reference output of the

digital-twin of the motorway and the results of lane detection by the MobilEye-630 image processing based open interface sensor is considered as the target of the NN.

The author of the dissertation was responsible for defining and implementing the measurement setup, performing the measurements, preparing the measurement data for further processing, and editing the corresponding section in the publication.

## Appendix B.

### Additional results

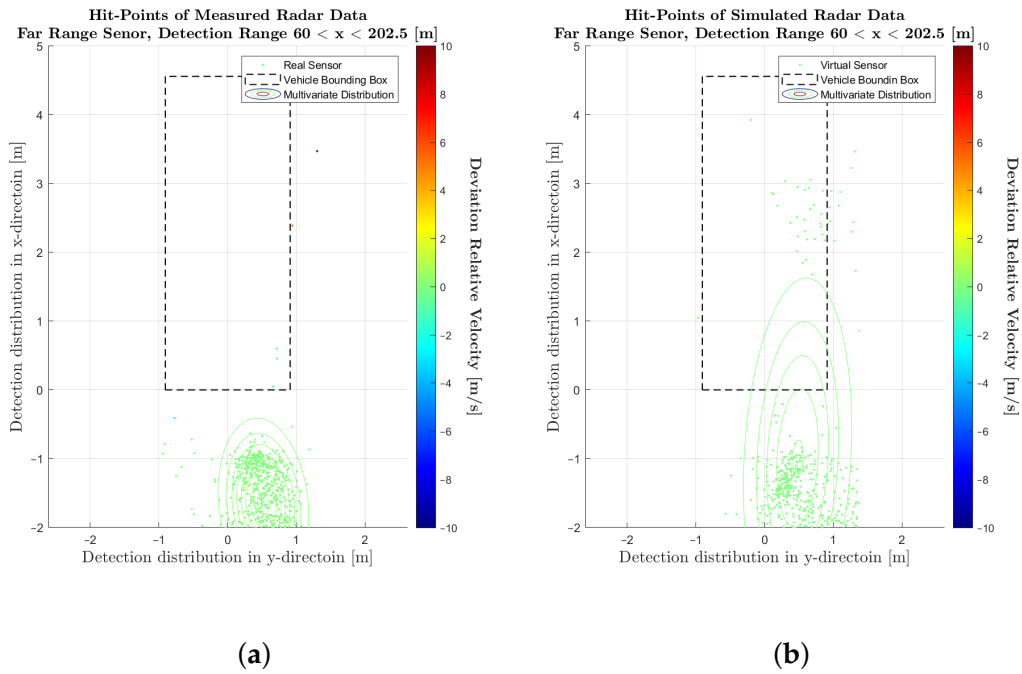


Figure B.1.: Visualisation of the measured and simulated radar point cloud data, cumulated over the entire measurement time, in the far-range detection sector. (a) Scatterplot of detections for the real sensor. (b) Scatterplot of detections for the sensor model.

## Appendix B. Additional results

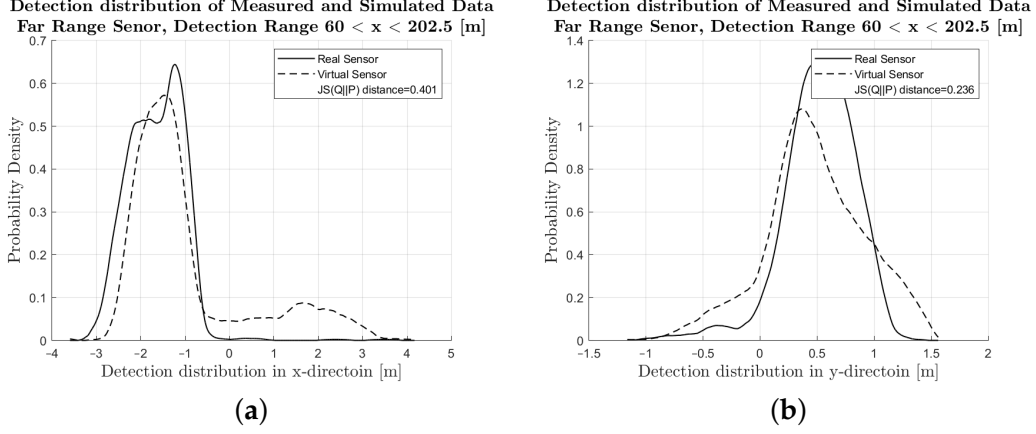


Figure B.2.: Visual comparison and evaluation of the probability distribution function (PDF) of the deviation of the measured and simulated radar point clouds with respect to the reference point in the far-range detection sector. (a) PDF of the deviation in the  $x$ -direction from  $\mathcal{P}_{ref}(x, y)$  of the real sensor and sensor model. (b) PDF of the deviation in the  $y$ -direction from  $\mathcal{P}_{ref}(x, y)$  of the real sensor and sensor model.

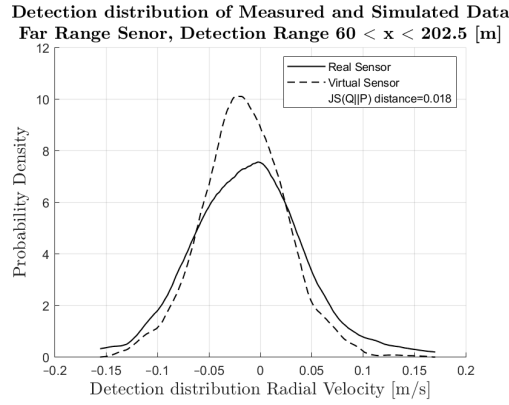


Figure B.3.: Visual comparison and evaluation of the probability distribution function (PDF) of the deviation of the measured and simulated radar point clouds with respect to the reference point  $\mathcal{P}_{ref}(x, y)$  in the far-range detection sector: PDF of the radial velocity deviation from the reference velocity.



## Appendix B. Additional results

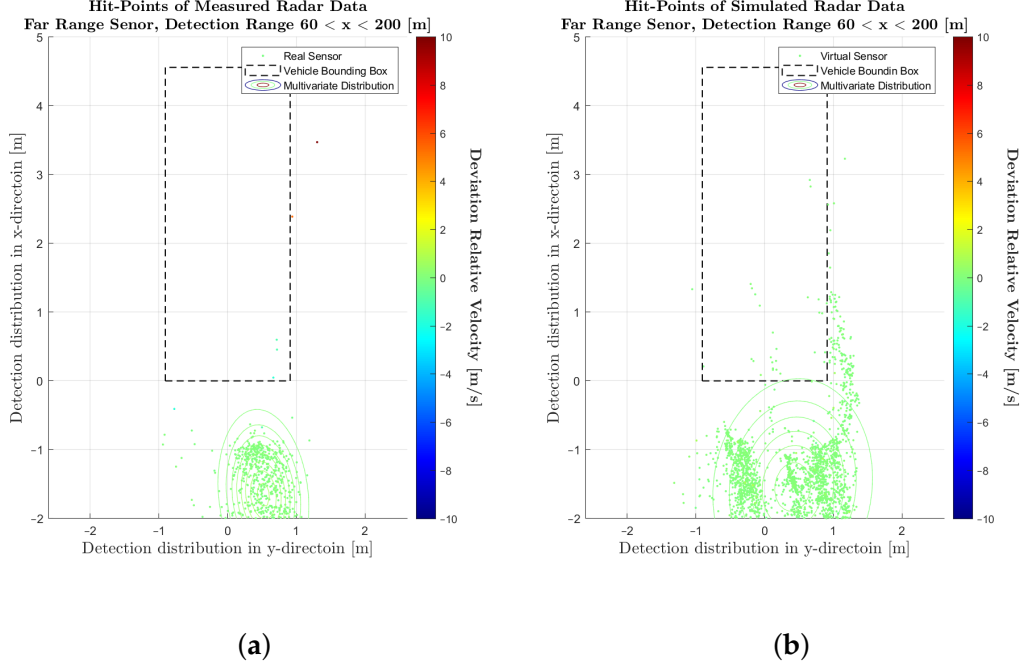


Figure B.4.: Visualisation of the measured and simulated radar point cloud data, cumulated over the entire measurement time, in the far-range detection sector. (a) Scatterplot of detections for the real sensor. (b) Scatterplot of detections for the sensor model.

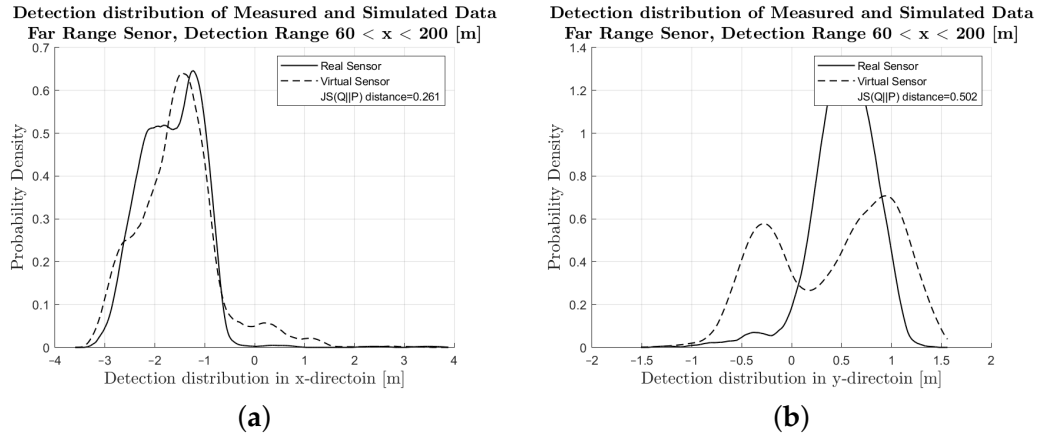


Figure B.5.: Visual comparison and evaluation of the probability distribution function (PDF) of the deviation of the measured and simulated radar point clouds with respect to the reference point in the far-range detection sector. (a) PDF of the deviation in the  $x$ -direction from  $\mathcal{P}_{ref}(x, y)$  of the real sensor and sensor model. (b) PDF of the deviation in the  $y$ -direction from  $\mathcal{P}_{ref}(x, y)$  of the real sensor and sensor model.

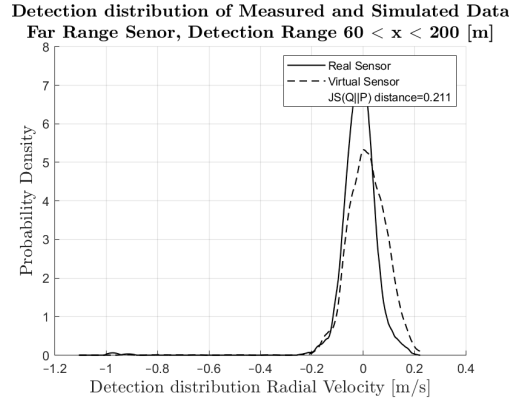


Figure B.6.: Visual comparison and evaluation of the probability distribution function (PDF) of the deviation of the measured and simulated radar point clouds with respect to the reference point  $\mathcal{P}_{ref}(x, y)$  in the far-range detection sector: PDF of the radial velocity deviation from the reference velocity.

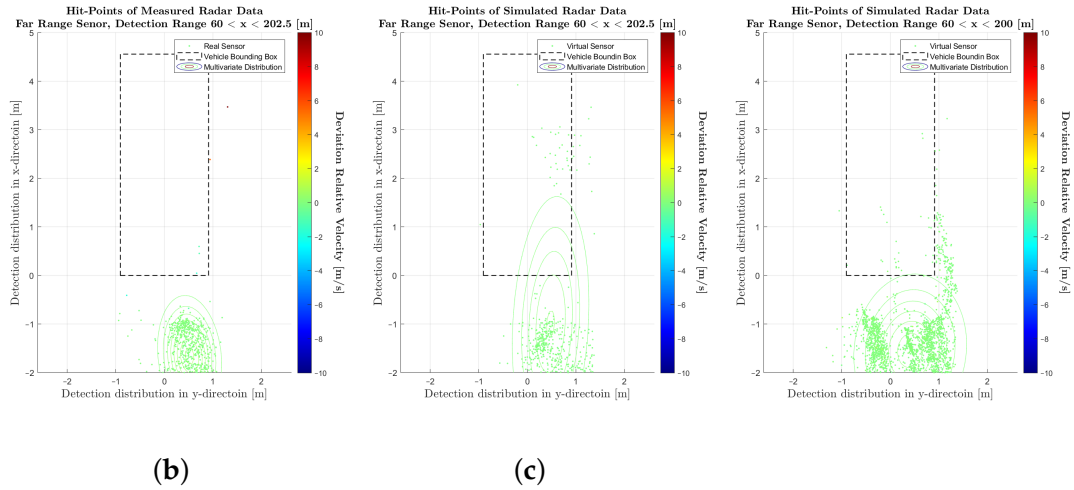


Figure B.7.: Visualisation of the measured and simulated radar point cloud data, cumulated over the entire measurement time, in the far-range detection sector. (a) Scatterplot of detections for the real sensor. (b) Scatterplot of detections for the sensor model presented in this paper. (c) Scatterplot of detections for the sensor model of commercial application.

## Appendix B. Additional results

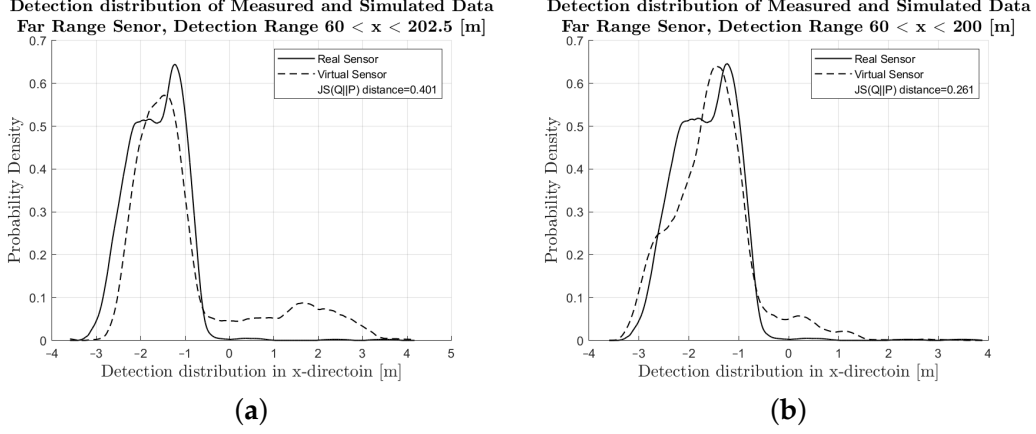


Figure B.8.: Visual comparison and evaluation of the probability distribution function (PDF) of the deviation of the measured and simulated radar point clouds with respect to the reference point in the far-range detection sector. (a) PDF of the deviation in the  $x$ -direction from  $\mathcal{P}_{ref}(x, y)$  of the real sensor and sensor model presented in this paper. (b) PDF of the deviation in the  $x$ -direction from  $\mathcal{P}_{ref}(x, y)$  of the real sensor and sensor model for commercial applications.

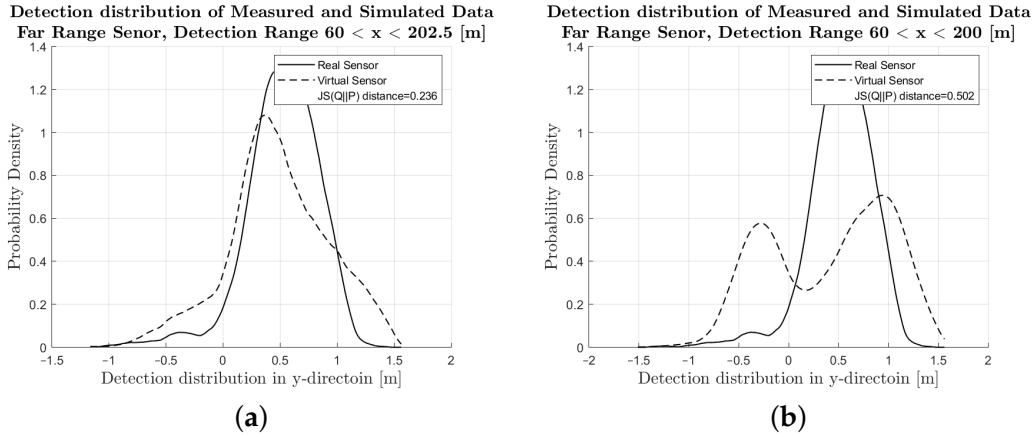
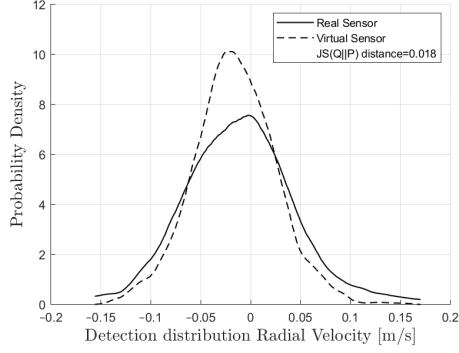


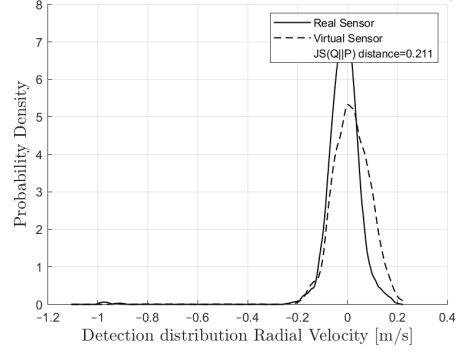
Figure B.9.: Visual comparison and evaluation of the probability distribution function (PDF) of the deviation of the measured and simulated radar point clouds with respect to the reference point in the far-range detection sector. (a) PDF of the deviation in the  $y$ -direction from  $\mathcal{P}_{ref}(x, y)$  of the real sensor and sensor model presented in this paper. (b) PDF of the deviation in the  $y$ -direction from  $\mathcal{P}_{ref}(x, y)$  of the real sensor and sensor model for commercial applications.

Detection distribution of Measured and Simulated Data  
Far Range Sensor, Detection Range  $60 < x < 202.5$  [m]



(a)

Detection distribution of Measured and Simulated Data  
Far Range Sensor, Detection Range  $60 < x < 200$  [m]



(b)

Figure B.10.: Visual comparison and evaluation of the probability distribution function (PDF) of the deviation of the measured and simulated radar point clouds with respect to the reference point  $\mathcal{P}_{ref}(x, y)$  in the far-range detection sector. (a) PDF of the radial velocity deviation from the reference velocity of the real sensor and sensor model presented in this paper. (b) PDF of the radial velocity deviation from the reference velocity of the real sensor and sensor model for commercial applications.